Neuromodulatory Control of Motivated Behavior in the Larval Zebrafish

Neuromodulatory Control of Motivated Behavior in the Larval Zebrafish

A dissertation presented

by

Caroline Lei Wee

to

The Division of Medical Sciences

in partial fulfillment of the requirements

for the degree of

Doctor of Philosophy

in the subject of

Neurobiology

Harvard University

Cambridge, Massachusetts

April 2016

Dissertation Advisor: Dr. Florian Engert Caroline Lei Wee

Neuromodulatory Control of Motivated Behavior in the Larval Zebrafish

Abstract

An animal's behavior is strongly influenced by homeostatic drives that are crucial for survival and reproduction, such as the drive to eat, or to escape from harmful threats. In vertebrates, an evolutionarily ancient brain structure, the hypothalamus, is particularly important for coordinating these essential survival functions. Here, I leverage the simple and transparent brain of the vertebrate larval zebrafish to dissect the conserved hypothalamic networks that regulate appetite and defensive behaviors, focusing on how these overlapping circuits interact with and influence each other.

By using an unbiased brain-wide activity mapping approach, I pinpoint hypothalamic oxytocin (OXT) neurons as a key hub for the control of defensive behaviors against pain. I show that OXT neurons integrate multiple noxious stimuli, in particular input from TRPA1 damage-sensing receptors, to drive pain avoidance behavior via co-release of OXT and glutamate in the hindbrain and spinal cord. Furthermore, OXT neurons can also integrate information about the animal's social context to control appetite, a separate homeostatic drive. These findings provide insight into how a single neuromodulatory circuit can exert flexible, context-dependent control over diverse social and non-social behaviors.

To further probe the hypothalamic networks controlling appetite, I have utilized whole-brain activity mapping to identify hypothalamic neural populations encoding

hunger and satiety. My results indicate that, similar to mammals, medial and lateral regions of the hypothalamus show anti-correlated activity patterns, which likely regulate distinct phases of appetite. In hungry fish, medial hypothalamic nuclei report an energy deficit, whereas more lateral regions may be involved in voracious eating. I demonstrate that one medial hypothalamic population, the serotonergic caudal periventricular hypothalamus, is an important regulator of lateral hypothalamic (LH) activity and food intake, and a separate serotonergic population, the superior raphe nucleus, is important for regulating food intake during satiety, also via the LH, but is dispensable during hunger. Thus, by dissecting serotonin circuit function in the context of other hypothalamic feeding networks, I show how a single neuromodulator can control food intake in a satiation state-dependent manner. Overall, these studies provide insights into the underlying evolutionary principles and logic governing hypothalamic function, and demonstrate how diverse neuromodulatory circuits in the hypothalamus and beyond can exert state-dependent control over an animal's most primitive, yet essential, survival drives.

TABLE OF CONTENTS

Acknowledgements

First and foremost, I would like to thank my colleagues and collaborators, who have made this work possible. This includes my supervisor Florian Engert, who makes everything seem better when prospects look gloomy, and unofficial co-supervisor Sam Kunes, who gives you a reality check when you need it. I first knew Adam Douglass as a large and, consequentially, slightly intimidating senior colleague, who later became a much-valued collaborator and supervisor from afar (i.e. Utah). He is a true mentor and an inspiration, and I look forward to continued collaboration with him.

Erin Song has been a close friend, confidante and collaborator, working alongside me throughout this journey. She has been unconditionally helpful in and out of the lab, and her scientific expertise and wealth of experience has really provided me with much needed guidance and support on a daily basis. Owen Randlett has been remarkably encouraging, helpful and easy to talk to (especially after Alex Schier's cocktails), and I have enjoyed our very fruitful collaboration. Max Nikitchenko has brought my work to a new and higher level with his immense scientific expertise, ambition and idealism. Robert Johnson, with his youthful enthusiasm, has taken the study of zebrafish behavior to new heights, and has been a true pleasure to work with.

In addition scores of labmates have contributed in one way or another to my work, and also made my time in the lab such a wonderful experience. On top of my current lab members, too many of which to name, I would like to thank Engert lab alumni, especially Isaac Bianco, Misha Ahrens, David Schoppik and Ahbinav Grama for the help, advice, criticism and mentorship they provided from day One. Jamie Gagnon

and the Schier lab have been incredibly helpful and accommodating in sharing their skills and resources. I would like to thank the students I have supervised, in particular Jim Bohnslav, for laboring on a project that would later become the cornerstone of Chapter 4 of this thesis. Steve Turney of the CBS imaging facility was immensely helpful and maintained a facility that has made much of this research possible.

I am grateful to my scientific mentors of past and present, including DAC members Dr. Naoshige Uchida, Dr. Bill Carlezon and Dr. Alex Schier, who provided helpful advice on my ever-changing projects and ideas, and past supervisors Dr. Teresa Gunn, and Dr. Tony VanDongen, who shaped my scientific thought process and ambitions. I would furthermore like to thank in advance Dr. Eve Marder, Dr. Rachel Wilson and Dr. Catherine Dulac of my dissertation committee for taking the time to read this thesis – I do hope you will find it enjoyable.

Finally, I would like to thank friends and family, in particular my classmates in the Program in Neuroscience, who have made my PhD journey a truly enjoyable experience, my friends from Singapore (especially Wang Yang), who accompanied me here in the US through thick and thin, Aaron Lenfestey, my first programming tutor and closest friend, and my family (i.e. the Wee and Chong clans), who have tolerated my infrequent communications and being far away from home for more than 8 years now. I will be seeing you again soon.

Chapter 1: Introduction

1.1. NEUROMODULATION

The brain consists of networks of neurons that process sensory stimuli to mediate behavior, and a primary goal of systems neuroscience is to identify how information is routed and transformed through each of these networks, from input to output. What has become increasingly apparent in the past decades is the extent to which these circuits can be modulated by the physical and social environment as well as by internal state, to drastically shape their functions[1–3].

Neural circuits are often shaped by *neuromodulators*, which are small molecules or genetically-encoded peptides that activate G-protein signaling pathways to induce molecular changes in a neuron's intrinsic or signaling properties. They are different from classical neurotransmitters in a number of respects: First, they tend to act broadly. In addition to the often-extensive projections of neuromodulatory neurons, neuromodulators can diffuse far from their axonal sources, and act on targets that do not necessarily receive direct synaptic inputs. Some neuromodulators are furthermore released into the circulation, and thus can act at distant locations throughout the brain and body[2,3]. In other words, neuromodulators are inherently promiscuous, targeting multiple neurons that control multiple behaviors.

Second, neuromodulators tend to act on longer timescales from synaptic neurotransmitters, due to the fact that they act via molecular cascades rather than direct

effects on ion channels. As a result their effects can potentially be extremely long-lasting, via the implementation of long-term cellular modifications or the regulation of gene transcription[4].

Another interesting property of neuromodulatory neurons is that they often co-express other neuromodulators, along with excitatory or inhibitory neurotransmitters, a phenomenon known as *co-transmission.* This phenomenon not only allows them to act on both short and long timescales, but also to exert diverse effects on downstream targets. For example, different neuromodulator/neurotransmitter types may be secreted depending on the activity pattern of the releasing neuron. Furthermore, the receptor expression patterns of downstream targets can confer selectivity towards one signaling molecule over another[5]. At the same time, simultaneously released molecules could both enhance or counteract each others' effects, either to energize downstream signals or to maintain stability and prevent runaway changes to circuit function[2,5].

Given their unique properties, neuromodulatory circuits are well-poised for conferring flexibility to hardwired circuits, in particular for allowing *state-dependent* control of circuit function, from sensory input to behavioral output. For example, in *Drosophila* the state of hunger, represented (in part) by dopamine (DA) neuron activity, can act on gustatory neurons to increase calcium influx, thus enhancing its sensory responsiveness to sugar[6]. In mammals a stressed state leads to release of opioid neuropeptides, which acts to inhibit pain transmission even at the first synapse in the dorsal horn of the spinal cord[7]. On the motor end, premotor neurons as well as central pattern generators are subject to intense neuromodulatory control[2,8]. For example,

socially-dominant cichlid fish, which are more colorful and thus subject to higher predation risk, have lower startle thresholds and higher excitability of the premotor Mauthner neuron that drives startle responses, due to differences in serotonin (5-HT) signaling[9]. Thus, even on a longer timescale an animal's social state (whether it is dominant or subordinate) can impact motor output, again via neuromodulators such as 5-HT.

The above are just a few examples from an ever-expanding list of how neuromodulators can shape circuits based on external context and internal state. These themes will also recur throughout the rest of this thesis. In the following sections, I will focus on the role of neuromodulators in evolutionarily conserved circuits that control fundamental behavioral drives crucial to an animal's survival and reproduction.

1.2 NEUROMODULATORS IN MOTIVATED BEHAVIOR

1.2.1 Motivation

An animal's behavior is controlled to a large extent by needs and desires that drive it towards seeking and achieving specific goals. A hungry animal seeks food, a sexually receptive animal seeks to mate, and an animal under stress seeks relief. Such drives (e.g. for defense, reproduction, energy/nutritional regulation, thermoregulation and fluid balance) are primitive but essential for survival, and are mediated by specialized neural circuits that integrate the internal needs of the animal with relevant external stimuli to mediate approach or avoidance behaviors[10,11]. These survival circuits are not isolated, overlapping and interacting heavily with those controlling reward, reinforcement, arousal and memory. They may also compete with each other; for example, an animal under threat may prioritize relief or escape over feeding[11]. When their functions are disrupted or imbalanced, maladaptive effects such as obesity or addiction may occur[12–14]. The approach and avoidance behaviors elicited by these survival circuits can broadly be referred to as "motivated behaviors", although precise definitions may differ across the literature [15]. In this section, I will focus on a number of motivated behaviors, highlighting in particular the role of neuromodulators involved as well as ideas or concepts relevant to my thesis research.

1.2.2 The hypothalamus in motivation

Many of the circuits involved in motivation can be found in the hypothalamus, a phylogenetically old forebrain structure that comprises numerous interconnected neuromodulatory circuits. The mammalian hypothalamus is divided into different regions, zones/areas, and nuclei, with sometimes-variable nomenclature and classification. I will highlight in the next few subsections various nuclei that are more immediately relevant to my thesis. They are:

1) The paraventricular (PVN) and supraoptic (SON) nuclei, which contains neurosecretory populations, including oxytocin (OXT), arginine-vasopressin (AVP) and corticotropin releasing factor (CRF) neurons that project to the pituitary gland as well as other parts of the brain.
2) The arcuate (ARC) nucleus, which appears to be specialized for appetite regulation, and contains intermingled hunger and satiety-promoting neurons expressing neuropeptides such as agouti-related protein (AGRP) and proopiomelanocortin (POMC).
3) The ventromedial (VMH) and lateral (LH) hypothalamic nuclei, which have diverse roles in regulating appetite, reward, aggression, fear and sexual behaviors, and also express many neuromodulators.[10,16,17]

Many of the putative functions of these hypothalamic regions were inferred by electrical stimulation and lesion studies conducted from as early as the 1920s. These studies were the first to demonstrate that different regions of the hypothalamus might be responsible for triggering specific goal-directed behaviors. In one of the earlier studies,

Bard (1928) showed using lesion studies that the hypothalamus was responsible for "rageful" behavior displayed by decorticate cats[18]. Other studies later further localized the responsible region to the medial hypothalamus[19], and it has been shown that stimulation of specific medial hypothalamic nuclei, for example the VMH, can triggered defensive and aggressive behaviors[20–22].

Electrical stimulation in lateral parts of the hypothalamus, including the LH, could elicit eating[23,24], drinking[25], gnawing[26] and predatory attack[27], whereas lesions in the same regions reduced food intake to the point of starvation[28,29] . On the other hand, stimulation of more medial regions of the hypothalamus, in particular the VMH, induced satiety[30], whereas lesions led to overeating[31], although such change in eating behavior could be partly due to the enhancement of defensive behaviors[30]. Interestingly LH stimulation was also shown to be positively-reinforcing[32,33], whereas VMH stimulation could be negatively-reinforcing[22]. These studies suggested opposing roles of the lateral and medial hypothalamus in the control of appetite, reward and punishment.

While the lack of cell-type specificity and discrepancies in electrode positioning limited the conclusiveness of these studies, they did implicate the hypothalamus as an important locus for the control of distinct and directed behaviors necessary for survival. Molecular/genetic dissection of hypothalamic and extra-hypothalamic circuits over the past fifty years have provided insights into the modulatory control of motivated behaviors, which I will describe in the following subsections.

1.2.3 Defense circuits: A focus on pain and stress

"Nature has placed mankind under the governance of two sovereign masters, pain and pleasure. It is for them alone to point out what we ought to do, as well as to determine what we shall do" - Bentham, 1907[34]

Defenses against pain and natural threats

To survive, an animal needs to defend itself against harm. Not surprisingly, organisms have evolved defense circuits to detect and avoid threats such as predators. In mammals, specialized circuits spanning the amygdala, medial hypothalamic nuclei (e.g VMH and premamillary nucleus) and periaqueductal gray (PAG) are tuned to naturally-threatening stimuli, such as predator odors, and can mediate defensive behaviors such as escape and freezing[11,35–37]. Interestingly, the defense behaviors mediated by hypothalamic stimulation tend to be more coordinated and goal-directed as compared to the downstream PAG, again suggesting that the hypothalamus does not just blindly drive, but coordinates the enactment of specific motor responses[19].

While successful avoidance of a threat is the ideal scenario, the animal also needs to respond when damage has already been inflicted. Tissue damage, for example from predator-induced injury, is first detected by primary afferent nociceptors, (PANs). PANs terminate onto distinct laminae of the dorsal horn of the spinal cord where they synapse onto second-order neurons. From there, they contribute to fast withdrawal reflexes within the spinal cord[38], but also send ascending signals to the brain, where they terminate on different regions of the brainstem, thalamus and cortex[7,39]. The central pathways that process pain are not as well understood, although

much progress has been made in the field. Painful stimuli are likely to be processed differently from other threats, particularly because the goals are different – not only does an injured animal need to escape (in some sense, even more urgently); it also needs to rest and recuperate, though the pathways mediating the latter process are unclear. In addition, while pain could increase the motivation to escape, intense pain can also interfere with ability to defend oneself from immediate threats, or make an animal more susceptible to attack; thus it may need to be temporarily suppressed or modulated[40,41].

Not surprisingly, evidence suggests that pain and predator cues activate distinct circuits. For example, predator and painful cues are conveyed through different amygdalar nuclei, the former through the basomedial and medial nuclei, and the latter through the central amygdala (cEA). Different parts of the hypothalamus may also be activated by painful and predatory stimuli. The anterior hypothalamus, which includes the PVN, is sensitive to noxious stimuli[42] and has been shown to coordinate defensive and anti-nociceptive responses to pain[43–45], whereas predator avoidance circuits tend to converge onto more medial/posterior regions of the hypothalamus, such as the VMH and pre-mamilliary nucleus[19,35].

An important function of central pain circuits is not simply to mediate defensive behaviors, but to modulate pain perception. For example, during threatening situations such as predatory attacks, a suppression of pain transmission can occur. This phenomenon is known as stress-induced analgesia, and may be beneficial in helping the animal defend itself appropriately[46]. On the other hand, stress, inflammation or

chronic activation can also sensitize pain circuits and facilitate pain responses. Thus, pain can be modulated in both directions depending on the context.

Numerous descending circuits have been shown to act at multiple stages of pain processing to either increase or decrease the gain of painful sensory input[7,39]. Modulation can occur even at the first synapse in the dorsal horn, suppressing pain transmission at its source. Neurons in the cortex, amygdala and hypothalamus convey pain information to the periaqueductal gray (PAG), an important site of pain modulation. The PAG in turn projects to different nuclei in the rostral ventromedial medulla (RVM) and dorsolateral pontine tegmentum (DLPT), which feed back onto dorsal horn neurons. The PAG, DLPT and RVM have been shown to contain distinct populations of cells that show opposing firing patterns ("ON" or "OFF") preceding the nociceptor-elicited withdrawal reflex, suggesting that they may control the gain of dorsal horn pain detection, by enhancing or inhibiting pain transmission respectively[47]. Thus, these opposing cell types confer bidirectional control over pain transmission.

Many neuromodulators act on the descending pain circuit to gate pain responses. The most prominent are endogenous opioids, which are well known for their ability to inhibit pain transmission. Opioids inhibit "ON" cells and increase the activity of "OFF" cells, underlining a potential mechanism for their potent analgesic effects[7]. Other neuromodulators involved in pain modulation include 5-HT, which has been shown to facilitate or inhibit pain transmission depending on receptor subtype, presumably by activating either the "ON" or "OFF" populations. Likewise, norepinephrine (NE) may also activate either population, though its effects on pain have been reported to be mostly

inhibitory. Recently, OXT and AVP-expressing neurons in the PVN have been shown to inhibit spinal nociception by suppressing dorsal horn neuron responses, as well as possibly modulate other pain-regulating areas such as the PAG and RVM[45,48–51]. Thus, pain transmission is an excellent example of how modulatory circuits exert flexible control over sensory circuits depending on internal state (e.g. stress) or other factors.

Stress and arousal states

On top of eliciting specific behavioral responses, threats can also induce widespread changes in neuromodulatory, autonomic and neuroendocrine responses, putting the organism into a stressed state. The stress response mounted by the organism could be conceived as its attempt to revert from a "threatened homeostasis" to its normal, pre-threat state [52,53].

One of the body's adaptations to stress is to increase general arousal and heighten attention to the surroundings, which is mediated by the release of neuromodulators such as NE, 5-HT and DA to diverse areas of the brain. The locus coeruleus (LC), one of numerous NE populations in the hindbrain, is a major controller of arousal. It integrates input from threat-detecting brain areas such as the amygdala and PVN, to widely influence activity of downstream areas including, but not limited to the cortex, hypothalamus, hindbrain and spinal cord, and modulate diverse processes such as pain perception and fear learning[54]. In addition, neurons of the sympathetic nervous system are also activated by stress, which secrete NE onto target tissue. Adrenal glands also secrete NE and epinephrine directly into the bloodstream. These autonomic responses cause system-wide changes in physiological functions, including

increased heart rate and blood pressure, sweat secretion and muscular blood flow, as well as reduced digestion, all of which aid the animal in responding to the threat[55].

During stress, certain peptide hormones are released into the circulation, the most prominent being glucocorticoids (GCs). Glucocorticoid secretion is triggered by a classical pathway known as the hypothalamic-pituitary-adrenal (HPA) axis. It involves first the activation of CRF-expressing neurons in the PVN of the hypothalamus, which causes the release of adrenocorticotropic hormone (ACTH) into the bloodstream from the pituitary gland, that in turn leads to secretion of GCs (e.g. cortisol) from the adrenal gland, into the bloodstream[53]. GCs, in addition to influencing the immune and metabolic systems also act on multiple regions of the brain to influence brain activity and behavior[55,56]. For example, GCs have been shown to affect multiple stages of fear learning, from the expression of freezing behavior to the consolidation of fear memories[55,57]. Interestingly, GCs can also feed back onto and inhibit hypothalamic CRF neurons, thus forming a negative feedback loop to prevent runaway increases in stress levels.

In the PVN, CRF neurons of the HPA axis are also intermingled with AVP and OXT neurons, which likewise are neuroendocrine populations involved in the stress response. A subset of AVP neurons co-express CRF, and both CRF and AVP act synergistically to induce ACTH secretion. AVP neurons also have an important role in maintaining water-electrolyte balance, and are activated by osmotic stress and dehydration. OXT neurons have been shown to respond to a wide range of stressful or noxious stimuli and may both regulate and be regulated by the HPA axis[48,58–62].

Furthermore, they may bidirectionally regulate CRF neuron activity in the PVN, possibly through local somatodendritic oxytocin release[63]. Their activity can also be potentiated by circulating GCs, thus forming part of a positive feedback loop to modulate stress responses[63]. The neural and peripheral effects oxytocin release during stress are still not well understood, but they have been proposed to mediate anxiolytic, anti-nociceptive, anti-inflammatory effects on downstream circuits, or to modulate defensive behavioral responses[64]. The role of OXT neurons in pain and stress will be further discussed in Chapter 2.

1.2.4 Appetite and energy regulation

"For the man who is extremely and dangerously hungry, no other interests exist but food. He dreams food, he remembers food, he thinks about food, he emotes only about food, he perceives only food and he wants only food" – Maslow, 1943[65]

Nutritional and energy deficits disrupt a different kind of homeostasis – the balance between a body's energy intake and expenditure. Unlike defense circuits, which are usually first triggered by external context, energetic needs are detected by interoceptive circuits, which are sensitive to levels of circulating nutrients, metabolites and hormones. A nutrient/energy deficit puts the animal into a "hunger" state, which is associated with an enhanced drive to seek and consume food, till homeostatic balance is restored, after which a "satiated" state is achieved.

The hypothalamus has long been recognized as a key locus for the enforcement of hunger and satiety based on electrical stimulation and lesion experiments that could drastically increase or abolish feeding behavior (see 1.2.2). While roughly anatomically segregated it contains genetically distinct neuromodulatory neurons and projections that are often intermingled and sometimes control opposing behaviors, making it difficult to cleanly dissect the neural circuits involved in controlling specific downstream behaviors[10]. Nevertheless, advances in genetic and pharmacological tools in past few decades have narrowed down specific neuronal cell-types that detect and respond to energy changes, while more recently, optogenetic and imaging techniques have provided novel insights into the activity and functions of these molecularly-defined populations.

Opposing appetite circuits in the arcuate nucleus

Energy balance is regulated by distinct and often antagonistic hypothalamic circuits, dysregulation of which can lead to obesity or starvation. The most widely studied of these circuits are the intermingled AGRP and POMC-expressing neurons in the ARC of the hypothalamus, which have been shown to report and promote "hunger" or "satiety" respectively.

The "satiety-promoting" POMC neurons co-express a host of neurotransmitters and peptides. In addition to POMC, a precursor protein that can be cleaved into melanocyte-stimulating hormones (α-, β-, and γ-MSH), β-endorphin, and ACTH, these neurons also express the cocaine-amphetamine regulated transcript (CART), all of which could mediate diverse effects on downstream targets. α-MSH is secreted by POMC neurons and can act through specific melanocortin receptors (MC3/4Rs) expressed on numerous projection targets, including the PVN, LH, amygdala and brainstem, to reduce food intake and increase energy expenditure[66]. Genetic deletion or mutations of POMC, MSH or MC3/4Rs also leads to obesity in rodents and humans, highlighting the importance of this conserved melanocortin signaling in the suppression of appetite and body weight[67–69].

The "hunger-promoting" AGRP neurons express AGRP, neuropeptide-Y (NPY) and GABA. Both NPY and AGRP are secreted peptides that stimulate feeding and reduce energy expenditure. In particular, AGRP acts as a MC3/4R antagonist that can oppose the appetite-suppressing effects of α MSH. AGRP over-expression thus leads to obesity[70]; however, knockouts of AGRP and NPY genes, even in combination, do not

result in appetite suppression[71]. Interestingly, acute ablation of the neurons themselves does reduce feeding, suggesting a more complex role for these neurons in appetite regulation, and the relevance of other co-expressed signaling molecules such as GABA[72–74]. In fact, AGRP neurons have been shown to inhibit neighboring POMC neurons via GABA signaling through local projections[75].

The sufficiency for AGRP and POMC neurons in respective stimulation and suppression of food intake respectively was confirmed through gain-of-function experiments. Acute pharmacogenetic or optogenetic activation of AGRP neurons was shown to trigger voracious feeding even during satiety, promote food-seeking behavior and induced weight gain after a day[76,77]. In contrast, extended (24 hrs) optogenetic stimulation of POMC neurons could partially reduce feeding and body weight through the melanocortin signaling pathway[77]. Interestingly, the acute AGRP neuron-induced increase in feeding was found not to depend on suppression of melanocortin signaling[77] or on POMC neuron activity[78]. Instead, other AGRP neuron projections within and beyond the hypothalamus, like the PVN, LH, anterior subdivisions of the bed nucleus of the stria terminalis (aBNST) and paraventricular thalamic nucleus (PVT) may be more important for mediating their appetite-stimulating effects[78,79]. In particular, AGRP neuron-mediated suppression of OXT neuron activity in the PVN via NPY and GABA secretion was both necessary and sufficient for acute AGRP neuron-induced feeding, although the contributions of other brain regions have certainly not been ruled out[78].

What cues are responsible for the activation of AGRP and POMC neurons? AGRP and POMC neurons have long been established as energy sensors that are

tuned to circulating hormonal and nutritional cues reporting the internal state of the animal[80]. Specifically, AGRP neurons have been shown to be activated by energy-deficit cues, such as the circulating hunger gut hormone ghrelin, and to be inhibited by energy-surfeit cues, such as glucose, insulin and the fat-derived hormone leptin[66]. In contrast, POMC neurons can be activated by leptin, and glucose[75,81]. Circulating cues may even mediate plasticity at these hypothalamic synapses. For example, ghrelin has even been shown to enhance synaptic inputs onto AGRP neurons, by increasing presynaptic glutamate release. This effect can be reversed by leptin via opioid (likely β-endorphin) release from POMC neurons, thus defining a molecular mechanism by which ghrelin and leptin exert opposing effects on AGRP neuron excitability[82].

However, the model that AGRP and POMC neuron are largely regulated by circulating nutrients and hormones that report energy status has recently been challenged by studies monitoring their activity in real-time in freely-behaving mice [83–85]. While these studies confirmed that AGRP and POMC neurons could be activated or inhibited respectively by energy deficit and related cues such as ghrelin, they also demonstrated that the sensory detection of food after fasting was sufficient to strongly reverse the activity of these neurons, even prior to food consumption. Such rapid sensory modulation of AGRP and POMC activity was unexpected given that the animal's energy status has not yet changed at this point. Instead, these neurons may be using external sensory information about food availability to predict their impending change in energy status, to drive behavioral changes from appetitive (food-seeking) to consummatory-type behaviors, or even to facilitate associative learning. In fact, the activation of AGRP neurons has been shown to represent a negative valence state,

reversal of which could condition flavor/place preference. Thus a fast drop in activity in response to the sensory cues of food could act as a teaching signal for the learning of food-predicting cues[85].

Interestingly, the immediate sensory-induced changes in firing rates of these neurons in response to food did not return their activity completely to baseline levels, demonstrating that, on a longer timescale, these neurons are still sensitive to the satiation state of the animal, and the lingering activation or inhibition of AGRP and POMC neuron activity respectively could still play a role in modulating food consumption[84,85]. Furthermore, AGRP and POMC neuron activity could be modulated by food cues in satiated mice, but only if the food was highly palatable, suggesting that the rewarding/hedonic properties of food could also directly influence activity of these neurons even in the absence of an energy deficit[83].

Overall, these studies suggest a more complex and integrative role of ARC neurons in the control of appetite that extends beyond energy sensing. Indeed, AGRP neurons may possibly have roles even beyond feeding. For example, while activation of AGRP neurons in the presence of food induces voracious eating, activation of the same neurons in the absence of food can trigger repetitive behaviors that cannot simply be explained by being in a negative valence state[86]. Thus, AGRP could possibly serve to influence other behaviors depending on environmental context, providing yet another example of state-dependent behavioral modulation by neuromodulatory circuits.

Opposing hypothalamic networks for appetite and beyond

The hypothalamic control of appetite extends beyond the ARC. In fact, classic lesion and electrical stimulation experiments pinpointed the VMH and LH as having opposing roles in satiety and hunger respectively (as described in Section 1.2.2), with the VMH able to suppress the appetite-promoting effects of LH stimulation[33]. However, unlike the ARC, which is thought to be specialized mainly for appetite-related functions, both the VMH and LH have been implicated in various other roles, including defensive, social (e.g. aggression, reproduction) and reward-related behaviors[10].

Nevertheless, the importance of the VMH and LH in appetite regulation has been well established. The VMH is replete with leptin receptors, and deletion of these receptors from specific VMH neurons leads to obesity, suggesting that independent of the ARC, the VMH is a critical regulator of energy homeostasis and body weight[87,88]. The VMH can potentiate POMC but not AGRP neuron activity in the ARC[89], and ARC neurons also project to the VMH, leaving plenty of opportunity for crosstalk and plasticity between the two satiety centers.

The LH is similarly well-connected to ARC neurons, and in itself comprises numerous modulatory populations, with intermingled neurons expressing hypocretin (orexin), which regulates both sleep/arousal and feeding, melanin concentrating hormone (MCH), an appetite stimulant, as well as neurotensin, galanin, glutamate and GABA[90,91]. Researchers had long recognized that these different cell types were likely to play distinct roles in feeding and other processes[90,92–94] and though many questions still abound, recent advances in genetic-based imaging, tracing and stimulation

techniques have finally permitted a more comprehensive understanding of the roles of these cell types in behavior.

For example, the GABAergic cells in the LH have been shown to be sufficient for stimulating food consumption, optical self-stimulation and place preference, with ablation of the same populations reducing feeding behaviors and weight gain[95]. In-vivo calcium imaging showed that different subsets of these neurons differentially represent appetitive and consummatory behaviors, confirming that they play important but diverse roles in coordinating behavioral responses to food. A combination of anatomical and electrophysiological studies suggest that these LH GABAergic neurons may project to the VTA to disinhibit dopaminergic neurons, thus linking the reinforcing effects of LH stimulation with an established locus for reward learning[90,96]. The close link between the LH and the reward system suggests that its role is more complex than simply making an animal “hungry”. For example, the LH may serve to increase the incentive values/ salience of food cues, or to reinforce appetitive food approach behaviors that precede consumption[92]. LH-lesioned rats, while eschewing normal chow, would still consume highly palatable foods, suggesting that a dysfunction in their subjective valuation of food, rather than a lack of “hunger” per se, may underlie their feeding deficits [29,93].

Other LH cell-types have also been investigated to various degrees. Interestingly, stimulation of glutamatergic LH neurons, unlike GABA, reduces feeding and is in fact aversive[97]. Activation of orexin neurons promotes food and addictive drug-seeking behaviors, but also wakefulness[98,99], and ablation of orexin neurons causes both narcolepsy and hypophagia[100], reflecting the overlap of arousal and feeding circuitry.

MCH has been shown to promote appetite and weight gain, but may also increase sleep and energy expenditure[93]. Thus, the appetite-stimulating effects of the LH must be taken into consideration along with other processes such as reward, arousal or metabolism. Clearly, a comprehensive understanding of the LH would involve careful characterization of its inputs, outputs, and the diversity of individual cell responses, ideally in the context of the entire brain network.

Monoaminergic control of appetite: A focus on serotonin

In addition to the hypothalamic neuropeptides, monoaminergic neurontransmitters such as DA, NE and 5-HT are important influencers of appetite. In fact, the earliest weight-loss drugs were 5-HT/NE or selective 5-HT reuptake inhibitors (SNRIs or SSRIs), suggesting that these monoaminergic systems acted to suppress appetite. Manipulations that increased endogenous serotonin, such as receptor agonists generally decreased food intake, whereas antagonists or knockout of specific 5-HT receptors (e.g. 5HT2C and 5HT1B) caused hyperphagia and weight gain[101]. In fact, one of the recently FDA-approved obesity treatments is *lorcaserin*, a specific 5-HT2C receptor agonist[102].

In mammals, 5-HT is secreted by the raphe nucleus, which sends projections to numerous targets within the hypothalamus. For example, 5-HT is thought to activate hypothalamic POMC neurons via 5-HT2C receptors, and inhibit AGRP neurons via 5HT1B receptors, thus promoting satiety via control of melanocortin signaling in the ARC[103–106]. 5HT is also released in the lateral hypothalamus, where it may affect the release of MCH and orexin[107,108]. To make matters more complex, serotonin can also be

secreted by enterochromaffin cells in the gut, which in fact forms the bulk of 5-HT in the body. Circulating 5-HT, while unable to cross the blood-brain barrier, can act on peripheral 5-HT3 receptors to increase gut motility, and is also able to suppress food intake, though mechanisms are not completely clear[102,109,110].

Finally, it is interesting to note that while generally known as an appetite suppressant in mammals, serotonin is predominantly appetitive in non-mammalian species such as leeches[111], C. *elegans*[112,113] and *Drosophila*[114]. The effects of 5-HT on appetite in non-mammalian vertebrate models are also not well understood. SSRIs and 5-HT agonists have been shown to reduce feeding in various fish species[115–117]. However, in blind Mexican cavefish, the SSRI fluoxetine was shown to increase food-seeking behavior; these fish also had more 5-HT neurons, higher 5-HT neurotransmission and enhanced food-finding abilities than their sighted, surface-dwelling counterparts[118,119]. Thus, while it is clear that 5-HT transmission is important for feeding behavior across numerous phyla, it has been difficult to achieve a consensus across vertebrate and invertebrate models on whether it promotes food seeking or satiety. Part of the complication may reflect the broad nature of serotonin function: it has been implicated in stress, arousal, reward as well as punishment, all of which may impact feeding behaviors[120,121].

The role of serotonin in appetite will be further explored in Chapter 4, using the larval zebrafish as a vertebrate model that could bridge the gap between mammalian and invertebrate studies. The role of dopamine in appetite will be elucidated in the next section (1.2.5).

1.2.5 Interactions between motivation circuits

"A crust eaten in peace is better than a banquet partaken in anxiety." – Aesop

Survival circuits such as those specialized for defense or appetite do not exist in isolation, but also interact with each other. For example, the activation of defense circuits can override the drive to eat, but intense hunger can motivate an animal to seek food even at the risk of predation. While integrating information from the outside world, they are tuned not only to their physical, but also social context[11]. At the same time, these survival circuits interact with more generalized motivational systems, such as circuits that mediate learning and arousal. In this section I will provide a few select examples of how more general motivational systems are involved in the regulation of basic survival drives.

Appetite and defense circuits interact with reward circuitry

Food is a naturally rewarding stimulus, and cues or behaviors that lead to food consumption are learned and positively-reinforced. However the subjective reward value of food can be modulated by an animal's internal energy status, or the food's palatability. For example, hunger may increase the value of nutritious but unpalatable food, whereas even in the absence of an energy deficit, highly palatable foods could still act as an incentive to drive approach behaviors or learning[122].

An important locus for reinforcement learning is the mesolimbic reward system, which includes VTA DA neurons and the downstream nucleus accumbens (Nac). DA

neurons in the VTA have been shown to encode the incentive value of a reward or its predicting cues, thus acting as a teaching signal that can facilitate learning[123,124]. Interestingly, the incentive value of food reward, represented by DA neuron activity, is subject to modulation by its caloric or nutritional properties, as well as the animal's current energy status.

A known pathway by which homeostatic appetite circuits can influence VTA reward processing is via the LH. Optical and electrical self-stimulation behavior can be elicited from the activation of LH neurons, and such behavior is modulated by satiation state[90]. Furthermore, GABAergic LH neurons have been shown to send projections to the VTA, where they may disinhibit DA neurons[90,125]. Thus, the LH may be involved in communicating an animal's energy needs to general reward processing circuits, which may modify an animal's subjective valuation of food, and thus its reinforcing properties. In fact, direct activation of LH-VTA neurons can motivate reward (sucrose)-seeking even in the presence of an aversive stimulus, possibly by artificially enhancing the incentive value of the reward to a point of compulsion[96] . The VTA/NAc in turn feeds back onto the LH and may communicate calculated signals (e.g. reward prediction error) back to the LH[96]. In addition, circulating hormones such as ghrelin and leptin have been shown directly affect VTA DA neuron activity, and thus could directly modulate the incentive value of food based on satiation state[126,127].

The palatability, or hedonic value of food, is also encoded by extrahypothalamic circuits, and likewise influences an animal's motivation to eat. Since LH/VTA lesions do not necessarily reduce hedonic responses to food (e.g. lip licking), and LH stimulation or

DA agonism do not enhance hedonic behavioral responses, other brain regions, for example opioid signaling pathways in the NAc and ventral pallidum (VP) are thought to be more important in the encoding of hedonic value[128–130]. In fact, stimulation of the VP leads to self-stimulation and affective “pleasure” responses, whereas VP ablation can reduce food-seeking and conditioned place preference behaviors[131]. Thus the hedonic value of food can also be reinforcing and stimulate appetite in the absence of an energy deficit.

Pain circuits also interact with reward pathways. For example, relief of pain has been shown to be rewarding and reinforcing by acting on mesolimbic reward circuitry[132,133]. In particular, specific NAc circuits downstream of DA neurons respond to both the onset and offset of painful stimuli, which may encode the motivational salience of pain and the reward value of pain relief respectively[134]. The overlap of pain and reward circuitry is also evident from the immense impact of opioid signaling on pain processing and relief, as discussed in Section 1.2.3. Opioid signaling is heavily involved in encoding the hedonic value of rewards, and also interacts with mesolimbic reward circuitry, thus allowing for interaction of pain circuits with reward and appetite circuits. In fact, sucrose consumption and food-predicting cues have been shown to relieve pain through an opioid-dependent mechanism, which may involve signaling from the VMH to the PAG and RVM[7]. Thus, coming full circle, both pain and appetite processing circuits intersect with reward pathways, allowing the learning of cues and behaviors that predict food reward, or pain relief.

Interactions between appetite and defense circuits

The state of stress, or "threatened homeostasis", can also exert a lasting impact on appetitive behaviors such as feeding. Interestingly, stress has bidirectional effects on food intake, either inducing anorexia, or hyperphagia[135,136]. It is clear that the HPA axis as well as monoaminergic arousal system are involved in the regulation of appetite circuitry. For example, CRF has been shown to be a potent and acute appetite suppressant, possibly by acting on receptors in the amygdala and VMH[57,136,137]. On the other hand, GCs are an appetite stimulant, possibly via the activation hypothalamic AGRP/NPY as well as POMC circuitry[138], or by interactions with ghrelin, leptin and insulin release and signaling pathways[136]. In addition, GCs and CRF have been shown to potentiate mesolimbic reward circuitry signaling, which could promote appetitive behaviors such as food consumption as a means of stress relief[135,139,140]. Monoamines such as 5-HT and NE, that are released in response to stressful stimuli to promote generalized arousal are also known to have potent anorectic effects[141] (see 1.2.3 and 1.2.4). Thus, appetitive and threat-processing circuits interact to shift the balance between different motivational behaviors or restore homeostasis via counteracting mechanisms.

Modulation by social context

A crucial external factor that interacts survival pathways is an animal's social environment. The presence of potential mates or threatening competitors is relevant to an animal's survival and procreation. Thus, these cues activate survival circuits such as those specialized for reproduction and defense, and also modulate other circuits, for

example appetite, reward or arousal. Yet social context can extend beyond sexual reproduction or aggressive interactions. The presence of fellow conspecifics is most often, except in a resource-scarce situation, beneficial to the animal, whether it is for safety in numbers, or more efficient foraging, learning or navigating. This is true even for simple organisms such as nematodes and fruitflies, which show complex social dynamics and interactions beyond stereotyped courtship or aggressive behaviors[142–144]. Thus even the mere presence or absence of fellow conspecifics is a relevant signal that may modulate survival circuits and behavioral output of the organism.

Here I will focus on a single example of how social information is integrated to modulate defense circuits that process pain and aversive stimuli. Numerous studies have demonstrated that an animal's stress levels in response to an aversive stimulus can be reduced by the presence of conspecifics, and that these behavioral effects are consistent with the downregulation of the HPA axis[145]. This phenomenon is known as "social buffering" of the stress response. Both OXT and opioid signaling have been proposed as candidates for mediating the effects of social buffering on the HPA stress response. OXT neurons, which are activated by stressful stimuli (see section 1.2.3), have been shown to inhibit the HPA axis via multiple mechanisms, such as suppressing hypothalamic CRF neuron activation, ACTH release and adrenal gland-mediated cortisol release[63,146]. Furthermore, opioid release may be induced by social interactions, leading to increased analgesia[147,148]. Thus, a possible mechanism for social buffering may involve oxytocin or opioid signaling ameliorating the stress response produced by HPA activation, though evidence is still scarce. While the underlying mechanisms are

still being explored, the social buffering effect is a clear example of how social context can modulate the function of innate defense circuits.

1.2.6 Open questions in the study of motivation

Given the complex and closely intertwined neuromodulatory networks underlying motivated behaviors, it is challenging to attain a comprehensive understanding of any individual circuit without understanding its roles in the context of other behaviors it controls, and other intersecting circuits in the brain. As described by LeDoux (2012):

"It is generally assumed that circuits underlying defense, energy, fluid balance, reproduction, thermoregulation, and other survival functions interact, but this has been not been studied to any significant degree. This is a particularly important topic that is best pursued by methods that allow evaluation of concurrent activity in the multiple brain areas, such as fMRI in humans and fMRI and molecular imaging in animals." [11].

A holistic understanding of these neuromodulatory circuits will also require precise genetic tools that allow for activity monitoring and manipulations at single cell resolution, which is especially necessary for understanding the functions of intermingled neural populations. Since many of these populations co-express multiple neuromodulators and neurotransmitters; more comprehensive loss-of-function, pharmacological and synaptic electrophysiological studies will be necessary to elucidate the specific roles of each modulator, and how they compensate for or complement each other as a whole. In the following section, I will describe why the larval zebrafish model may be useful in tackling some of these questions.

1.3 ZEBRAFISH AS A MODEL FOR MOTIVATED BEHAVIOR

"Nothing in biology makes sense except in the light of evolution" – Dobzhansky, 1973[149]

1.3.1 Zebrafish as a Model for Systems Neuroscience

Understanding how intersecting neural circuits process information to produce behavior is a key goal in systems neuroscience. Multiple models, from simple (e.g. nematodes) to very complex (i.e. humans) each have their advantages and disadvantages with respect to achieving this goal. Here, I will focus on why the larval zebrafish (3-29 days post-fertilization or dpf) is an exceptionally useful model for dissecting circuit function during behavior.

In the quest to comprehend the human brain, researchers often turn to model organisms for two major reasons: 1) Reduced complexity, which allows for a more complete and detailed understanding of circuit function and 2) the feasibility of executing controlled manipulations of brain activity or gene function. The former is an important criterion for systems neuroscience; however, another factor that needs to be taken into consideration is how similar this simple "model" brain is to a mammalian, or human brain. While evolution makes certain that there are bound to be commonalities, the neural circuits and neurochemistry of vertebrate models tend to be much more homologous to humans in terms of anatomical structure and connectivity, as compared to invertebrate models. Thus, a simple brain with chemical and structural homologies to a more complex one might potentially (on a case-by-case basis) be more helpful in unraveling the function of its "more complex" counterpart. In this regard, the larval zebrafish forms a unique compromise between brain simplicity and anatomical

homology.

Being a vertebrate model, the larval zebrafish brain bears many structural similarities to mammalian brain organization[24]. Although lacking a cortex, many interesting subcortical areas of the zebrafish brain are highly conserved. The telencephalic pallium is believed to contain homologs to the mammalian olfactory cortex (posterior dorsal pallium), amygdala (dorsomedial pallium) and hippocampus (ventral dorso-lateral pallium), whereas the telecephalic subpallium has been proposed as the homolog to the mammalian basal ganglia[150]. The diencephalon is also heavily conserved, with the habenula, for example, similarly implicated in learning behaviors as in mammals[151–154]. Furthermore, the hypothalamus forms a significant part of the larval zebrafish brain and bears many homologies to the mammalian hypothalamus, which will be described in the following section. Neuromodulatory populations, such as the norepinephrinergic locus coeruleus and serotonergic raphe nucleus can be found in zebrafish. The perhaps intriguing exception are the midbrain DA neurons which are heavily involved in reward processing in mammals, but do not exist in zebrafish, although other DA populations abound[155,156].

While exhibiting clear homologies to the mammalian brain, the larval zebrafish brain is much smaller than the brain of any mammalian model. Less than 500μm thick at larval stages, and with only around 100,000 neurons, it presents a tractable brain size for exhaustive analyses of activity and connectivity patterns[150]. Another ancillary benefit of a simple (and transparent) brain, as in the case of the larval zebrafish, is that it is possible to monitor brain activity from large portions, if not the entire network, at single

cell resolution, thus permitting a fuller perspective of the interconnected brain networks that control brain function. In fact, the tools for monitoring activity from a large number of neurons at the same time have expanded greatly in the past few years. While classical serial-scanning two-photon microscopy methods have allowed for brain-wide calcium imaging that extends to deep regions of the zebrafish brain[157], new computational and optical techniques now allow for even faster and deeper-penetrating two-photon imaging, by using tools such as acousto-optic deflectors, parallelized multifocal scanning and spatial light modulators[158–160]. Furthermore, one-photon techniques such as light sheet[161–163] or light field microscopy[164] permit fast volumetric imaging that, although poorer in resolution for deep tissue and requiring exposure to visible light, still are capable of capturing activity from the entire zebrafish brain. Combined with tethered or fictive behavioral monitoring, these techniques allow the assessment of whole-brain neuronal activity simultaneously with behavior, providing insights into how distributed brain networks act in concert to control behavioral output[165].

In addition, a novel method developed in the Engert lab (MAP-mapping) has allowed for the high-throughput mapping of brain activity across multiple stimuli through the use of a fast (~1 minute) reporter of neuronal activity, phosphorylated-Extracellular signal-regulated kinase (ERK/MAPK)[166]. This method, which quantitatively compares activity patterns across groups of fish under different treatment conditions, and overlays the activity patterns onto anatomically mapped brain regions, allows for the identification of candidate brain areas that are activated by specific stimuli. Although limited in time resolution, this whole-brain activity mapping technique has allowed for the characterization of brainwide responses to numerous stimuli, a method that is more

tedious to achieve in mammalian models.

The second major rationale for studying model organisms is the capacity to functionally dissect neuronal circuitry, in order to establish causal relationships between activity patterns and behavior. Optical, optogenetic and genetic tools have successfully been used in zebrafish to ablate, silence or activate neurons of interest and study their effects on behavior, and novel, more effective tools are constantly being developed. These include nitroreductase mediated cell-specific ablations, which causes specific cell death in genetically-specified populations under exposure to a pro-drug[167], channelrhodopsin or halorhodpsin-mediated activation or inhibition of neurons[168], chemical activation of neurons via exogenous TRP channels[169], two-photon laser mediated cell lesioning[170,171] or the expression of neurotoxins (e.g. tetanus toxin) that prevent synaptic signaling[172]. Furthermore, novel genetic manipulation techniques such as CRISPR-mediated mutagenesis now allow for fast and precise genetic editing to analyze the roles of conserved genetic networks in neural function[173]. Finally, the development of viral circuit tracing and electron microscopy techniques in larval zebrafish, also from the Engert lab, should allow for the dissection of circuit connectivity to form more biologically-accurate models of circuit function. Many of the tools described above have been utilized in Chapters 2-4 of this thesis.

In summary, the sheer scale, complexity and optical impenetrability of the mammalian brain makes it difficult to assess the breadth and distribution of changes that occur during any behavior with high spatial resolution. The simpler but anatomically homologous larval zebrafish brain may complement mammalian studies in providing a

wider and more comprehensive viewpoint of brain function across multiple brain networks and multiple behaviors.

1.3.2 Using Zebrafish to Study Motivated Behaviors

In his perspective piece "Rethinking the Emotional Brain", LeDoux (2012)[11] highlighted key topics that require further exploration in order to advance our understanding of motivated behaviors. On the list he stressed that:

"More comparative work is needed to elucidate similarities and differences in survival functions and circuits between various groups of vertebrates. Particularly pressing are studies of non-mammalian vertebrates."

The rationale is clear -- non-mammalian vertebrates were the first organisms in which hypothalamic survival circuits developed (survival circuits are also present in invertebrates, but tend to be much less conserved), and thus understanding the functions of these hypothalamic circuits in simple vertebrates should provide insights into the logic and principles that guided their evolution into the more complex manifestations that we see in mammals. LeDoux further argues that although the precise behavioral outputs that an animal produces may be different across various species, the motivational circuits underlying these behaviors that generate drives and shift priorities, are likely very similar between mammals and simple organisms. In this section, I will propose that a specific non-mammalian vertebrate model, the larval zebrafish, provides the exquisite opportunity to bridge the current evolutionary gap in our understanding of the circuits underlying purposeful, motivated behaviors.

Conserved neuromodulatory networks for motivated behaviors

Motivated behaviors are controlled by neuromodulatory circuits concentrated in (though not restricted to) various subcortical brain regions, including the hypothalamus, amygdala and monoaminergic populations. Most, if not all of these regions have their counterparts in the zebrafish. In the zebrafish hypothalamus, the neuroscretory preoptic area that expresses OXT, AVP and CRF neurons, among many other peptides, is similar to the mammalian PVN/SON, and the ventral periventricular hypothalamus may be homologous to the ARC due to the expression of AGRP, MSH, Kisspeptin, Growth Hormone Releasing Hormone and Neurokinin B[174]. At the same time, many regions of the zebrafish hypothalamus do not appear to have a mammalian counterpart. For example, the caudal periventricular hypothalamus, which contains mainly DA and 5-HT neurons, does not exist in mammals, although DA and 5-HT are important regulators mammalian hypothalamic function. As part of my thesis work, my colleagues and I have characterized the expression of various neuropeptides in the zebrafish hypothalamus, to elucidate the similarities and differences between the zebrafish and mammalian brain (more in Chapter 4).

The strong homologies between larval zebrafish and mammalian hypothalamic circuits will clearly facilitate the generalization of discoveries from one organism to the other. At the same time, the differences may also be illuminating. For example, they could provide insights into which hypothalamic circuits have been strictly preserved over evolution, and likely maintain core specific functions, and which are more flexible, have

had their functions overtaken by alternative circuits, or may have transformed over evolution to suit mammalian needs.

As described previously, an additional benefit of the larval zebrafish is its tractable brain size and transparent brain, both of which are advantageous for the large scale monitoring of brain networks controlling motivated behaviors (see Section 1.3.1 for available techniques). I will use the hypothalamus as an example: The human hypothalamus is about the size of an almond[17]. The mouse hypothalamus, while much smaller (roughly 2mm long on each axis) is still larger than the entire larval zebrafish brain. The larval zebrafish hypothalamus, while forming a remarkably large fraction of the ventral half of its brain, is only about 100-200μm long on each axis, thus, by volume estimates is about 1000 times smaller than that of the mouse. Along with the fact that the entire larval zebrafish brain has just 100,000 neurons, which is likely smaller than the total number of neurons in the rodent hypothalamus, it presents a clearly tractable brain size for comprehensive circuit dissection, and also allows the possibility of imaging not just across the entire hypothalamus, but the entire brain.

Recent advances in in-vivo recording/imaging techniques in rodents have allowed for monitoring of population activity at high temporal and spacial resolution within specific hypothalamic nuclei during free behavior, a procedure that admittedly has not yet been achieved in larval zebrafish. However, these tetrodes or head-mounted microendoscopes do not even span the entire nucleus of interest, and can only sample a small number of neurons per mouse[84,85,95]. For example, one recent study using tetrode recordings identified a total of 100 ARC (AGRP and non-AGRP) neurons across

15 mice[84], and another study using a microendoscopic device could only image about 20 AGRP neurons per mouse[85]. In reality, the mouse ARC has about 10000[79] AGRP neurons and 3000 POMC neurons[67,79]. Thus, at this point researchers are literally peering through a pinhole in the rodent brain, and while it is possible that the activity they are recording is representative of the entire population, it may be useful to complement these studies with brain-wide imaging approaches only possible in simpler, smaller vertebrate brains.

Furthermore, these methods are insufficient to elucidate how diverse motivated circuits interact, since this would require mapping of brain activity beyond a single locus. Recently, a technique called frame-projected independent-fiber photometry (FIP) has been used to record from multiple regions of the brain[175]; however, in addition to its highly invasive nature, this method measures bulk activity from brain regions and rely on genetic specificity to distinguish between multiple intermingled cell types.

In short, while technical advances in brain imaging and electrophysiology make the rodent model highly appealing and suitable for dissecting the circuits underlying motivated behavior, the larval zebrafish model is likewise advantageous, both from an evolutionary standpoint, to elucidate the similarities and differences between mammalian and teleost motivational systems, and from a systems neuroscience perspective, by contributing towards a comprehensive understanding of motivation in the vertebrate brain.

The current state of motivated behavior research in the larval zebrafish

What is the state of motivated behavior research in the larval zebrafish? The large majority of systems neuroscience-based studies of the larval zebrafish have cashed in on their repertoire of stereotyped, reflexive behaviors, in order to probe sensorimotor integration pathways across the entire brain. A number of recent studies have started to probe neuromodulatory regulation of simple behaviors, such as locomotion, optomotor or escape reflexes. Behavioral paradigms for motor or operant learning have been developed in the larval zebrafish, allowing for the study of circuits underlying more complex behaviors. More recent forays into appetite regulation, developed by others and myself in the Engert lab, have only just started to tease apart how internal state can modulate the prey-capture reflex. Below, I will describe the most relevant studies with regards to motivated behavior in the larval zebrafish.

i. Defense/Stress/Arousal

One of the most commonly studied defensive behaviors in the larval zebrafish is its escape reflex. This is a fast, robust, high-angle and stereotyped behavior (the C-bend) that is made in response to a variety of threatening visual, tactile or vibrational-acoustic stimuli. This C-bend is driven by the large Mauthner cell, which receives ipsilateral sensory input to drive a turn to the contralateral side, allowing for fast, directional escape from a threat. However a Mauthner-mediated escape is energetically costly and thus the “decision” to escape is gated and subject to modulation, both from neighboring interneurons[171] and neuromodulatory populations such as DA and 5-HT[176,177]. Interestingly, the DA neuron population that modulates escape behaviors is

situated in the caudal periventricular hypothalamus. In Chapter 4 of this thesis, I will explore how intermingled 5-HT neurons within the same area control appetite. In addition to the escape reflex, zebrafish also react to heat and noxious chemicals[178–180]. However, neuromodulatory pathways that govern these behaviors are completely unknown and are the focus of Chapter 2 of my thesis.

Zebrafish also clearly show stress-related behaviors. Zebrafish CRF neurons have been shown by calcium imaging to respond to stressors such as low pH or high salinity, displaying enhanced activation and recruitment with stressor intensity[181]. A glucocorticoid receptor mutant identified from a forward genetic screen was shown to have higher cortisol levels due to the impairment of GC-mediated transcription, thus preventing negative feedback regulation of the HPA axis activation[182]. In both larvae and adults, this GC receptor mutant also demonstrated enhanced stress behavior[182,183]. In particular, mutant larvae had lower spontaneous locomotor activity but higher startle responses to a vibrational acoustic stimulus. Interestingly, SSRIs were shown to ameliorate these stress-related phenotypes, suggesting an interaction of 5-HT signaling with the HPA stress axis[182,183]. Thus, the function of the zebrafish HPA axis parallels that of humans, and may provide insights into the mechanisms of SSRI-based anti-anxiety drugs. Furthermore, 5-HT has also been implicated in arousal in the larval zebrafish. Larval zebrafish show short-term heightened arousal and responsiveness to visual stimuli after a brief pulse of waterflow, which was shown to be mediated by the dorsal raphe nucleus[184]. Thus, 5-HT may be important for mediating arousal state-dependent modulation of sensory processing.

ii. Appetite

From 5 dpf, the developing larval zebrafish begins to hunt for food, by executing a coordinated sequence of orienting movements in response to prey, such as eye convergences and small turns (J-bends), followed by a forward swim ("strike") which if implemented successfully culminates in the capture of the prey[185]. This behavior has long been characterized as a stereotyped, reflexive action pattern triggered by the movement of a small object across its visual field[185]. My colleagues and I have now demonstrated that prey capture behavior can be strongly modulated by hunger state, even after food deprivation for as short as 2 hours[186] (see also Chapter 4). Again, the mechanisms underlying how internal state modulates appetite are completely unknown in the larval zebrafish, and are the subject of my thesis research.

iii. Social behavior

Even less is known about social behaviors in the larval zebrafish. While adult zebrafish are highly social, larvae have not been established as such[187]. In fact, a recent study characterizing the development of social behaviors in zebrafish concluded that robust conspecific preference, as well as synchronization of behavior with other fish, only arises at around three weeks, and could be disrupted by exposure to ethanol, similar to findings in adult zebrafish[188]. However, other studies have suggested that much younger larval zebrafish may already be capable of social behaviors – in particular, one study showed that visual access to conspecifics could be used as a "social reward" to condition place preference[189]. However, since these results contradict other studies that have assayed conspecific preference in larval zebrafish, their capacity

for social interactions at this age remains to be elucidated. In Chapter 3, I will describe results indicating that larval zebrafish brain activity and behavior can in fact modulated by social context.

iv. Learning

The larval zebrafish is capable of both associative and non-associative learning, although again not as robustly as in adults[190]. On the simpler end of the spectrum, larval zebrafish show habituation of the Mauthner-mediated startle response, which, in the case of long-term habituation, can last up till 18 hours after training. Larval zebrafish are also capable of adaptive motor learning, retaining the memory of having experienced high or low gain for at least 10 seconds after the end of the stimulus[165].

They are furthermore capable of classical and operant learning, which has been shown most commonly with aversive stimuli such as electric shock or heat[154,190]. In particular, the habenula was shown to be crucial for avoidance learning with electric shock in ~3 week old larvae[154]. Recent work from Drew Robson and Jennifer Li in the Engert lab has also demonstrated that larval zebrafish are capable of operant learning and that neural representations, for example in the habenula, may reflect changes that happen across learning. In adult zebrafish, ventral habenula signaling to the median raphe nucleus may encode punishment expectation[153], thus, the established role of the habenula in mammalian learning can likely extend to the zebrafish.

While reward-driven learning has been demonstrated in adult zebrafish, no clear reward-learning paradigm has been established in the larval zebrafish. However, given

the clear capacity of the larval zebrafish for associative and non-associative learning, it is a matter of time before the behavioral repertoire of the larval zebrafish will be greatly expanded to include more complex learning and memory paradigms.

Overall, while still in its early days, the larval zebrafish most certainly has the potential to become a highly effective model for investigating the neural bases of motivation and neuromodulation. The rest of this thesis will describe the beginning of an effort to dissect motivation circuits and their interactions in the larval zebrafish brain.

Chapter 2:

Descending oxytocin neurons form a parallel pain avoidance circuit in the larval zebrafish

2.1 INTELLECTUAL CONTRIBUTIONS

The following chapter is adapted from a manuscript entitled "Descending oxytocin neurons form a parallel pain avoidance circuit in larval zebrafish" that has not yet been submitted for review. I am first on the author list, but Dr. Maxim Nikitchenko (MN), Sasha Luks-Morgan (SLM), Dr. James Gagnon (JG), Dr. Erin Song (ES), Dr. Owen Randlett (OR), Dr. Isaac H. Bianco (IHB), Alix Lacoste (AL), Dr. Ahbinav Grama (AG), Dr. David G.C. Hildebrand (DGCH), Dr. Alexander Schier (AS), Dr. Samuel Kunes (SK), Dr. Florian Engert (FE) and Dr. Adam D. Douglass (ADD) also contributed to the manuscript. I conceived of the project with help from ADD, FE, MN, ES and SK, wrote most of the manuscript, did most of the experiments and analyzed most of the data. ADD revised the introduction of the manuscript and supervised the project together with FE. MN developed hardware and software for calcium imaging/behavior experiments also designed and performed experiments and analyzed data. SL and ADD performed/analyzed free-swimming channelrhodopsin experiments, and OR performed/analyzed some MAP-mapping experiments. ES and also performed experiments. IHB built the optogenetic stimulation setup and advised experiments. JG and I generated the oxytocin CRISPR mutant. ADD and I generated the *Tg(oxt:Gal4)* line. AG and DGCH generated the *Tg(HuC:GCAMP6s)* line. AS supervised JG, OR and AL and advised the project.

2.2 SUMMARY

Oxytocin (OXT) is an evolutionarily ancient neuropeptide that is well known for its pro-social functions. However, it is also involved in many non-social and negative processes, including pain, anxiety, fear and stress. Here, we use brain-wide activity mapping to identify a specific role for hypothalamic OXT neurons in pain processing. Using a novel optical approach for activating TRPA1 receptors, we found that zebrafish OXT neurons showed robust responses to TRPA1 activation, which correlates with large-angle tail bends, a pain avoidance response. OXT neurons project to the hindbrain and spinal cord; and both optogenetic activation of OXT neurons, and bath application of OXT to a reduced preparation, were sufficient to elicit high angle tail bends. Since OXT neurons co-express both glutamate and OXT, we used CRISPR-mediated mutagenesis to demonstrate that lack of OXT attenuates OXT neuron effects on locomotion, but does not abolish it completely. Overall, our results demonstrate a functional role for OXT neurons in promoting an avoidance response to painful sensory stimuli.

2.3 INTRODUCTION

An animal's physiological and behavioral responses to pain enable it to avoid physical threats while placing it into a state of elevated sensory awareness. The autonomic, neuroendocrine, and central mechanisms that underlie these responses are complex and coordinately regulated by the hypothalamus. By integrating and responding to a wide range of physiological pain signals of neuronal and non-neuronal origin, the hypothalamus serves a crucial role in the behavioral and affective components of pain across species.

Increasing attention has been directed toward the hypothalamic peptide neurohormone oxytocin (OXT) in the context of pain. In addition to its well-studied roles in social and affiliative behaviors, parenting, and childbirth, it has become clear that OXT released in response to threatening and injurious stimuli is a crucial modulator of behavior. In particular, OXT neurons have been shown to respond to noxious thermal, mechanical and chemical stimuli[42,191], electric shock[192,193], emotional stress[194–196], seizures[59] and inflammation[197]. Recent work has suggested that OXT may promote relief from these stimuli through its anti-nociceptive, anti-inflammatory and anxiolytic effects[51,58,197–199]. Furthermore, OXT may drive defensive avoidance responses by enhancing locomotion and escape[192,200], and reducing freezing behavior[64].

Attempts to understand OXT's diverse roles in pain and other behaviors have been complicated by the fact that it can operate as both a neuroendocrine hormone, via its release into the bloodstream through the pituitary, and as a centrally acting modulatory neurotransmitter. Much more is known of the neuroendocrine actions of

OXT, than of behavior driven by its neuromodulatory action. Indeed, it is only recently that OXT projections from the hypothalamus to other regions of the CNS have begun to be identified and characterized. These projections appear to be especially important for OXT's role in pain. OXT has been shown to suppress pain sensation by modulating the activity of dorsal root ganglion sensory neurons[48,51,197,201,202]. In addition, OXT can enhance spinal motoneuron activity in spinalized rodent preparations, suggesting a role in modulating spinal locomotion[203–205]. Pharmacological activation of OXT receptors in the amygdala reduces learned freezing behaviors in fear-conditioned rats, as does optogenetic activation of OXT neurons projecting from the hypothalamus to the amygdala[64]. Such central modes of action clearly need to be considered alongside the hormonal models of OXT activity to understand its contributions to pain-related behaviors.

Many of OXT's behavioral roles are remarkably well conserved throughout evolution, with OXT-like peptides mediating social, reproductive, and aversive functions in species ranging from nematodes to mammals[206–209]. In fish, homologs of OXT and the related nonapeptide arginine-vasopressin (AVP), have been implicated in sociosexual behaviors such as parental care, aggression and pair bonding[210–214]. Teleost OXT neurons are mainly located in the neurosecretory preoptic-hypothalamic area (NPO), which is thought to have differentiated into the paraventricular nucleus (PVN), supraoptic nucleus, and accessory nuclei of the hypothalamus in mammals[215,216]. This region also contains other neuroendocrine cells of the hypothalamic-pituitary-adrenal (HPA) axis, including AVP, corticotropin-releasing hormone, thyrotropin-releasing hormone and somatostatin-expressing neurons[216]. As in

mammals, OXT neurons in fish project beyond the pituitary, sending axons to disparate parts of the brain, including other hypothalamic regions, the hindbrain and spinal cord[217–220].

Here, we exploit the experimental leverage offered by the larval zebrafish to demonstrate a novel role for hypothalamic OXT neurons in mediating pain avoidance. Using pERK-based activity mapping and calcium imaging, we show that noxious stimuli, in particular TRPA1 receptor stimulation, activate OXT neurons, whose activity correlates strongly with large angle tail bends, a pain avoidance behavior. Experimental activation of these descending OXT neurons also drives large-angle tail bends. OXT contributes partially to this pain avoidance response, but other co-expressed transmitters, likely glutamate, are also involved. We thus propose that OXT neurons form part of a parallel neuromodulatory circuit that generates an appropriate motivated behavior in response to painful sensory input.

2.4 RESULTS

Whole-brain activity mapping reveals OXT neuron activation by noxious stimuli

Whole-brain activity mapping using phosphorylated ERK (i.e. MAP-mapping) is a novel approach that allows rapid, high-throughput analysis of brain responses to a wide range of stimuli during natural behavior[166]. We utilized this MAP-mapping approach to identify specific neuronal networks that might be involved in the processing of painful stimuli, including mustard oil, electric shock and noxious (37°C) heat. In each of these treatments, strong activation was observed in the neurosecretory preoptic area, overlapping with OXT neuron expression (Fig. 2.4.1A, 2.4.1B). This region is homologous to the PVN/supraoptic/accessory nucleus of the hypothalamus in mammals [216]. In contrast, dish taps, a stressful but non-noxious vibrational-acoustic stimulus, did not strongly activate the preoptic region (Fig. 2.4.1A). These results suggested that preoptic OXT neurons may form part of a core network specifically involved in pain processing.

To confirm the specificity of OXT neuron activation, we first compared pERK signals within the OXT preoptic region (Diencephalon - OXT Cluster 1 in Preoptic Area, as annotated in the Z-brain atlas) across a wide range of appetitive, neutral and aversive stimuli. We found that only aversive stimuli could induce activation of the preoptic OXT region (Fig. 2.4.1C). In particular, we observed stronger activation by painful stimuli such as heat, mustard oil and electric shock than with a stressful stimulus such as dish taps (Fig. 2.4.1A,C).

Figure 2.4.1: Whole-brain activity mapping reveals OXT neuron activation by noxious stimuli (A) Activity maps from MAP-mapping experiments probing brain-wide neural responses to a range of aversive stimuli. Intersection maps across multiple experiments were used to increase reliability. The neurosecretory preoptic area (PO) consistently showed enhanced activity after (i) electric shock (intersection of three experiments), (ii) mustard oil (intersection of a 10uM and 25uM exposure conditions) and (iii) 37°C heat (intersection of two experiments), but less PO activation in response to (iv) dish taps (intersection of two experiments). Regions within the brain are outlined. Mustard oil treatment also induced pERK expression outside of the brain, especially skin and muscle tissue. Scale bar = 100μm. PO = preoptic area, PT = posterior tuberculum, Pit = Pituitary gland, LC = Locus coeruleus, cHy = caudal hypothalamus, HB = hindbrain, OTc = Optic Tectum. A = anterior, L = Left, V = Ventral. **(B)** (i) Projection image of ventral planes of a single MAP-map for electric shock, registered to the Z-brain atlas. PO is strongly activated (ii) Tg(Oxt:GFP) transgenic line registered to Z-brain atlas (iii) Z-brain outline of OXT neurons in the PO area, used for ROI-specific analysis of PO OXT neuron activation in (C). Scale bar = 100μm. **(C)** Comparison of PO OXT neuron activation in response to a range of appetitive (cocaine, amphetamines, food), neutral (optomotor gratings) and aversive (dish taps, 37°C heat, mustard oil, electric shock) stimuli. Zebrafish subject to heat, mustard oil and electric shock showed significant activation of the PO OXT neuron region, cocaine treatment significantly reduces PO OXT neuron activity ($p = 0.027^{*}/0.193/0.883/0.301/ 0.4148.133\times10^{-7}{}^{***}/ 3.048 \times10^{-5}{}^{***}/ 0.000488^{***}/ 6.145\times10^{-8}{}^{***}$. Wilcoxon sign rank test against median of 1).

Figure 2.4.1 (Continued): (D) (i) Projection image of *Tg(oxt:GFP)* fish show projections from the PO to the pituitary gland (Pit), hindbrain (HB) and spinal cord (SC), among other regions. Scale bar = 100μm. (ii) Higher magnification image of PO and posterior (postr) OXT neurons. Scale bar = 20 μm. (**E**) (i) There is a significant increase in pERK/tERK ratio of individual *Tg(Oxt:GFP)*-positive neurons across multiple fish. Preoptic cluster is shown in red. Electric Shock: n=7/8 fish, ***p = 0.000311; 25μM Mustard oil: n = 12/12 fish, ***p = 3.658×10^{-5}; 37°C heat: n = 15/15 fish, ***p = 0.000136. Posterior population is shown in blue. Electric Shock: n=7/8 fish, ***p = 0.000621; 25μM Mustard oil: n = 12/12 fish, ***p = 0.000308, 37°C heat: n = 15/15 fish, p = 0.648, Wilcoxon rank sum test. (ii). Probability distribution (kernel density estimate) of pERK/tERK ratios for preoptic population (red) of OXT neurons shows a significant shift in pERK/tERK ratio in response to electric shock (n = 256/281 neurons, ***p = 5.1983×10^{-56}), mustard oil (n =385/464 neurons, ***p = 1.0398×10^{-85}) and 37°C heat (n = 796/882 neurons, ***p = 2.1029×10^{-12}). (iii) Probability distribution (kernel density estimate) of pERK/tERK ratios for posterior population (blue) of OXT neurons shows a significant shift in mean pERK/tERK ratio in response to electric shock (n = 120/128 neurons, ***p = 2.1522×10^{-19}), mustard oil (n =223/205 neurons, ***p = 1.1497×10^{-26}) and 37°C heat (n = 284/278 neurons, *p = 0.0158). Two-sample Kolmogorov-Smirnov test. For (ii) and (iii), Box width spans pERK/tERK ratios from 0 to 2.

Figure 2.4.1 (Continued): (F) Average calcium activity of 13 OXT neurons (from a single example fish) labeled by *Tg(oxt:Gal4;UASGCaMP5G*) in response to electric shock (2.6V/cm, represented by dashed line). Scale bar: 5% Δf/f (vertical), 5 sec (horizontal). Inset: Projection image of *Tg(oxt:Gal4;UASGCaMP5G)*-expressing neurons from the same example fish (PO cluster). Scale bar = 20μm. **(G)** OXT neurons, as labeled by *Tg(oxt:Gal4; UAS:GCaMP5G)* or *Tg(otp:Gal4;UAS:GCaMP5G)* respond more strongly to electric shock (2.6V/cm) than to taps. A supra-threshold tap stimulus that has been calibrated to trigger Mauthner-mediated escapes was used. Fraction of labeled neurons that respond at least once to stimulus, mean of the maximum Δf/f value within 5 seconds after stimulus, integrated Δf/f within 5 seconds after stimulus was significantly higher for electric/shock treatments. Different fish were used for tap and shock stimuli. *Tg(oxt:Gal4;UAS:GCaMP5G):* Fraction responsive: *p = 0.0180*;* Mean peak Δf/f: **p = 0.0038*;* Mean integrated Δf/f: **p = 0.0027; n = 7shocks/11 taps. *Tg(otp:Gal4;UAS:GCaMP5G):* Fraction responsive: *p = 0.043*;* Mean peak Δf/f: ***p=7.5453x10^{-4}; Mean integrated Δf/f: ***p =3.4659x10^{-5}; n= 14 shocks/12 taps. Wilcoxon sign rank test.

Figure 2.4.1 (Continued):

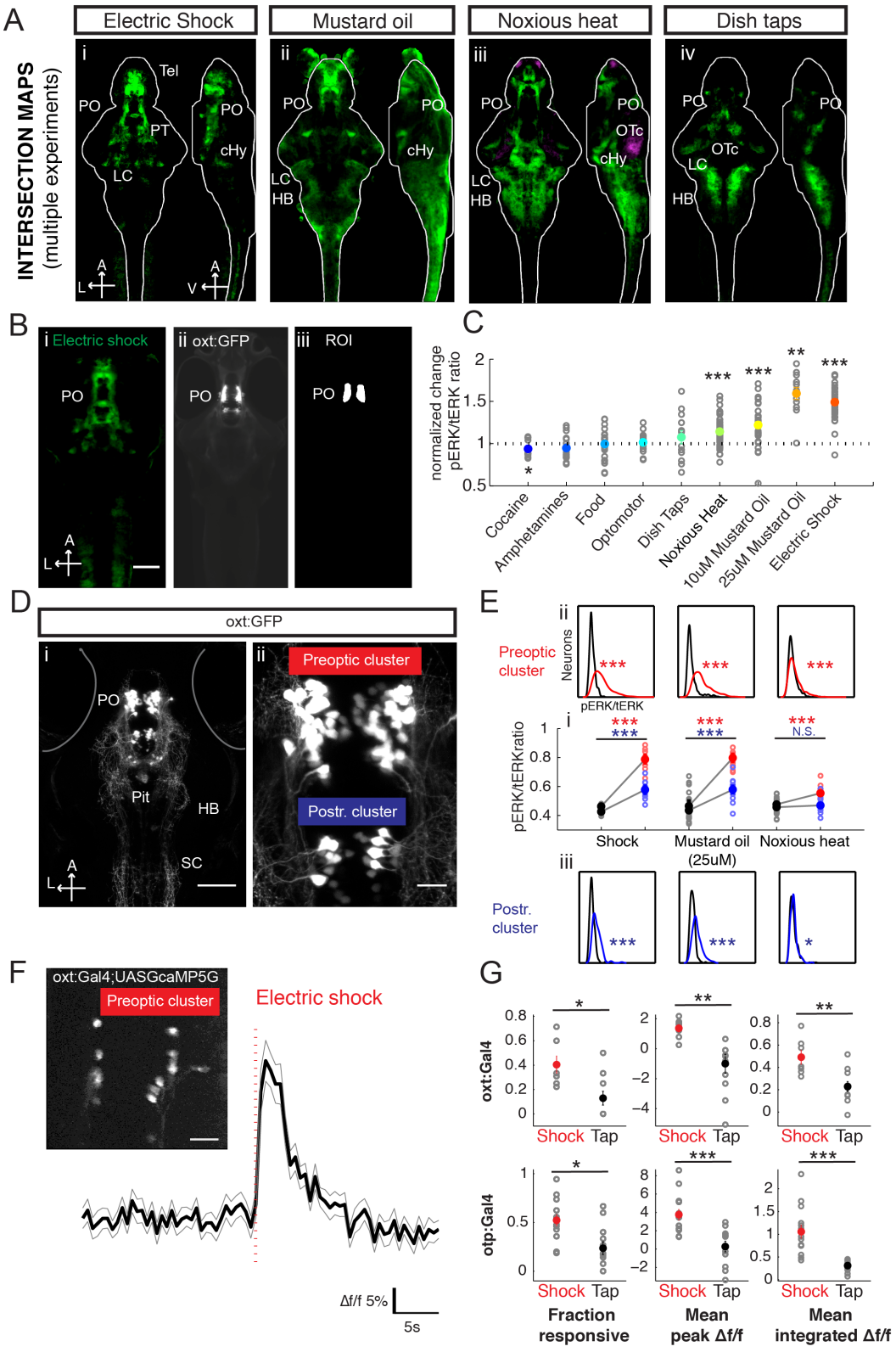

Since other neuropeptidergic neurons are interspersed with OXT neurons in the preoptic area[216], we asked if pERK signals were enhanced specifically in OXT-expressing neurons. To that end, we performed MAP-mapping experiments on transgenic fish expressing *Tg(oxt:GFP)*, which specifically labels OXT neurons[219] (Fig. 2.4.1D, 2.4.2A-B). In mammals, OXT neurons can generally be divided into two subclasses: magnocellular neurons, which are larger, express higher levels of OXT and project to the pituitary gland, and parvocellular neurons, which are smaller, express less OXT and project to other regions of the brain, including the hindbrain and spinal cord[221,222]. Likewise in zebrafish we observed a bimodal distribution of OXT-positive neurons into two subgroups – one with higher OXT expression, that are likely to be magnocellular neurons (~33% of neurons), and another with lower OXT expression, that form the majority (~67%) of OXT neurons labeled by *Tg(oxt:GFP).* Similar to mammals, the putative magnocellular neurons were more anteriorly positioned as compared to the parvocellular ones (Fig. 2.4.2).

We confirmed that normalized pERK activity averaged across individual OXT-positive neurons (both magnocellular and parvocellular combined) in the preoptic OXT cluster was significantly increased after exposure to electric shock, mustard oil and heat, as compared to controls (Fig. 2.4.1D). Interestingly, 37°C heat, which has been shown to be a strong noxious stimulus for zebrafish[179] and which causes widespread activation across the entire brain (Fig. 2.4.1A), caused a smaller overall change in pERK levels than mustard oil or electric shock, with only a subset of neurons showing an increase in activity.

Figure 2.4.2: Anatomical characterization of oxytocin and orthopedia-expressing neurons (A) The preoptic (PO) and posterior cluster of *Tg(oxt:GFP)* neurons (i) overlap with antibody staining against OXT (ii). (iii) Overlay of GFP expression and anti-oxt staining. A = Anterior, L = Left. Scale bar = 20μm. (iv) OXT neurons color-coded according to oxytocin antibody staining intensity. Colorbar: Red (>3000), Orange (2000-3000), Yellow (1500-2000), Cyan (1000-1500), Blue (<1000). Neurons expressing higher levels of OXT, likely magnocellular neurons, are located more anteriorly. M = magnocellular (putative) P = parvocellular (putative). (v) Histogram showing distribution of OXT peptide levels (i.e. oxt antibody staining intensities) of individual *Tg(oxt:GFP)* positive neurons for five different fish. **(B)** (i) Histogram showing the bimodal distribution of normalized OXT levels (i.e. oxt antibody staining intensities) in five larvae combined. OXT expression level for each neuron was normalized to the mean intensity of all neurons of each fish. We used K-means clustering (k=2) to divide the neurons into two categories, likely representing magnocellular and parvocellular cell types. The first group (parvocellular, blue) comprised 104/156 (66%) of the population (normalized intensity = 0.797±0.0234) and the second group (magnocellular, red) comprised 52/156 (33%) of the population (normalized intensity = 1.7975±0.0514). (ii) Histogram showing the distribution of normalized *Tg(oxt:GFP)* intensities in five larvae combined, which, unlike for OXT peptide, was not bimodal. For purpose of comparison to (i), we similarly used K-means clustering (k=2) to divide the neurons into two categories**.** The first group comprised 97/156 (62%) of the population (normalized intensity = 0.7831±0.0247) and the second group (magnocellular) comprised 59/156 (38%) of the population (normalized intensity = 1.4522±0.0420).

Figure 2.4.2 (Continued): (iii) Although their distributions are different, *Tg(oxt:GFP)* expression in each neuron correlated with anti-OXT staining, suggesting that it could be used to estimate oxt expression levels. R= 0.534, p =7.2512×10^{-13} (Pearson's correlation). (iv) *Tg(oxt:GFP)* levels showed a weak correlation with pERK activity for 25μM mustard oil treatment (R = 0.1982, p = 1.7052×10^{-5}) but not for electric shock (R = -0.0723 p = 0.2273) or heat (R = 0.0259, p = 0.443). Pearson's correlation. **(C)** In-situ hybridization shows overlap of OXT mRNA with the *Tg(oxt:GFP)* line. Stronger mRNA expression is observed more anteriorly, which likely corresponds to magnocellular cell types. **(D)** (i) Maximum intensity image showing overlap of *Tg(oxt:Gal4)* (magenta) and *Tg(oxt:GFP)* (green) expression. *Tg(oxt:Gal4)* labels fewer neurons in the posterior cluster. Scale bar = 20μm. (ii) Lower magnification maximum intensity projection of *Tg(oxt:Gal4)* and *Tg(oxt:GFP)* expressing fish showing extensive OXT neuron projections to many parts of the brain, including the pituitary gland and hindbrain/spinal cord. Scale bar = 100μm. **(E)** *Tg(oxt:GFP)* overlaps with *Tg(otp:Gal4)* expression, though *Tg(otp:Gal4)* may label more posteriorly-located (i.e. parvocellular) cells. We observed no obvious overlap of *Tg(otp:Gal4)* with the poster OXT cluster. Scale bar = 20μm. **(F)** Sparse labeling of OXT neurons by injection of the *oxt:Gal4* construct into embryos expressing *Tg(UAS:ChR2-YFP)*. Examples from three fish are shown. OXT neurons in the preoptic area project to the pituitary gland, hindbrain and spinal cord.

Figure 2.4.2 (Continued):

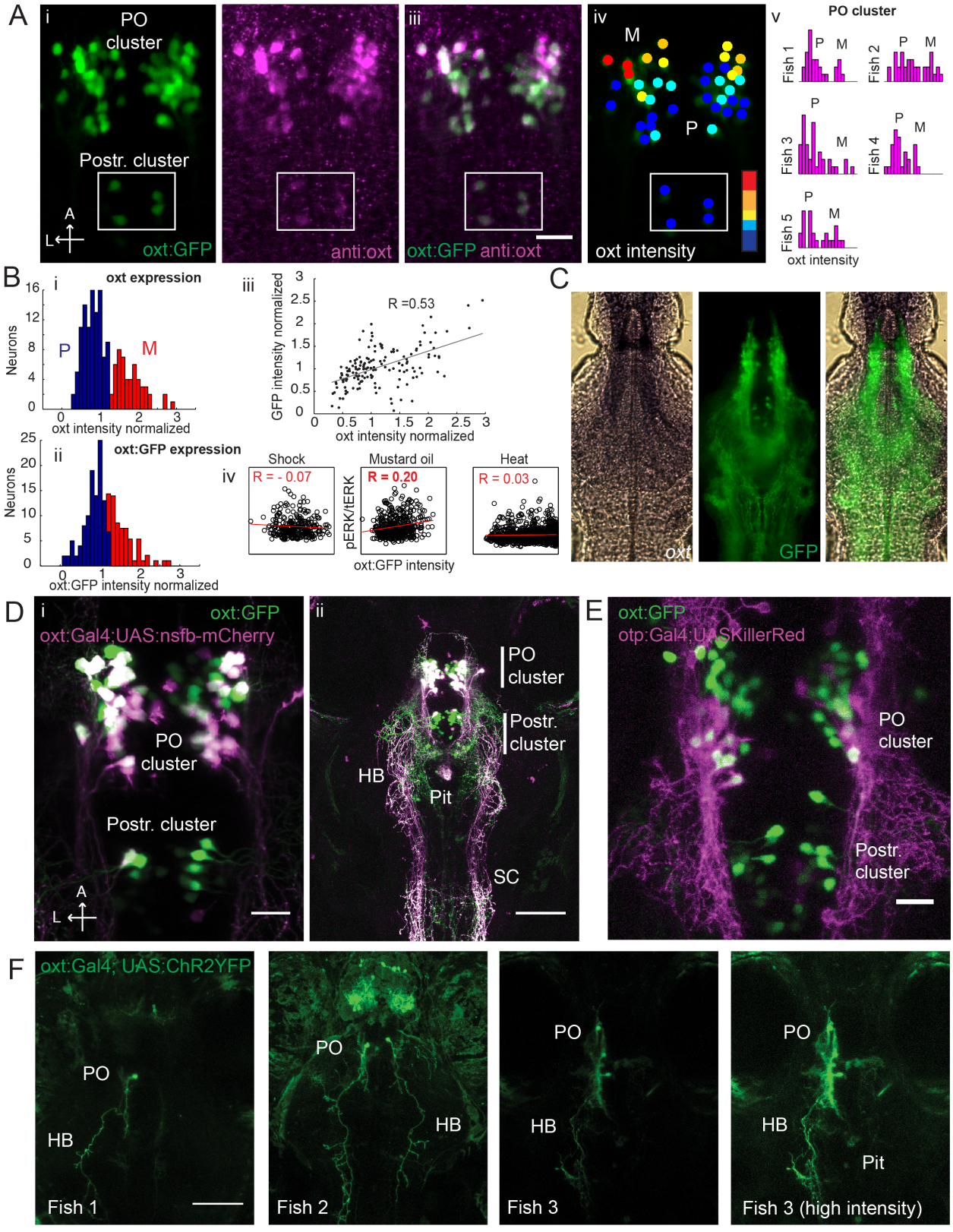

Although *Tg(oxt:GFP)* expression can in principle be used as a readout of endogenous OXT gene expression[219], the distribution of GFP expression, unlike for OXT immunostaining, did not look bimodal (Fig. 2.4.2), thus we were unable to use oxt:GFP expression alone to definitively distinguish between magnocellular and parvocellular cell types. However, since GFP expression correlated with OXT protein levels (Fig. 2.4.2), we asked whether there was any relationship between the degree of activation of OXT neurons (i.e. pERK signal) and OXT expression (approximated by GFP intensity). Interestingly, we found that while electric shock and heat seemed to evenly activate OXT neurons across-the-board, there was a weak but positive correlation between *Tg(oxt:GFP)* expression and pERK signals for mustard oil treatment, raising the possibility that magnocellular neurons might be more significantly activated by mustard oil. Such activation of more anterior parts of the preoptic area can also be visualized from our whole brain activity maps (see Fig. 2.4.1A).

We also compared preoptic OXT neuron activation with a more posterior/ventral population of OXT neurons (posterior cluster) labeled more sparsely by the *Tg(oxt:GFP)* line, which also express lower levels of OXT (Fig. 2.4.2A). Unlike the preoptic neurons, the homologous population of the posterior cluster in mammals is unknown. Again, a smaller but significant increase in pERK levels was also observed in the posterior cluster in response to electric shock and mustard oil, but not to heat.

We further verified our MAP-mapping results by performing calcium imaging in OXT neurons. We used two different transgenic lines to label OXT neurons. The first was a novel *Tg(oxt:Gal4)* line, which we generated using the same promoter sequence as in the previously-published *Tg(oxt:GFP)* (Fig. 2.4.2C). Since this line only labels the

posterior cluster very sparsely, we did not focus on those neurons in our analysis. We also utilized the orthopedia *Tg(otpb.A:Gal4)* [referred to as *Tg(otp:Gal4)*] line, which has been previously shown to overlap strongly with preoptic OXT neuron expression[223] (Fig. 2.4.1D). In both mammals and zebrafish, the transcription factor orthopedia (otp), plays a conserved role in the development of OXT neurons (as well as other neuropeptides), and has been proposed to form part of a network that coordinates responses to stressful stimuli in the zebrafish[224]. We found that electric shock strongly activated preoptic OXT neurons, whereas a vibrational-acoustic tap stimulus, which generates an escape response[171] but is presumably non-noxious, induced at most weak activation (2.4.1F-G). Thus, our calcium imaging results complement our MAP-mapping data in demonstrating strong OXT neuron activation in response to painful stimuli.

TRPA1 stimulation drives large-angle tail bends that correlate with OXT neuron activity

Painful chemical stimuli such as mustard oil, but not heat, activate the Transient Receptor Potential Cation Channel, TRPA1[178,179,225]. We thus decided to investigate if TRPA1 channel activation could excite OXT neurons. We took advantage of a recently published small molecule, Optovin[226], which is inactive in the dark but can be photoconverted into a TRPA1 agonist in the presence of low intensity UV/blue light. After the UV/blue light is switched off, Optovin converts back to its original conformation within seconds[226]. Thus, by immersing the fish in Optovin and stimulating them with brief pulses of UV/Blue light, we could activate TRPA1 in a spatially and temporally controlled manner.

As expected from a noxious stimulus, photochemical activation of TRPA1 receptors enhanced locomotion and drove large angle tail bends (Fig. 2.4.3A-B). Using simultaneous 2P calcium imaging and behavioral monitoring in pan-neuronal GCaMP6s fish (Fig. 2.4.3A), we found that cell bodies in the preoptic area, including OXT neurons, were activated by TRPA1 stimulation (Fig. 2.4.3C-E, 2.4.4A). By co-expressing *Tg(oxt:Gal4;UASnfbCherry)*, we could specifically extract activity traces from OXT neurons. We found that mean OXT neuron activity was strongly correlated with TRPA1-induced large angle tail bends (Fig. 2.4.3D-F). On occasions when stimulation with UV light alone induced tail bends, or when spontaneous tail bends occurred, OXT neurons were also concurrently activated, suggesting that OXT neuron activity was more correlated with behavior than with the stimulus per se (see Fig. 2.4.4 for examples). These experiments provide evidence that OXT neurons receive sensory input from TRPA1-expressing sensory neurons and might potentially be involved in modulating behavioral responses to TRPA1-activation.

Figure 2.4.3: TRPA1 stimulation drives large-angle tail bends that correlate with OXT neuron activity (A) Schematic of TRPA1 stimulation behavioral setup for two-photon calcium imaging. A custom-built two-photon laser-scanning microscope was used for calcium imaging. The fish was stimulated using a 405nm laser aligned parallel to the fish's anterior-posterior axis and focused on the center of its tail (see inset), with the fish facing away from the laser beam to reduce visual stimulation. A custom-built shutter controlled by a servomotor was positioned above the objective and used to block the imaging light path whenever the UV laser was turned on, to prevent saturation of the PMT. **(B)** (i) Distribution of peak tail angles within one second of stimulation in DMSO (black) and Optovin (red). UV stimulation produces larger angle tail bends in Optovin (114.83±4.05 degrees) than in DMSO (34.22±3.40 degrees). Data shown are for *Tg(HuC:GCaMP6s)* fish (n=8). (ii) Mean peak tail angle and area under tail angle trace (an approximation for amount of movement) within 1s of stimulation is significantly higher in Optovin than in DMSO (Peak tail angle: ***$p = 2.3927x10^{-5}$; Integrated Area: ***$p = 3.8876x10^{-4}$, Paired Student's t-test). **(C)** Pixel-by-pixel analysis of *Tg(HuC:H2B:GC6f)* fish, which express GCaMP in the nucleus, shows that cell bodies in the PO and also PT are specifically activated by UV stimulation in the presence of Optovin but not DMSO. Heat maps shows the average Δf/f per pixel in 5s window after UV stimulation.

Figure 2.4.3 (Continued): (D) Mean OXT neuron activity (Δf/f) and cumulative angle traces, plotted side by side in DMSO and Optovin conditions. Red dots indicate time of UV stimulation (5 stimulations shown, 1 minute inter-stimulus interval). The same OXT-positive neurons were identified for DMSO and Optovin conditions by co-expression of *Tg(oxtGal4;UAS:nsfbCherry)* in pan-neuronal *Tg(HuC:GCaMP6s),* fish, and averaged to obtain mean OXT activity. Scale bar: 10% Δf/f (vertical) or 50 degrees (vertical), 5 secs (horizontal). **(E)** Top: Average OXT neuron activity (8 fish, 25 stimulations per fish in Optovin and DMSO, for GCaMP6s fish. Bottom: Average tail deflection magnitude in Optovin and DMSO conditions. OXT neuron activity and average tail angles are larger in Optovin than in DMSO. Slightly higher baseline movements in Optovin are due to spontaneous tail twitching movements which begin to occur after repeated stimulations in Optovin, but do not correlate with OXT neuron activity (see Fig. 2.4.4 for examples). Scale bar: 0.5% Δf/f (vertical) or 5 degrees (vertical), 1 sec (horizontal). **(F)** Mean OXT neuron activity (integrated activity over 5 second window after stimulation) correlates with (i) peak and (ii) integrated tail angles (within a 1s window after stimulation). A longer time window was chosen for calcium fluorescence due to the slow rise/fall kinetics of GCaMP fluorescence, as shown in (E). Red = Optovin, Black = DMSO. Correlation coefficient was calculated across both DMSO and Optovin conditions. Peak tail angle: $R = 0.565$, $^{***}p = 4.1141 \times 10^{-35}$; Integrated tail activity: $R = 0.486$, $^{***}p = 4.5149 \times 10^{-25}$ (Pearson's correlation).

Figure 2.4.3 (Continued):

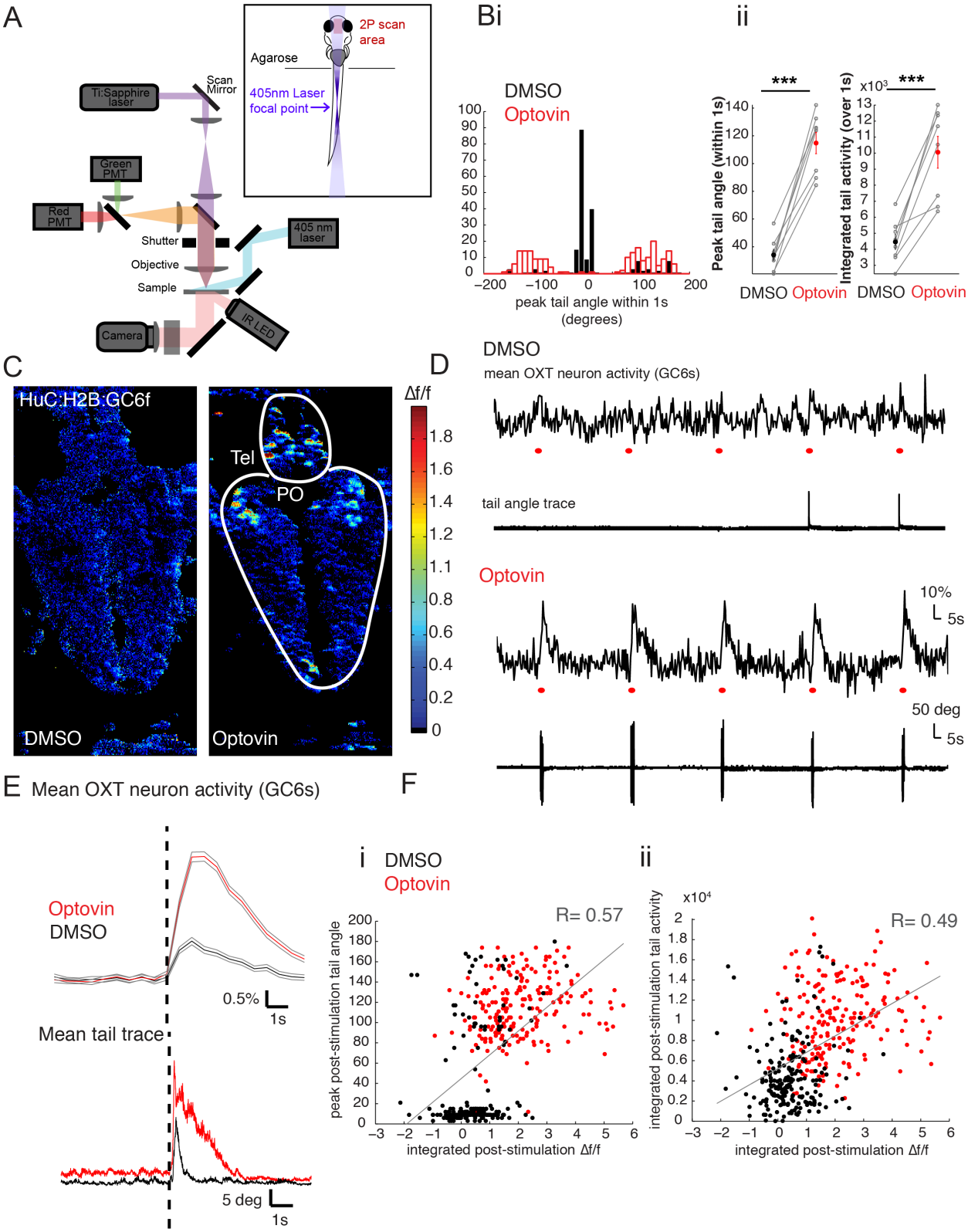

Figure 2.4.4: TRPA1 stimulation drives large-angle tail bends that correlate with OXT neuron activity – additional supporting data (A) TRPA1 stimulation and simultaneous imaging of OXT neurons using a confocal microscope setup. A 405nm laser (10% power) was used to stimulate the head of *Tg(oxt:Gal4;UAS:GCaMP5G)* fish, in either DMSO and Optovin. Behavior was not monitored during these experiments. Top image: *Tg(oxt:Gal4;UASAGCaMP5G)* expression from a single fish Bottom image: Hand-drawn ROIs delimiting individual OXT neurons from the same fish. Plots show calcium activity (Δf/f) of circled neurons in DMSO (top) or Optovin (bottom). A 100ms pulse of UV is administered at 30, 90 and 150s (grey lines). **(B)** OXT neurons, as labeled by *Tg(oxt:Gal4;UAS:GCaMP5G)* or *Tg(otp:Gal4;UAS:GCaMP5G)* respond more to UV stimulation in Optovin than in DMSO. The fraction of visible neurons that respond at least once to stimulus, mean peak Δf/f within 5 seconds post-stimulation, and integrated Δf/f within 5 seconds post-stimulation was significantly higher in Optovin. The same fish was used for DMSO and Optovin treatments. *Tg(oxt:Gal4;UAS:GCaMP5G):* Fraction responsive: ***p = 0.000322; Mean peak Δf/f: ***p = $3.099 \times 10^{-5;}$ Mean integrated ***p = 5.420×10^{-5} (n = 6 fish). *Tg(otp:Gal4;UASGCaMP5G):* Fraction responsive: ***p = 8.718×10^{-5}; Mean peak Δf/f: ***p = 2.014×10^{-5}; Mean integrated Δf/f: ***p=2.856×10^{-5} (n=7 fish) Paired Student's T-test.

Figure 2.4.4 (Continued): (C) More example traces of tethered swimming behavior in DMSO and Optovin, in *Tg(HuC:H2B:GC6f)* fish. (i) Multiple OXT neuron responses during Optovin stimulation correlate with multiple tail responses (ii) Example of a strong OXT neuron response during DMSO stimulation, which correlates with a large angle tail bend (iii) Example of spontaneous tail twitching during Optovin condition, that does not correlate with OXT neuron responses (iv) Examples of weak OXT neuron responses in DMSO condition (occasionally in absence of stimulation, see green box) that correlates with tail bends. Also note tail twitching in Optovin condition that does not correlate with OXT neuron activity. (v) Top: Average OXT neuron activity (5 fish, 24 stimulations per fish) in Optovin and DMSO, *for Tg(H2B:GCaMP6f)* fish. Bottom: Average tail deflection magnitude in Optovin and DMSO conditions. OXT neuron activity and average tail angles are larger in Optovin than in DMSO. Scale bar: 0.5% Δf/f (vertical) or 5 degrees (vertical), 1 sec (horizontal). (vi) and (vii) Mean OXT neuron activity (integrated activity over 5 second window after stimulation) correlates with (vi) peak and (vii) integrated tail angles (within a 1s window after stimulation). A longer time window was chosen for calcium fluorescence due to the slow rise/fall kinetics of GCaMP fluorescence. Red = Optovin, Black = DMSO. Correlation coefficient was calculated across both DMSO and Optovin conditions. Peak tail angle: $R = 0.4707$, $p = 1.239 \times 10^{-14}$; Integrated tail activity: $R = 0.448$, $p = 3.239 \times 10^{-13}$ (Pearson's correlation).

Figure 2.4.4 (Continued):

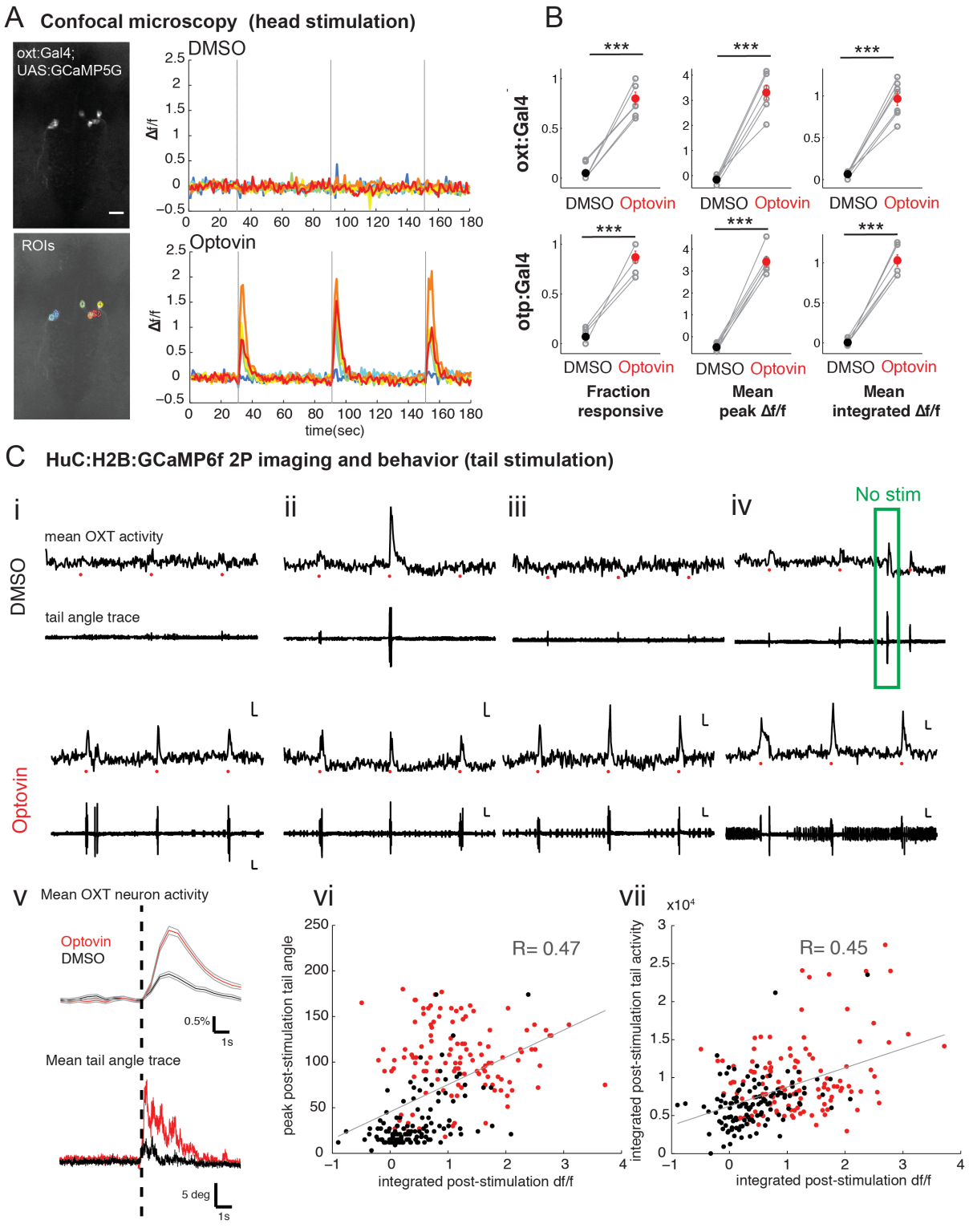

Optogenetic activation of OXT neurons drives large-angle tail bends

Since OXT neuron activity correlates with large angle tail bends, we hypothesized that it may drive such pain behavior in response to noxious stimuli. To investigate the functional role of OXT neurons in pain processing, we expressed channelrhodpsin (ChR2) in OXT neurons using our *Tg(oxt:Gal4)* line (Fig. 2.4.5Ai). Concentrating blue light specifically onto the preoptic area (Fig. 2.4.5Aii) of *Tg(oxt:Gal4;UAS:ChR2-YFP)* larvae evoked strong swimming behavior, but not sibling controls, demonstrating that the behavior was not visually-evoked (Fig. 2.4.5B-C). Interestingly, despite high light intensities (6mW/mm^2), long stimulation durations were required in order to achieve a high probability of response, on the order of seconds (Fig. 2.4.5C-D). Response frequencies and latencies were highly variable, and the mean latency of response was on the order of seconds (Fig. 2.4.5B-D, F). We also observed a similar enhancement in locomotion in free-swimming *Tg(oxt:Gal4; UAS:ChR2-YFP)* fish (Fig. 2.4.5F), and in *Tg(otpGal4;UASChR2-YFP)* fish (Fig. 2.4.6A-E), supporting a role for preoptic OXT neurons in driving locomotion.

More detailed analysis of the behavioral kinematics of ChR2-induced behavior revealed that stimulation of OXT neurons predominantly produced large-angle tail bends, that had much larger cumulative tail angles than escape behaviors induced by vibrational-acoustic stimuli (Fig. 2.4.5E, Fig. 2.4.6E). Even within the same fish, and for the same stimulation, tail bends in both directions could be observed (Fig. 2.4.5B). The laterality of tail bends in each fish did not correlate with the number of ChR2-expressing neurons on either side of the midline, suggesting that they were not simply being produced by asymmetrical ChR2 expression (Fig. 2.4.6F). These large-angle tail

bends were kinematically distinct from startle escape responses mediated by zebrafish hindbrain escape circuitry (i.e. Mauthner and Mauthner-homolog-mediated C-bends), suggesting that OXT neurons form an independent diencephalospinal network that drives large-angle turns (Fig. 2.4.5E, 2.4.7E). The high-angle, highly lateralized turning behavior was also apparent from swim trajectories when we stimulated OXT neurons in blind, freely-swimming fish (Fig. 2.4.5F). Thus, activation of OXT neurons can drive behavioral responses that are kinematically similar to those observed during TRPA1 activation.

Figure 2.4.5: Optogenetic activation of oxytocin neurons drives large-angle tail bends (A) (i) Maximum intensity projection of *Tg(oxt:Gal4;UAS:ChR2-YFP)* fish shows strong PO expression and projections to the hindbrain and spinal cord. (ii) Photo-conversion of *Tg(oxt:Gal4;UAS:Kaede)* fish delimits neurons that are exposed to light during optogenetic stimulation. Scale bar = 100μm. **(B)** Maximum intensity projection images showing behavior of a representative *Tg(oxt:Gal4;UAS:ChR2-YFP)* during different time periods after blue light onset. The first tail bend of this fish occurs between 0.5s-1s, and a mixture of tail bends is seen in both directions. **(C)** Rastor plot of responses of a single example fish 100ms and 5s stimulation, showing variability in response frequency and latencies. Each vertical black line represents a detected swim bout. Only the first 100ms stimulation produced a response (other depicted bouts were spontaneous). Stimulation period (100ms or 5s) is highlighted in blue **(D)** (i) Probability of response (making at least one bout within 6s post-stimulation) and (ii) normalized frequency of response (number of bouts per second) to blue light stimulus increases with stimulation duration in *Tg(oxt:Gal4;UASChR2-YFP)* fish and is significantly higher than for controls. Response probability: ***$p = 1.1185 \times 10^{-25}$; Response frequency: ***$p=5.9862 \times 10^{-21}$, n = 29/13, Two-way ANOVA. Data was pooled over multiple clutches. (iii) and (iv) Histogram of response latencies in head-embedded fish, for a (iii) 2s (1.37±0.08s, n = 36 responses from 10 fish) and (iv) 5s (1.80±0.13s, n = 51 responses from 10 fish) stimulation. A response is defined as the first bout within 6s of stimulation. Data is from a single clutch.

Figure 2.4.5 (Continued): (E) Optogenetic activation of OXT neurons drives large angle tail bends. (i) Example of tail angle traces elicited by *Tg(oxt:Gal4;UASChR2-YFP)* stimulation, as compared to a typical escape response elicited vibrational-acoustic (tap) stimulus. (ii) Histogram showing distribution of peak tail angle per bout for responses to a 5s stimulus from *Tg(oxt:Gal4;UASChR2-YFP)* fish (blue), overlaid with a histogram of tail angles from an independent set of fish experiencing a vibrational-acoustic tap stimulus (magenta). The mean tail angle is significantly larger for *Tg(oxt:Gal4;ASChR2-YFP)* stimulation (100.108±1.93 degrees, n=246 bouts from 10 fish) than for taps(68.963±3.0887, n = 75 bouts from 10 fish), ***p = 2.0610×10^{-9} (Wilcoxon rank sum test) **(F)** ChR2-driven free-swimming behavior in blind fish. The eyes of *Tg(oxt:Gal4;UAS:ChR2-YFP)* fish, or their non-expressor siblings, were removed at 6dpf. At 7dpf, fish were then stimulated for 5s with a blue LED illuminating the entire arena (2cm diameter) from below. (i) Example swim trajectories from 4 representative ChR2-positive fish and 4 controls. Red = pre-pulse swim trajectory, Blue = post-pulse swim trajectory. Eyeless fish do not move much spontaneously. Note the high rates of turning. (ii) ChR2-positive fish showed a significant increase in distance traveled during the light pulse (normalized to total distance traveled). Positive: 0.7163± 0.0370; Controls: 0.5280±0.0230; n = 14/6, *p = 0.015, Wilcoxon Rank Sum test. (iii) Histogram of mean latencies per fish for ChR2-positive (blue, 2.357± 0.412s) and control (gray, 3.204±0.785s) fish. Note that many control fish did not swim at all, hence there are fewer data points depicted.

Figure 2.4.5 (Continued):

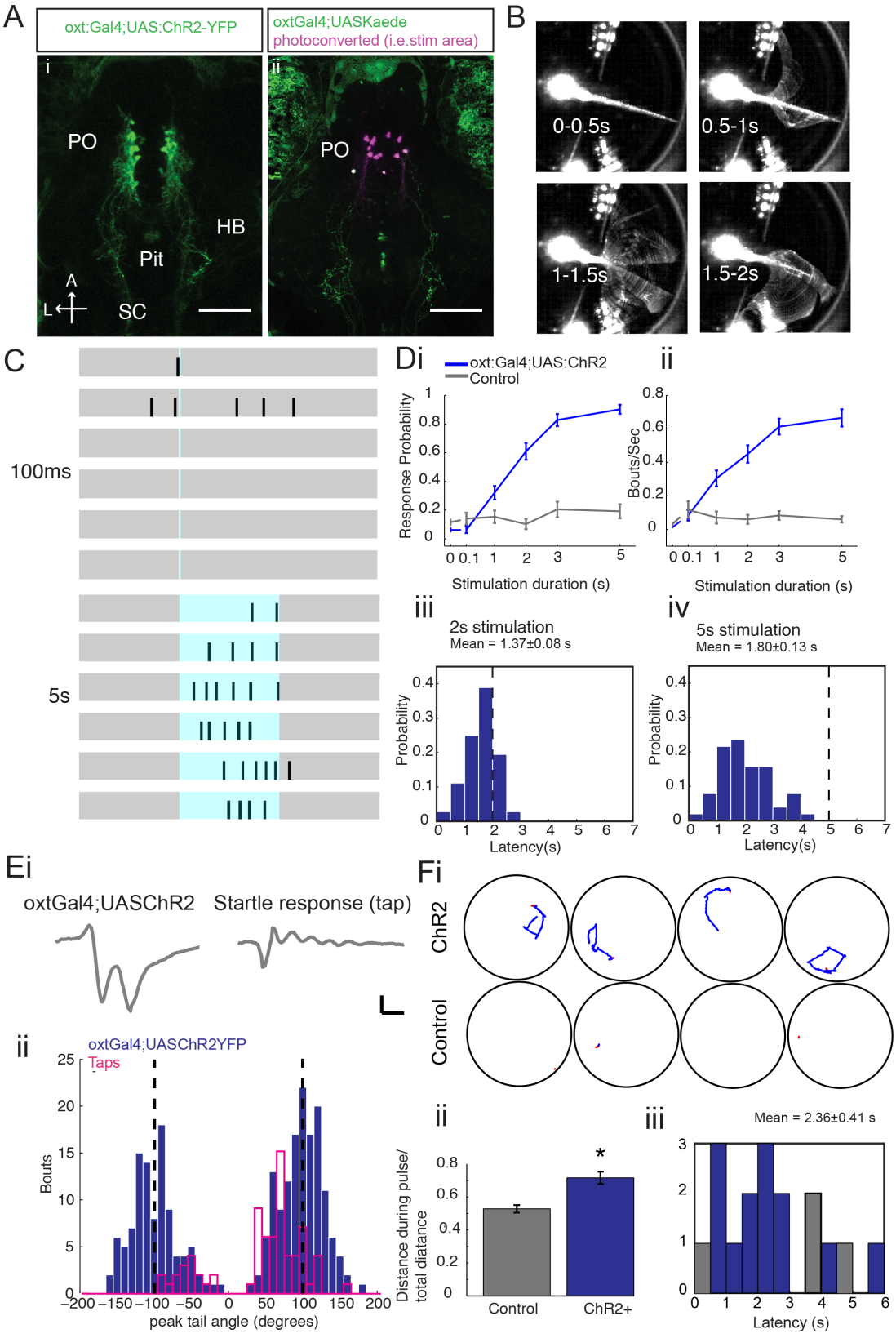

Figure 2.4.6: Further characterization of optogenetically-driven behavior

(A) (i) Photoconversion of *Tg(HuC:Kaede)* fish using our optogenetic stimulation setup, which depicts the illumination area used for tethered *Tg(oxt:Gal4;UAS:ChR2-YFP) and Tg(otp:Gal4;UAS:ChR2-YFP)* stimulation experiments. (ii) Photoconversion of *Tg(otpGal4;UASKaede)* fish showing the subset of otp-expressing neurons that are exposed to light during stimulation. (iii) Maximum projection image of *Tg(otp:Gal4;UASChR2:YFP)* line used in channelrhopsin experiments, which labels more neurons than the *Tg(oxt:Gal4).* Scale bar = 100μm. (B) Response probability (making at least one bout) and normalized response frequency (number of bouts per second) to blue light stimulus increases with stimulation duration in *Tg(otp:Gal4;UASChR2-YFP)* fish. The stronger responses for Tg(otp:Gal4) fish are likely due to a larger number of preoptic neurons labeled. Response probability: ***p = 2.8741×10^{-58}; Response frequency: ***p = 4.2884×10^{-51}; n = 12/21 with pooled controls, Two-way ANOVA. **(C)** Histogram showing response latencies during 5s stimulation of *Tg(otp:Gal4; UAS:ChR2-YFP)* fish (mean= 1.94±0.15s, n = 60 bouts from 10 fish, blue); overlaid with responses from stimulating a subset of trigeminal neurons in *Tg(isl2b:Gal4;UAS:ChR2-YFP)* fish (mean = 0.32±0.10s, n = 16 bouts from 3 fish, magenta). Stimulating trigeminal neurons produces predominantly short-latency responses, unlike for stimulating otp (or oxt)-expressing neurons. **(D)** Blind *Tg(otp:Gal4;UASChR2-YFP)* fish, homozygous for the *chk* mutation show similar responses to blue light as sighted siblings. Response probability (blind vs sighted): p = 0.6628 (N.S.); Response frequency (blind vs sighted): p = 0.3035 (N.S.); n =12 (blind)/18 (sighted), Two-way ANOVA.

Figure 2.4.6 (Continued): (E) Comparison of tail kinematics between optogenetic stimulation of different neuron populations, or a vibrational-acoustic tap stimulus (i) Diagram defines parameters that are used to compare bout kinematics across different stimuli. Example responses to a tap stimulus or a 5s long *Tg(oxt:Gal4;UASChR2-YFP)* optogenetic stimulation are shown. (ii) Bout kinematic parameters quantified across different stimuli. These include the integrated area under the entire bout (bout area), integrated area under the first tail bend (1^{st} bend area) and first and second tail bends (1^{st} + 2^{nd} bend area), bout duration, duration of the first tail bend (1^{st} bend duration), magnitude of the first tail bend, which can be used to define a turn versus a forward swim [170], and number of undulations. For each of these parameters, asterisks denote groups with kinematics that are significantly different from *Tg(oxt:Gal4;UASChR2-YFP).* Corrected $p<0.05$ (one-way ANOVA), Tukey-Kramer correction, n = 9/9/20/20/10. **(F)** The laterality of *Tg(oxt:Gal4; UAS:ChR2-YFP)* expression across midline does not correlate with the laterality of tail bends, suggesting that the large angle tail deflections are not a product of stochastic asymmetries in ChR2 expression. Tail laterality = number of neurons on left/total number of neurons; Neuron laterality = sum of tail angles towards the left/sum of all tail angles. A higher index depicts more tail bends or neurons to the left. While most animals make more/larger angle tail bends to the left (for reasons unclear), neuron expression is mostly symmetric across the midline and cannot explain the lateralized tail responses.

Figure 2.4.6 (Continued):

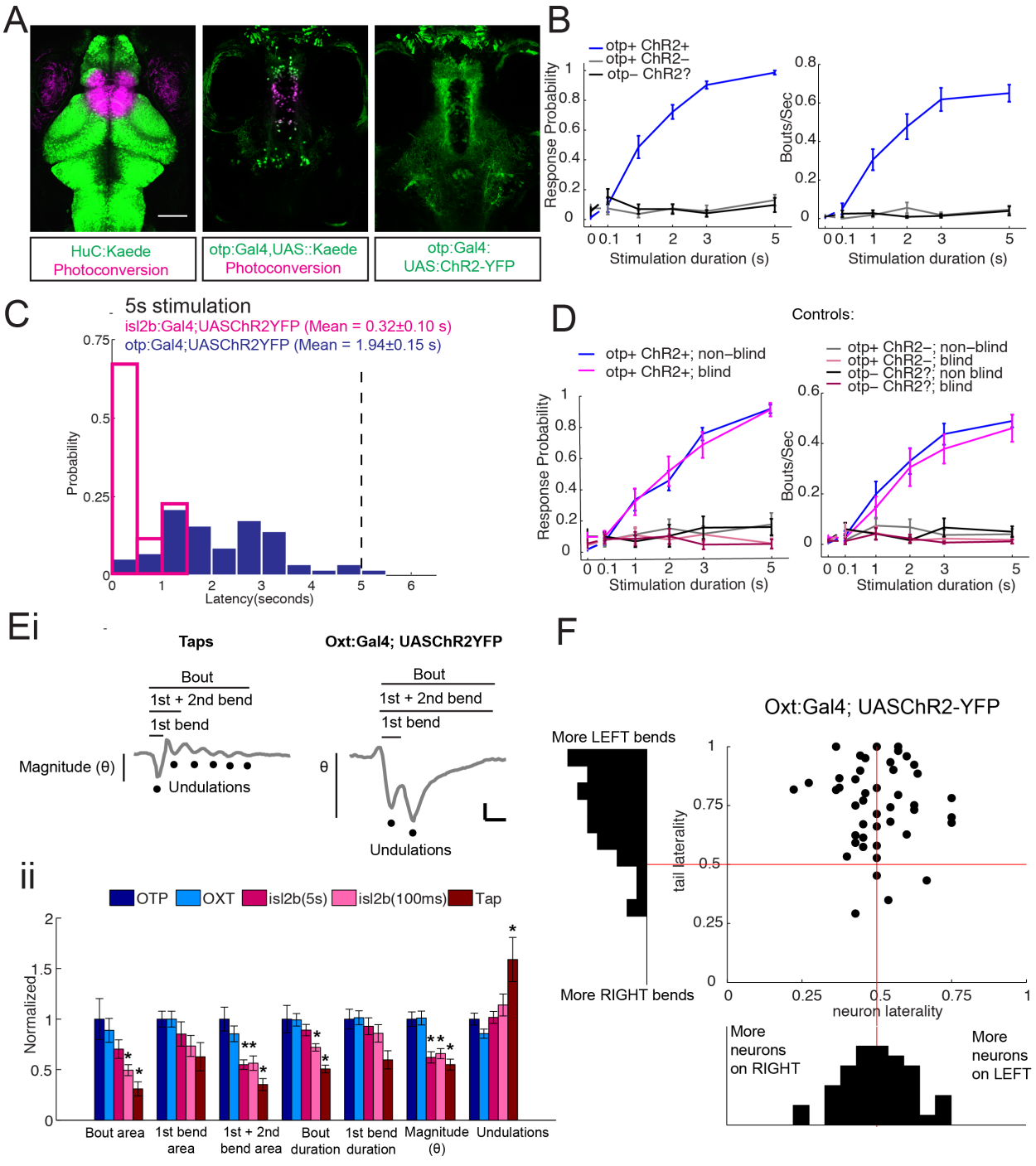

OXT neurons mediate their effects through both OXT and glutamate

Since preoptic OXT neurons project to the hindbrain and spinal cord of the zebrafish (Fig. 2.4.1D, Fig. 2.4.2F), they are well-poised to modulate hindbrain/spinal circuitry though the secretion of OXT. However, as commonly observed in neuromodulatory neurons, OXT neurons in the preoptic area also co-express glutamate (Fig. 2.4.7A). This raised the question of the specific role of the neuropeptide OXT in driving ChR2-induced behavior. We performed two complementary experiments to answer this question. First, we developed a reduced zebrafish preparation in which brains were transected at the midbrain/hindbrain boundary, and all tissue anterior to the hindbrain, including OXT neurons was removed. Fish in this preparation survived for hours in culture solution and produced bouts of small amplitude tail undulations, possibly due to reduced inhibition of hindbrain reticulospinal circuitry (Fig. 2.4.7B). Interestingly, the addition of OXT (5μM) to the bath led to a large burst of swimming activity about 5 minutes after, most of which were large-angle tail bends as quantified by tail angle distributions (Fig. 2.4.7C, 2.4.7D). Consistent with observations in neonate mouse spinal cords[203], OXT induced locomotion lasted for only around 5 minutes, before returning to a slightly enhanced baseline (Fig. 2.4.7B). This data suggests that OXT can act directly on hindbrain/spinal circuitry, even in a reduced preparation, to modulate forward swims into large-angle turns.

Figure 2.4.7: OXT neurons mediate their effects through both OXT and glutamate

(A) (i-iii) Z-projection images show *Tg(oxt:GFP)* neurons overlapping with glutamate-expressing neurons labeled by *Tg(VGlut2a:dsRed)* (iv) Higher magnification view. Scale bar = 20μm. **(B)** (i) Maximum projection images of a tethered fish in a reduced preparation from a 5 minute interval before addition of OXT, and 5 minutes after addition of OXT (final concentration of 5μM). (ii) Example of a cumulative tail angle trace from a reduced preparation before and after addition of OXT. **(C)** OXT promotes large angle tail bends. Distribution of peak tail angle per bout is for a 10-minute period either before (blue) and after (magenta) addition of OXT, for the same example fish shown in B). Peak tail angles are significantly higher after addition of OXT. Before: 16.573±0.166 degrees, n = 278 detected bouts. After: 42.494±1.308 degrees, n = 576 detected bouts. ***p = 2.2660×10^{-61} (Wilcoxon Rank Sum test). **(D)** Across 5 fish, mean integrated bout area and peak tail angles are higher in the 10 minutes after addition of OXT than in the 10 minutes prior. (Bout area: **p= 0.00620, Peak tail angles: **p = 0.00974, n=5 fish, paired Student's T-test) **(E)** (i) Diagram: schematic showing the zebrafish OXT gene. Exons 2 and 3, which include the sequence coding for the OXT peptide sequence (magenta), are deleted in the *oxt* mutants. Genetic sequence encoding the OXT peptide is shown in magenta. Amino acid sequences for the WT *oxt* gene, and the *oxt* mutant are also denoted. (ii) Antibody staining against OXT confirms the absence of the peptide in homozygous oxt mutants. Scale bar = 50 μm.

Figure 2.4.7 (Continued): (F) Response probability, frequency and the number of responses per stimulus are reduced in OXT CRISPR mutants. Data shown is aggregated over multiple clutches of fish, and examples of data from individual clutches are shown in Fig. 2.4.8. Difference in Response probability: ***p = 3.2159×10^{-6}; Number of bouts: ***p = 3.2992×10^{-7}; Normalized frequency: ***p = 2.6796×10^{-7}, n = 92(heterozygous)/51 (mutant) fish, two-way ANOVA. Latency for a 5s stimulation is significantly longer for mutants than for their heterozygous siblings. Uncorrected p = 2.584×10^{-4}, n = 422/212 bouts (Wilcoxon rank sum test).

Figure 2.4.7 (Continued):

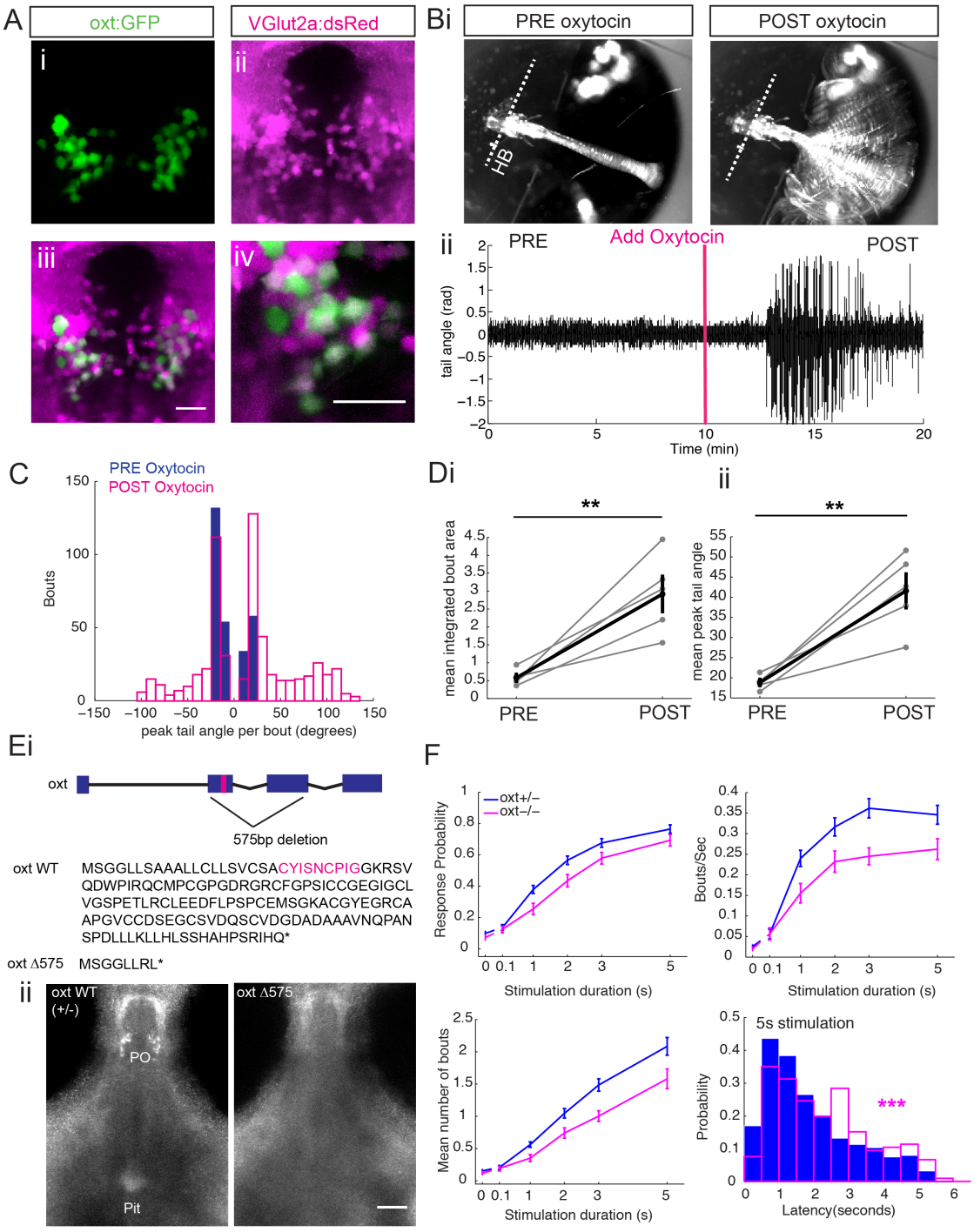

In addition to sufficiency, we decided to explore if OXT was necessary for ChR2-induced behavior. To do this we used the CRISPR/Cas9 system to generate an OXT null mutant line in zebrafish. We injected embryos with Cas9 protein and a set of short guide RNAs (Gagnon et al., 2014), and identified a 575bp deletion predicted to be a null allele. We confirmed that this was a null allele by immunostaining using an OXT antibody (Fig. 2.4.7E).

Interestingly, the absence of OXT significantly reduced the frequency of a ChR2-evoked response, but did not completely abolish ChR2-evoked swimming behavior, and response latencies were also significantly longer for 5s stimulations (Fig. 2.4.7F). This was despite the fact that the average number of ChR2-expressing neurons remained the same between mutant and wildtype fish (Fig. 2.4.8C-D). Taken together, our results suggest that although OXT may be sufficient to enhance locomotion in a reduced preparation, OXT neurons can still mediate behavior in the absence OXT, and thus other neurotransmitters are also important for mediating its effects on downstream hindbrain/spinal circuitry. Co-expression analysis has suggested that OXT neurons do not co-express other neuropeptides known to be present in the same region[227], thus glutamate is a likely candidate for supplying much of the locomotor drive provided by OXT neurons.

Figure 2.4.8: OXT neurons mediate their effects through both OXT and glutamate – additional supporting data (A) We found no significant difference in the number of ChR2-positive OXT neurons in a clutch of heterozygous and null mutants expressing *Tg(oxt:Gal4;UASChR2-YFP)* (p = 0.3495, n = 12/9, Wilcoxon rank sum test) **(B)** We found no significant differences in peak turn angles between heterozygous and null mutants. Mean peak turn angles: 75.540 ±2.156 degrees, vs 68.175±1.280, n =704/253, p = 0.5267 (N.S), Wilcoxon rank sum test. **(C)** Data from a single clutch (incrossed hets). Response probability: p=0.281 (WT vs het), *p=0.047 (WT vs null), p= 0.155 (het vs null); Number of bouts: p=0.593 (WT vs het), *p = 0.0135 (WT vs null), *p=0.0333 (het vs null); Response frequency: p=0.4856 (WT vs het), *p=0.0168 (WT vs null), p = 0.0577 (hets vs null), n = 13, 17, 6, Two-way ANOVA. **(D)** Data from a single clutch (hets vs null). Response probability: **p=0.0048; Number of bouts: ***p= 0.0003; Bout frequency: ***p = 0.0006, n = 21/16**,** Two-way ANOVA.

Figure 2.4.8 (Continued):

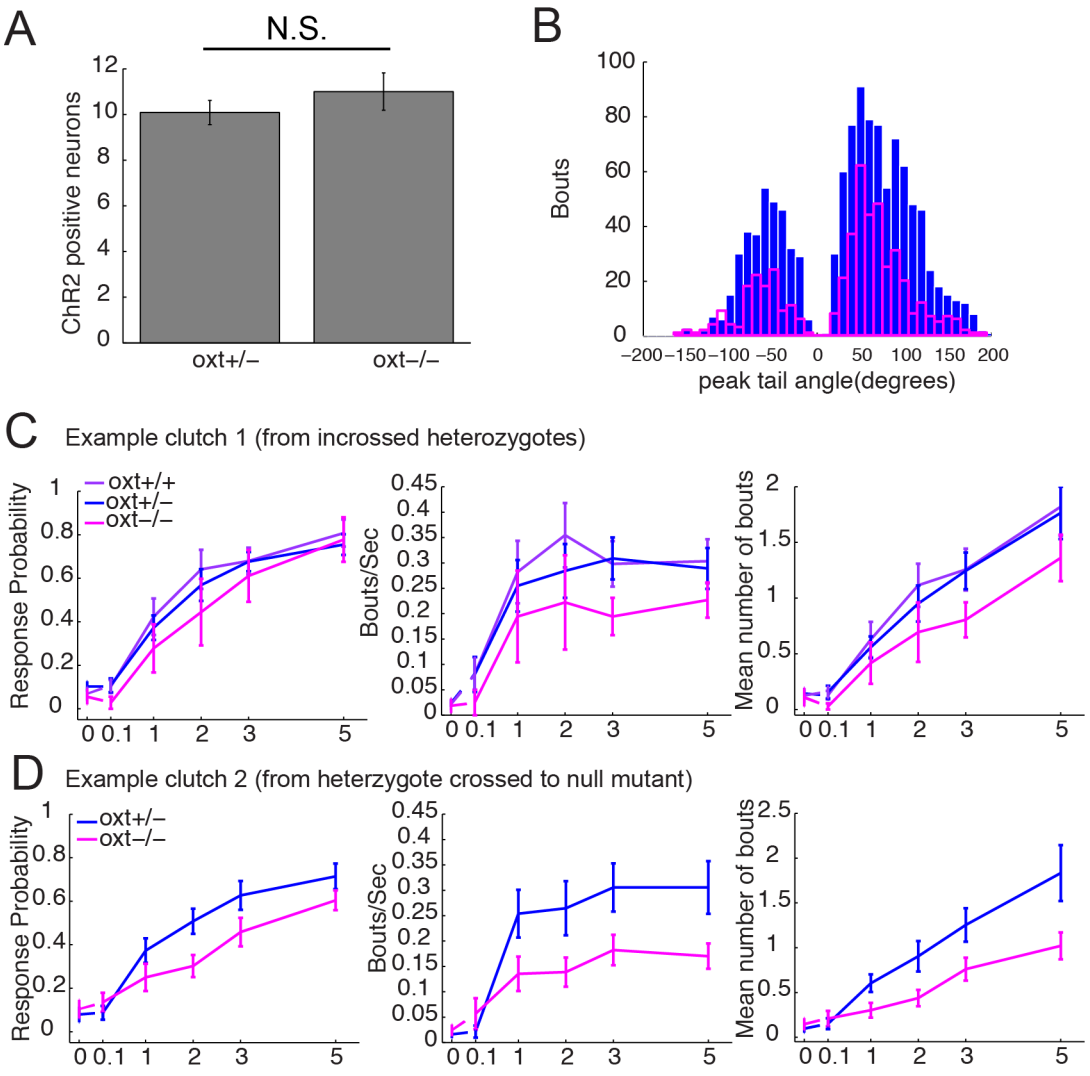

2.5 DISCUSSION:

A novel modulatory circuit for pain

Pain, a stimulus associated with tissue-damaging events, is a critical experience that enhances an animal's chances of recovery and survival. Specialized peripheral and central circuits have evolved both for rapid detection of painful stimuli and to the generation of appropriate behavioral responses. On the sensory end, the highly-conserved the transient receptor potential (TRP) family of ion channels are important transducers of noxious stimuli, with TRPV1 channels responding to noxious heat, and TRPA1 channels both to exogenous irritant chemicals (e.g. mustard oil) and endogenous products of tissue injury and inflammation[228,229]. In addition to detecting a painful stimulus, TRPA1 activation itself can also trigger inflammation, and has thus been characterized as a "gatekeeper" for pain[225,229]. However, the central circuits downstream of TRP channel activation that control of pain sensation and behavior are still being uncovered[39].

TRP channels emerged early in evolution, and have maintained a conserved function as crucial damage sensors in insects, zebrafish and mammals[178,230–233]. Thus, the larval zebrafish, a vertebrate genetic model with a transparent brain and highly conserved neuroanatomy and neurochemistry, can be used to understand how phylogenetically old brain circuits evolved to sense and react to physical pain and damage. Here, we used a novel and high-throughput brain-wide activity mapping approach to reveal central circuits in the larval zebrafish that respond specifically to pain, and have identified hypothalamic OXT neurons as a key node onto which multiple

painful stimuli converge. We demonstrate the first known link between peripheral TRPA1 receptor activation to central OXT circuitry, corroborating an emerging hypothesis that OXT may play a crucial role in pain processing, particularly pain induced by exogenous or endogenous chemicals[199]. Interestingly, we have also observed weaker activation of a subset of OXT neurons by heat, which acts through TRPV1 channels in zebrafish[179]. This could be explained in part by overlapping TRPA1 and TRPV1 expression on sensory neurons, since in both zebrafish and mammals, TRPA1-expressing neurons form a subset of TRPV1-expressing neurons[179,234]. Given the diverse nature of aversive stimuli that activate OXT neurons, it is likely that OXT neurons play a more general role in the encoding of aversive stimuli beyond TRPA1.

In our paper, we focus on the most salient behavioral outcome of OXT neuron activation – the enhancement of locomotor drive to the hindbrain/spinal cord, which results in large angle tail bends that may help to facilitate escape from a noxious environment. Pain response behaviors are known to be fast, reflexive and driven by hindbrain or even spinal circuits. In contrast, OXT neurons are embedded deep within the diencephalon, with dendritic processes extending into the telencephalon. We propose that OXT neuron activity may not be strictly necessary for a behavioral response, but may be integrated with fast hindbrain/spinal reflex circuits to serve as a parallel modulatory circuit for the control of pain avoidance behavior.

We speculate that OXT neurons may also serve other functions beyond that of driving an acute behavioral response to pain. For example, OXT release in response to painful stimuli could mediate anxiolytic, anti-inflammatory or anti-nociceptive effects, as

suggested by multiple studies in the literature[51,58,197–199]. It may furthermore be involved in modulating pain responses based on external context, internal state or past experience. Since both mammalian and zebrafish OXT neurons are widely-projecting and can release their peptides both into the circulation and to diverse regions of the brain[217–220], they are well-poised to coordinate system-wide responses to pain, much of which remain to be elucidated.

While we highlight descending OXT neurons as a modulatory circuit that can exert direct control on locomotor output, our results also suggest that it forms only one of many redundant layers of pain control. The preoptic area also contains non-overlapping peptidergic populations such as vasopressin and corticotropin receptor-expressing neurons, which may also play a role in pain and stress responses[53]. Beyond the preoptic area, our brain-wide analysis has identified other neuromodulatory populations that also respond to noxious or aversive stimuli such as the monoaminergic caudal hypothalamus and norepinephrinergic locus coeruleus. It will be interesting to elucidate the respective roles of these different loci in coordinating behavioral responses to pain, and to contrast their functions to those of OXT.

Diencephalic control of locomotion and the role of co-transmission

Our study is also the first to demonstrate direct control of locomotor output by central OXT neurons in a vertebrate animal. It complements a number of published zebrafish studies demonstrating control of specific locomotor behaviors by optogenetic activation of sensory[235–237], motor[238–241] or neuromodulatory[176,242] populations, highlighting the utility of the zebrafish model in studying transformations of sensory

information into action. While the optical activation of OXT neurons requires longer stimulation durations and produces behaviors at long latencies, we argue that these may simply be due to lower locomotor drive under baseline conditions. When coupled with a salient stimulus like pain, OXT neuron activation would likely sum up with other sources of drive at the level of the reticulospinal neurons, and thus be able to contribute to short-latency behaviors.

Many neuromodulatory neurons express more than one neurotransmitter type[5]. Zebrafish and mammalian OXT neurons co-express both OXT and glutamate, and thus are an interesting system for understanding how neurotransmitter co-release affects circuit output[64,243,244]. As proposed early on by Kupfermann (1979)[245], neuromodulators, unlike neurotransmitters, not simply excite or inhibit an electrically excitable cell, but are rather involved in altering the effects of other events occurring at the cell. In the case of OXT neuron control of locomotion, direct application of OXT itself to the hindbrain/spinal cord amplifies existing swim patterns and promotes the generation of large-angle tail bends. This phenotype is consistent with that observed in neonate rodent spinal cords, where OXT has also been shown to enhance motor neuron activity [203,246]. At the same time, it is clear that glutamate released from OXT neurons is also capable of driving swimming and large angle turns, since genetic knockout of OXT reduces but does not abolish effect of OXT neuron activation on swim kinematics. Though the attenuation of ChR2-induced swimming behavior in *oxt* mutants could arguably be caused by developmentally induced deficits or delay, we did not observe any differences in baseline locomotor behavior in *oxt* mutants as compared to their wildtype siblings.

While we have not directly proven that glutamate is the neurotransmitter responsible for a large portion of OXT neuron effects on locomotion, we argue that it is the most likely candidate, since co-expression studies of OXT neurons in larval zebrafish have found little evidence for co-expression of other neuropeptides in OXT neurons[227]. Thus, we propose that OXT may play a role in boosting glutamatergic transmission at hindbrain/spinal synapses, in order to increase the robustness and reliability of OXT neuron function. It will be interesting to explore how exactly OXT can change neural dynamics at the cellular or network level to induce such dramatic changes in behavior.

Another possible benefit of OXT and glutamate co-release is that OXT can be co-opted for other functions beyond that of driving locomotion. For example, given the vast literature suggesting that OXT has inflammatory or anti-nociceptive effects[51,58,199], OXT release in the hindbrain/spinal cord or bloodstream may help to suppress pain sensation or promote wound healing at the same time that a locomotor response to pain is triggered, allowing the animal to more effectively escape a noxious stimulus. Furthermore, OXT co-release may be important for exerting more sustained effects on hindbrain/spinal circuitry such as sensitization, plasticity and learning. These hypotheses remain to be explored. Overall, our data emphasizes the importance of co-transmission in neuromodulatory circuits.

A non-social function for OXT

In the past few years, the established concept of OXT function has been rapidly evolving. While initially renown for its pro-social functions, including pair bonding, trust, mating, and parental care[244,247–249], more recent studies suggest that it may also be

involved in aversive social learning[250], aggression, negative social emotion and other anti-social behaviors[251,252], leading to the hypothesis that it may serve to enhance the salience of both positive and negative social stimuli[253]. In addition, numerous studies have linked OXT and non-social, negative processes such as pain, anxiety, fear and stress[58,60], suggesting that its effects may span both social and non-social phenomena. Indeed, it has recently been proposed that OXT may play a more general role in controlling both the approach and avoidance of motivationally-relevant stimuli, and is not limited to social contexts[254].

OXT/vasopressin-like nonapeptides have been present for more than 600 million years[215,255], and thus studying its functions in simpler organisms may provide clues to its conserved functions. Consistent with its social and reproductive role in mammals, OXT/vasopressin-like peptides have been shown to facilitate reproductive-like behaviors such as copulation and egg-laying in invertebrates such as nematodes, annelids and molluscs[206–209]. Interestingly, in nematodes and molluscs, OXT/vasopressin-like peptides are also important for non-social functions, in particular avoidance learning[256,257].

Our study dissects OXT circuits in the larval zebrafish, an evolutionarily ancient and immature organism devoid of complex social and reproductive behaviors. Our results implicate OXT in an essential and primitive function – that of regulating behavioral responses to painful stimuli. At the same time, it is very likely that OXT is important for functions beyond that of pain processing in the zebrafish. In other fish species, OXT and AVP have been implicated in sociosexual behaviors such as parental

care, aggression and pair bonding[210–214]. Whether these social functions of OXT are already emerging in young zebrafish, or only manifest in adulthood, remain to be explored. In addition, it will be interesting to discover how OXT neurons integrate both social and non-social stimuli to produce relevant behavioral outputs, as well as how these social and non-social stimuli interact. For example, it is well known that social context can affect pain behaviors (a phenomenon known as social buffering), and OXT has been suggested as a likely candidate linking these two processes[145,199,258] . We propose the larval zebrafish as an ideal model for tackling such questions surrounding OXT system evolution and function. Taken together, our results have expanded the current understanding of OXT by identifying an evolutionarily conserved role for these hypothalamic neurons in the control of pain, a non-social and negatively motivated behavior.

2.6 FUTURE DIRECTIONS

How important is OXT signaling in directing pain responses? Loss- and gain-of-function experiments aimed at elucidating the influence of OXT neurons and OXT signaling on pain response behaviors are still ongoing. We also do not know how exactly OXT neurons mediate their effects on hindbrain/spinal circuits, or which classes of downstream neurons they exert their effects on. We also do not know how the action of symmetrically projecting neurons to the spinal cord can lead to asymmetrical and lateralized bending of tail muscles. Some of these questions can be answered by a more detailed anatomical deconstruction of OXT neuron projection patterns, as well as of OXT receptor expression to identify potential targets. On the network level, it may be possible to perform large scale imaging of hindbrain and spinal areas during ChR2 stimulation of OXT neurons, or application of OXT in a hindbrain preparation, to elucidate how firing dynamics of the entire network change under these perturbations. For truly satisfactory answers, electrophysiological recordings from OXT neuron targets would be necessary to identify, at the cellular level, the effects OXT exerts on cells that drive locomotion. A reduced preparation amenable to fictive and patch clamp recordings, such as those used by David McLean and colleagues[259] would be useful for this set of experiments.

2.7 EXPERIMENTAL PROCEDURES

Fish Husbandry

Larvae and adults were raised in facility water and maintained on a 14:10 hr light:dark cycle at 28°C. All protocols and procedures involving zebrafish were approved by the Harvard University/Faculty of Arts & Sciences Standing Committee on the Use of Animals in Research and Teaching (IACUC). All larvae were fed with an excess of paramecia daily starting from 5dpf.

Transgenic lines

The following transgenic lines were also used: *Tg(otpb.A:Gal4) [referred to as otp:Gal4 in text]* [223]; *Tg(isl2b:Gal4)* [260], *Tg(VGlut2a-dsRed)* [261], *Tg(UAS-E1b:Kaede)*[262]; *Tg(UAS:nsfb-Cherry)* [263], *Tg(UAS:mKillerRed)* [264], *Tg(UAS:GCaMP5G)* [166], *Tg(UAS:ChR2-YFP)*[171] and *Tg(HuC:H2B:GC6f)* (Chao-Tsung Yang and Misha Ahrens, manuscript under review). *Tg(HuC:GC6s)* was generated by Ahbinav Grama. Tg(oxtl:Gal4) was generated by Adam Douglass using the *Tg(oxtl:GFP)*[219] plasmid provided by Eric Glasgow.

Generation of oxt mutant using CRISPR/Cas9

Ten Cas9 target sites within the oxt open reading frame were chosen using CHOPCHOP[265], Cas9 protein was mixed with all ten sgRNAs and injected into embryos at the 1-cell stage[173]. Clutches from outcrosses of these injected fish were screened by PCR using flanking primers and Sanger sequencing to identify a 575bp deletion allele.

Lack of *oxt* expression was confirmed by immunostaining with an anti-oxt antibody (see Fig. 2.4.7). *Oxt* mutant fish were genotyped using a three primer PCR-based strategy.

MAP-MAPPING

6-7dpf larvae were divided evenly into control and treatment groups in 85-mm dishes and exposed to specific behavioral stimuli. The protocols for optomotor and aversive stimuli (taps, electric shock, heat) were previously published in Randlett et al (2015)[166]. For the food stimulus, filtered paramecia was added to a dish of larvae that had been food-deprived for 2hrs prior, with paramecia-water added to the control. For addictive drug stimuli, fish were exposed to 1uM cocaine-HCL (Sigma) or 3μM D-amphetamine hemisulfate (Sigma) or solvent (water) control. After 15 minutes (45 minutes for addictive drug stimuli), larvae were quickly funneled through a sieve, which was then quickly dropped into 4% paraformaldehyde, immunostained, imaged and analyzed as described below. For quantification of pERK/tERK ratios over individual OXT neurons, pERK experiments were performed on nacre *Tg(oxt:GFP)* fish. pERK/tERK intensities of individual GFP-positive neurons were measured using ImageJ and quantified using MATLAB. See also Randlett et al (2015)[166].

Antibody staining and in-situ hybridization

24 hours after fixation (4% paraformaldehyde (PFA) in PBS + 0.25% Triton (PBT)), fish were washed in PBT, incubated in 150mM Tris-HCl pH 9 for 15min at 70°C, washed in PBT, permeabilized in 0.05% Trypsin-EDTA for 45min on ice, washed in PBT, blocked in blocking solution (10% Goat Serum, 0.3% Triton in BSS) for at least an

hour and then incubated in primary and secondary antibodies for up to 3 days at 4°C diluted in blocking solution. In between primary and secondary antibodies, fish were washed in PBT and blocked for an hour. The following antibodies were used: rabbit anti-pERK antibody (Cell Signaling, #4370, 1:500 dilution), mouse anti-ERK (p44/42 MAPK (Erk1/2) (L34F12) (Cell Signaling, #4696, 1:500 dilution). For immunostaining against oxytocin, we used either a commercial rabbit anti-oxytocin (Used in Fig. 2.4.7, AHP71, AbD Serotec, 1:300); or a rabbit anti-oxytocin (Used in Fig. 2.4.2, VA10, 1:5000) [266] that originated from Dr. Harold Gainer's laboratory (NIH, Bethesda, USA). In our hands, the latter antibody was more sensitive to oxytocin. Secondary antibodies conjugated with alexa-fluorophores (Life Technologies) were diluted 1:500.

For in-situ hybridization, brains were fixed in 4% paraformaldehyde +5% sucrose, dissected out and then processed according to the protocol in Thisse and Thisse (2008)[267]. Following development with a BCIP reagent, brains were mounted in glycerol and imaged on an Olympus BX51WI compound fluorescence microscope.

Functional imaging and Photochemical TRPA1 activation

6-8dpf larvae of the mit1fa-/- (nacre) background were embedded in 1.5% agarose. For experiments that involved simultaneous behavioral tracking, the tails of the larvae were freed. OXT neurons were either labeled with *Tg(oxt:Gal4;UASGCaMP5G)/ Tg(otpb.A:Gal4;UASGCaMP5G)*[166] or with *Tg(oxt:Gal4;UAS:nsfbCherry)* fish also co-expressing *Tg(HuC:GCaMP6s)* or *Tg(HuC:H2BGCaMP6f).* Tap and shock experiments were performed without freeing the tail. We delivered taps by striking the imaging platform with a solenoid (Guardian Electric 28P-I-12D). Electric shocks were 100-ms

pulses of 40 V delivered by a Grass Stimulator over a 6-cm dish, with the anode and cathode attached to the dish using crocodile clips aligned to the head and tail of the fish, respectively. For TRPA1 photoactivation experiments, fish were stimulated first in DMSO, then in Optovin (10μM). For both conditions, fish were first incubated in the respective solutions for 30-45 minutes. We observed that a >30 minute incubation period in Optovin was essential for eliciting consistent behavioral responses in head-embedded fish, whereas in free-swimming fish, incubation is not required (except for habituation purposes). In both conditions, the tail of the fish was stimulated for 100ms with a 405nm laser that focused on the middle of the tail and aligned along the AP axis of the fish to avoid asymmetrical stimulation (1.15mW at sample), with a 1-minute inter-stimulus interval. Tail behavior was simultaneously monitored at 200fps, and tail coordinates extracted online using custom LabView software.

Calcium imaging analysis

All calcium imaging data was analyzed using custom MATLAB software. The general protocol for analysis, also used in subsequent chapters was 1) image registration (alignment) to correct for motion artifacts 2) Extraction of fluorescence signals from aligned images using manually-drawn ROIs 3) Analysis of Δf/f signals from individual traces and alignment to tail traces, if relevant to the experiment.

For fish expressing *Tg(UAS:GCaMP5G)* directly in *oxt/otp*-expressing neurons, ROIs were drawn over all visible oxytocin neurons (from a maximum projection image) and raw fluorescence traces were extracted as the summed pixels within the ROI. For fish co-expressing *Tg(oxt:Gal4;UASnsfbCherry)* with a pan-neuronal GCaMP line

(*Tg(HuC:GCaMP6s)* or *Tg(HuC:H2B:GCaMP6f)*), ROIs were drawn in the red channel, and fluorescence traces from the respective aligned green channel were extracted.

Δf/f values were then calculated using the average fluorescence over the time period before the first stimulus as the baseline over which all traces were normalized. For most experiments, the maximum and integrated Δf/f within a 5s window from the time of stimulation was computed on raw Δf/f traces. These parameters were then compared to tail kinematics from aligned tail traces. For some experiments, we also quantified the number of neurons that were "responsive" to stimulation, by applying zero-phase digital filtering to rectified Δf/f traces, and then setting a pre-calibrated threshold such that any change in fluorescence activity exceeding this threshold was counted as a response. If a neuron responded at least once out of three stimulations, it was classified as being responsive.

Head-embedded optogenetic experiments

6-8dpf larvae were embedded in 1.5% agarose and their tails freed. Stimulation was using a fluorescent microscope (Olympus BX51WI) through a 40x water-dipping objective. The light source for most experiments was a mercury Arc lamp (Ushio USH-102D halogen bulb). The stimulation area was 150um in diameter (A-stop open, F-stop closed), and can be visualized by Kaede photoconversion (Fig. 2.4.6). The light intensity at the sample was calibrated to be 6mW/mm^2. The light path was gated with a digital shutter (Uniblitz) and fish were stimulated for durations of 100ms, 1s, 2s, 3s and 5s every 30 seconds (6 presentations each, randomly shuffled for each fish). Tail coordinates were automatically extracted at ~400fps using custom LabView software,

and further analysis of tail kinematics performed using custom MATLAB software. OXT mutant clutches were tested using the same protocol and genotyped post-hoc.

Free-swimming optogenetic experiments

6dpf larvae were lightly anesthetized in 0.1% MS-222; the eyes were then manually removed using forceps. Fish were then returned to warmed Ringer's Solution and allowed to recover for 12 hours. Behavioral experiments were performed with the fish singly placed into a 1in cut-out agarose circular mold. This arena was placed onto a platform of filter paper, above a light array consisting of 15 far-red LEDs. A quad blue LED was mounted in the center of the far-red array. Fish were allowed to habituate for 10 minutes before beginning testing. A baseline recording was made for 5 sec at 435Hz, followed by 5 seconds of recording during blue light stimulation, and an additional 5 seconds of recording after the end of the stimulus. Each fish was recorded over 10 iterations with a 60s interval between trials. A custom LabView program was used to control the acquisition of the data as well as to control the blue LED trigger. Location of the fish was tracked in MATLAB, and measurements of velocity were extracted. Ratios of distance traveled during the pulse divided by the distance traveled during the pre-pulse and pulse were measured for each fish.

Reduced Preparation

7dpf larvae of the WIK background were embedded in 1.5% agarose and solution was then replaced with zebrafish ACSF. A thinned tungsten wire to remove eyes and brain above the mid-brain/hindbrain. Lack of responses to gentle touch stimuli

on the head (at locations anterior to the cut) was used to establish that all forebrain/midbrain tissue had been successfully removed. Regular spontaneous twitching of the tail (resembling forward swim bouts, but with much lower low amplitude) usually occurred after 5 minutes of tissue removal. We waited at least 5 minutes after commencement of movement before beginning to record baseline tail movements, and pipetted OXT to a final concentration of 5uM 10 minutes after the start of recording. Equidistant points along the tail of the fish were extracted online at 100fps using custom LabView software, and cumulative tail angles plotted/analyzed using custom MATLAB software.

Statistics

All error bars show mean ± SEM over fish. Significance was reported as follows: *p<0.05, **p<0.01, ***p<0.001. Significance was determined using the Paired Student's T-test for paired data and the Wilcoxon rank sum test for independent samples. The two-sample Kolmogorov–Smirnov was used for comparing distributions of pERK/tERK ratios in the presence or absence of noxious stimuli. The Wilcoxon signed rank test was used in Fig. 2.4.1C for comparing the distribution of normalized OXT ROI signals across different behavioral stimuli to the null hypothesis of median 1. One-way or two-way ANOVA were used when comparing fish using multiple parameters or multiple stimulation conditions.

Chapter 3:

Social regulation of appetite by the neuropeptide oxytocin

3.1 INTELLECTUAL CONTRIBUTIONS

The following chapter will be written into a manuscript entitled “Social state-dependent regulation of appetite by the neuropeptide oxytocin” that has not yet been submitted for review. Order of authorship has not yet been finalized. Contributions are as follows:

I conceived of the project with Dr. Erin Song (ES) and Dr. Samuel Kunes (SK). ES and I designed all experiments under supervision from SK. Dr. Florian Engert (FE) provided some input. ES and her undergraduate thesis student Sandy Wong (SW) performed most experiments and analyzed some data. I helped with experiments involving mutant/transgenic lines. I performed imaging for MAP-mapping experiments, and analyzed MAP-mapping data as well as data from pERK experiments on dissected brains. Dr. James Gagnon (JG) and I generated the oxytocin CRISPR mutant (also used in Chapter 2). Dr. Adam D. Douglass (ADD) and I generated the *Tg(oxt:Gal4)* line (also used in Chapter 2). Koichi Kawakami generated and kindly provided the *Tg(UAS:Botox:GFP)* transgenic line. I wrote this chapter and plotted all figures.

3.2. SUMMARY

Neuromodulators often exert widespread effects on brain circuits and behavior, making them a challenge to understand. The neuropeptide oxytocin (OXT) is no exception, having been implicated in numerous functions such as social behavior, pain, and appetite, among many others. Loss of OXT neurons, for example Prader-Willi syndrome, is characterized by diverse symptoms such as severe overeating, social deficits and a high pain tolerance. We previously showed that OXT neurons are activated by noxious stimuli and promote pain avoidance behaviors. Here, we further leverage the accessible neural circuitry and genetics of the larval zebrafish to explore the evolutionary logic underlying OXT's broad effects on social and non-social behaviors. We found that the brain activity and behavior of one-week old larval zebrafish are robustly modulated by social context, contradicting the widely accepted notion that zebrafish larvae are inherently non-social. Interestingly, we discovered that OXT neurons increase their activity during social isolation, which correlates with a profound reduction in appetite, and manipulations of OXT signaling can reverse this effect. Our results not only recapitulate oxytocin-related phenotypes present in mammals, but also provide insight into how OXT neurons can represent social context to modulate downstream behaviors in a state-dependent manner.

3.3. INTRODUCTION

Neuromodulators not only mediate responses to acute stimuli, but also represent external context and internal state to shape brain activity patterns and behavior. Their ability to encode information and modulate behaviors across multiple timescales and across different contexts makes them an indispensable component of brain function, but at the same time complex to understand.

OXT, with its ability to act both as a neuromodulator and circulating hormone, is a prime example of how a simple peptide that originated more than 600 million years ago has accrued numerous and diverse functions across evolution[255]. It has been implicated in a wide spectrum of behaviors ranging from reproduction, pair bonding, parental care and social support, to stress, pain, aversive learning and appetite suppression[58,61,247–249,268]. Its proposed roles often appear to contradict each other – for example, it has been shown to both facilitate and reduce pro-social behavior, enhance or diminish stress and regulate both positive and negative emotions[253,254].

Diseases affecting OXT signaling are also fascinating as they affect diverse aspects of social and non-social behavior. Prader Willi syndrome, characterized by a loss of OXT neurons, manifests in poor social behaviors, extreme hyperphagia, and reduced pain sensitivity[269]. On the other hand, patients with William's syndrome, which may be associated with high OXT levels[270–272], show high sociability, high anxiety in non-social contexts, but also a diminished appetite, which may partially be caused by feeding difficulties[273].

Here, we sought to explore the breadth of OXT function in a simple vertebrate model, the larval zebrafish, in an attempt to understand how an evolutionarily conserved circuit can integrates multiple stimuli to regulate diverse downstream behaviors. The anatomical similarities of zebrafish OXT circuitry to those of mammals is striking – zebrafish OXT neurons predominantly reside in the neurosecretory preoptic area, which has been shown to be homologous to the paraventricular nucleus of the hypothalamus in mammals[216]. Magnocellular OXT neurons project to the pituitary gland, where OXT is released into to the circulation, and parvocellular cells project also to other parts of the brain, including the hindbrain, spinal cord and hypothalamic areas. Thus, they are well poised to control multiple behaviors on multiple timescales.

This chapter builds on our previous work demonstrating activation of a large majority OXT neurons in response to noxious sensory stimuli. We show that a majority of OXT neurons are also activated by short-term social isolation, albeit to a weaker extent. Isolation also suppresses food intake, and we demonstrate that this is mediated by enhanced OXT signaling in the isolated state. Importantly, the effect of OXT on appetite was social state-dependent, suggesting that OXT circuitry could have evolved to suppress appetite in specific social contexts. Taken together, our results highlight a crucial role of OXT at the intersection of both social and non-social behaviors.

3.4. RESULTS

Social isolation increases OXT neuron activity

Larval zebrafish are not known to be social animals[188]. However, this does not mean that they are oblivious to their social context. We decided to a use whole brain activity mapping technique (MAP-Mapping)[166] to compare the neural activity of briefly (2hr) isolated larvae to those that remained with conspecifics, hypothesizing that any differences in brain activity caused by social context would reveal modulation by social state not immediately apparent from behavior (Fig. 3.4.1A).

Interestingly, despite the higher levels of sensory stimulation caused by the presence of other fish, isolated fish consistently had on average higher total brain activity than isolated fish (Fig. 3.4.1B). Isolated fish showed very specific enhancement of brain activity, restricted mostly to the telencephalon and preoptic area (homolog of the hypothalamic PVN)[216] (Fig. 3.4.1B). Given the abundance of OXT neurons in the preoptic area, we measured average pERK signals within the preoptic OXT neuron region of interest (Diencephalon - OXT Cluster 1 in Preoptic Area, as annotated in the Z-brain atlas). We found that pERK signals in the OXT region was higher in isolated than non-isolated fish, and the difference increased as group size became larger (Fig. 3.4.1C).

Since the preoptic area contains many intermingled cell types, we measured the pERK activity of individual *Tg(oxt:GFP)*-positive neurons. Similarly, we found that OXT neuron activity was higher in isolated fish, as demonstrated by a right-shifted probability

distribution (Fig. 3.4.1D-E). We had previously shown that OXT neuron activity was enhanced by noxious stimuli such as mustard oil, electric shock and heat. Not surprisingly, the increase in OXT neuron activity was smaller in an isolated fish than in fish exposed to mustard oil, confirming that social isolation was not activating it as strongly as an acutely painful stimulus (Fig. 3.4.1D). Thus, the brain activity of larval zebrafish is modulated by social context, and OXT neurons form part of the network activated by social isolation.

Figure 3.4.1: Social isolation increases oxytocin neuron activity (A) Schematic of experimental paradigm for MAP-mapping experiments. Larvae were raised in groups of ~40 from spawning, which is how they are normally raised in a lab setting. They were fed excess paramecia from 5dpf onwards. At 7-8dpf, they were split into smaller (35mm) dishes, some of which contained only one larva (isolated) and others that contained groups of larvae (3 or 5, depending on the experiment). To prevent stress from overcrowding, a larger (55mm) dish was used for a group of 10. For MAP-mapping experiments, paramecia were provided in excess, to mimic pre-experiment conditions. After 2hrs, the larvae were fixed, stained with pERK and tERK and imaged for MAP-mapping experiments. **(B)** Activity map shows significant activation (green) of preoptic area and telencephalon in respond to short-term social isolation (Isolated vs group of 10). Scale bar = 100μm. PO = preoptic area, PT = posterior tuberculum, Tel = Telencephalon. . A = anterior, L = Left, V = Ventral **(C)** (i) Projection image of ventral planes of the same MAP-map (isolated vs group of 10) registered to the Z-brain atlas. PO is strongly activated (ii) *Tg(oxt:GFP)* transgenic line registered to Z-brain atlas (iii) Z-brain outline of OXT neurons in the PO area, used for ROI-specific analysis of PO OXT neuron activation in (iv). Scale bar = 100μm (iv) Comparison of PO OXT neuron activation in isolated fish normalized to controls of increasing group size. Isolated relative to group of 3 (Fold change =1.07±0.0303, p = 0.053, n= 49), isolated relative to group of 5 (Fold change =1.124±0.0279, **p =0.0016, n=17), isolated relative to group of 10 (Fold change=1.21 fold ± 0.0754, *p = 0.0171, n = 13). Wilcoxon sign rank test against median of 1.

Figure 3.4.1 (Continued): (D) Individual *Tg(oxt:GFP)*-positive neurons are activated by social isolation. Probability distribution (kernel density estimate) of pERK/tERK ratios of preoptic OXT neurons shows a significant shift in pERK/tERK ratio for isolated fish as compared to non-isolated fish of different group sizes. Distribution for mustard oil (25μm) is shown for comparison. (i) Mustard oil vs control (***p = 1.0398×10^{-85}, n = 385/464 neurons) (ii) Isolated fish vs group of 10 (***p = 3.3559×10^{-21}, n =399 isolated/296 control) (iii) Isolated fish vs group of 3 (***p = 6.0299×10^{-15}, n = 513 isolated/732 control), Two-sample Kolmogorov-Smirnov test. The mean pERK/tERK ratio of all neurons per fish was also significantly higher in isolated fish vs controls. (Mustard oil: ***p = 3.658×10^{-5}, n = 12/12 fish, Isolated vs group of 10: ***p = 3.1080×10^{-4}, n = 7/8 fish; Isolated vs group of 3: *p = 0.0116, n = 9/12 fish, Wilcoxon Rank Sum test) **(E)** (i) High resolution representative images of pERK staining in dissected brains of isolated and non-isolated (group of 3) fish. OXT neurons in the preoptic area, as well as the posterior cluster of OXT neurons show higher pERK fluorescence in isolated fish vs non-isolated fish. OXT neurons are outlined based on *Tg(oxt:GFP)* expression in a different channel (not shown). Other neurons in the posterior tuberculum (PT) are also activated by isolation. (ii) Higher magnification view of preoptic pERK staining shown in (i) Scale bar = 20μm. (iii and iv) Probability distribution (kernel density estimate) of OXT neuron activity in isolated vs non-isolated fish from the same set of dissected brain pERK experiments.

Figure 3.4.1 (Continued): (iii) Higher pERK fluorescence was observed in preoptic OXT neurons (***p = 7.29×10^{-8}, n = 224 control/660 isolated, Two-sample Kolmogorov-Smirnov test) and the (iv) posterior cluster (***p = 5.31×10^{-5}, n=96 control/115 isolated, Two-sample Kolmogorov-Smirnov test). These dissected were not co-stained for tERK but staining conditions were kept as similar as possible. The mean pERK fluorescence per fish was also significantly higher in isolated fish vs controls (Preoptic: *p = 0.0317; Posterior: *p= 0.0159, n = 5 single/4 isolated, Wilcoxon Rank Sum test).

Figure 3.4.1 (Continued):

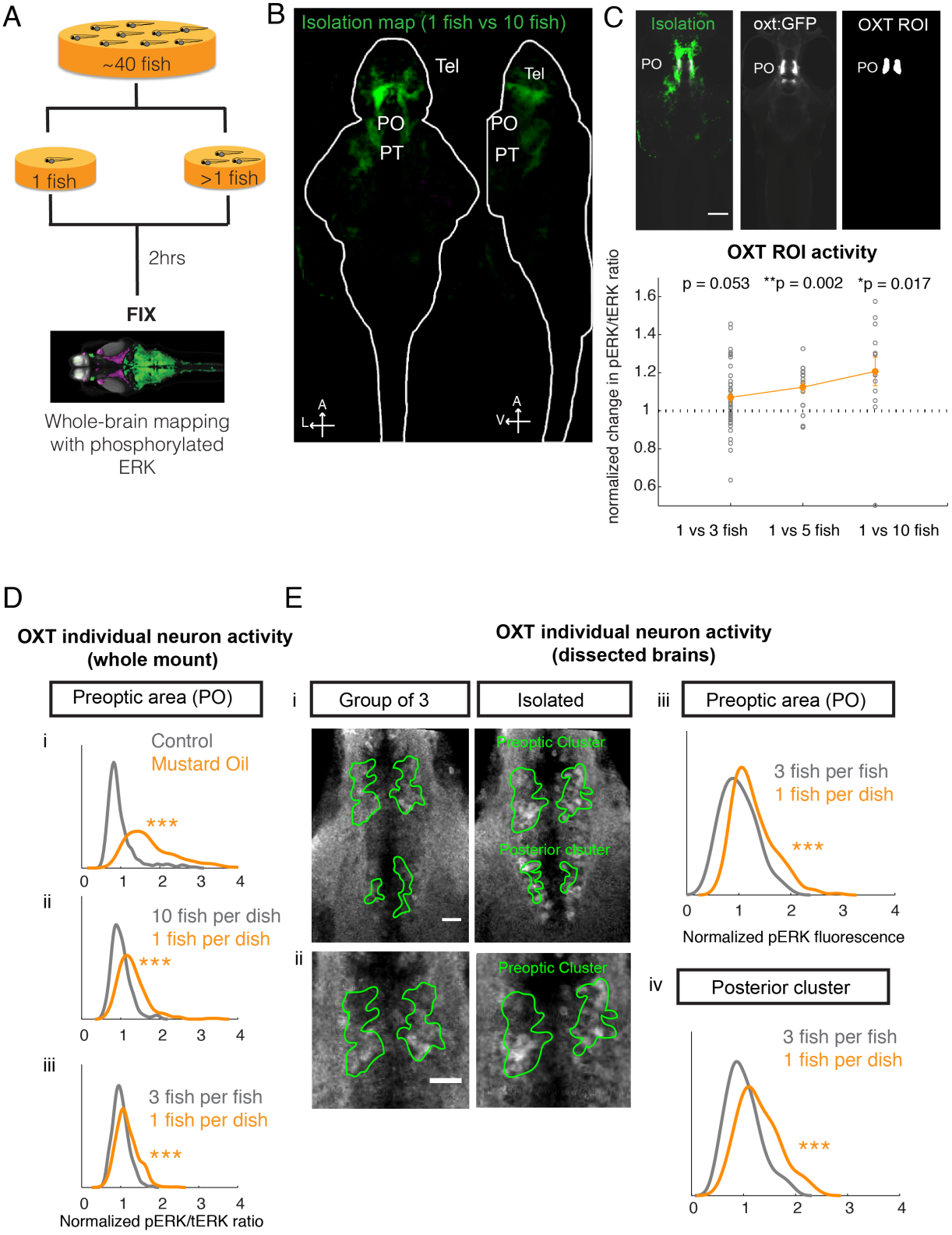

Social isolation suppresses appetite in larval zebrafish

We next asked if behavior may also differ in isolated versus non-isolated fish. We reasoned that if oxytocin activation during isolation were an aversive or stressful state similar (though to a smaller degree) to the experience of noxious stimuli, it would suppress appetitive behaviors such as feeding. To that end, we fed a large excess of fluorescent dye-labeled paramecia, a natural prey, to isolated and non-isolated fish, and compared food intake between these two groups (protocol adapted from Shimada et al, 2012)[115] (Fig. 3.4.2A). Interestingly, we found that isolated fish consumed less food per capita than non-isolated fish (Fig. 3.4.2B). This is despite the fact that the same amount/density of food was available for both isolated fish and fish in a group. Food intake increased with group size in a dose-dependent manner (Fig. 3.4.2B). Thus social isolation suppresses food intake, or conversely, the presence of conspecifics enhances food intake.

What social sensory cues might rescue the suppressive effect of isolation on food intake? We first allowed isolated larvae visual access to conspecifics through a plastic barrier, and found that this could not increase their food intake (Fig. 3.4.2C). Next, we conditioned fish water with age-matched larvae (not necessarily kin) for 2hrs, and then added the conditioned water to isolated fish prior to feeding. Interestingly, the addition of conditioned fish water was sufficient to rescue the effects of isolation on feeding (Fig. 3.4.2C). These results suggest that olfactory pheromone(s) might be sufficient for the enhancement of food intake by conspecifics.

What is the nature of this olfactory cue(s)? Since many pheromones are excreted as waste, we conditioned fish water with fish that had either been fed continuously, or unfed (these fish still retain sustenance from their yolk sac). Interestingly, only conditioned water from fish that had been previously and recently fed was able to enhance food intake in isolated fish (Fig. 3.4.2C). Thus, we postulate that the social cue is a digested food product excreted in either urine or feces, although its exact nature remains to be explored.

Figure 3.4.2: Social isolation suppresses appetite in larval zebrafish (A) Schematic of experimental paradigm for food intake. At 7-8dpf, larvae were split into smaller (35mm) dishes, some of which contained only one larva (isolated) and others that contained groups of larvae (usually 3). After 2 hours, and equal amount of exccess labeled paramecia was added to each dish, regardless of number of fish. After 30 minutes of feeding, the larvae were fixed and their gut fluorescence imaged and quantified. **(B)** (i) Example of food intake data from a single experiment. Isolated fish eat less per capita than fish in groups of 3. **p = 0.0058, n = 21 (group) /17 (isolated). (ii) Food intake increases with group size. Data is normalized to group of 3. Asterisks represented corrected p-value < 0.05 (one-way ANOVA). n = 36/7/52/29. (iii) Olfactory but not visual cues can enhance food intake during social isolation. (Isolated control vs group control: ***p = 1.1577×10^{-4}; isolated control vs isolated with odor (from fed fish): *p = 0.0435; n=76/74/41/75/10/17/11, Wilcoxon rank sum test.

Figure 3.4.2 (Continued):

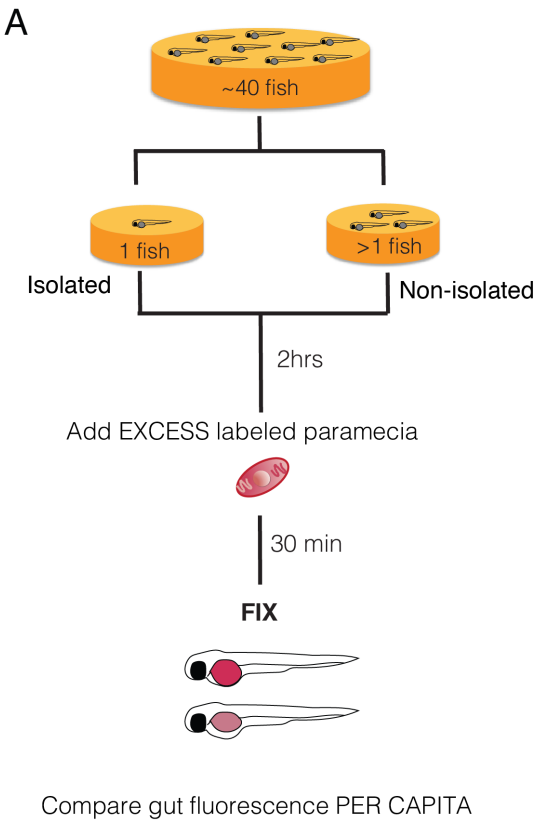

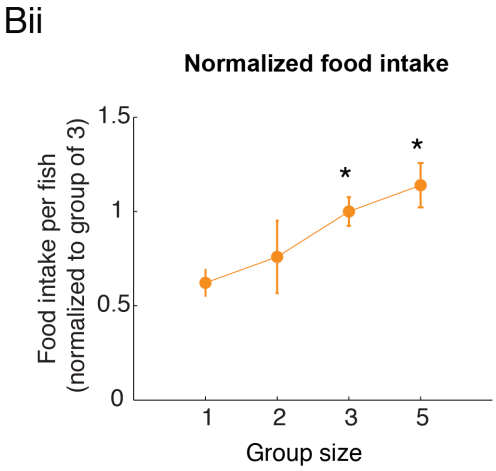

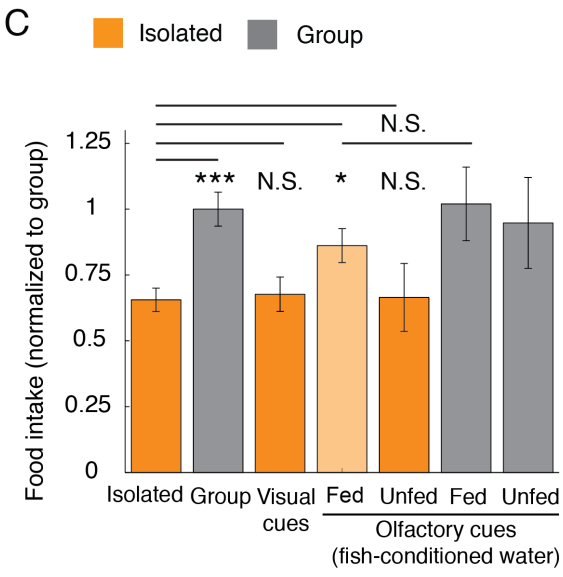

Oxytocin neurons mediate the social regulation of appetite

Given that isolation enhances OXT neuron activity and suppresses food intake, we hypothesized that OXT neuron signaling would mediate this regulation of food intake by social context. This would furthermore be consistent with the known appetite-suppressing effects of OXT neurons, and may form part of a coordinated response to stress.

To determine the effect of OXT neuron signaling in this process, we used a chemical-genetic method to specifically ablate OXT neurons, by expressing bacterial nitroreductase *in Tg(oxt:Gal4)* neurons, and exposing these fish (or sibling controls) to Metronidazole two days before the experiment (Fig. 3.4.3A). We found that, unlike in controls, ablation of OXT neurons enhanced food intake in isolation, while leaving food intake of non-isolated fish unchanged (Fig. 3.4.3B). Similarly, constitutively silencing OXT neurons by expressing the botulinum toxin light chain *Tg(UAS:Botox:GFP)* in the *Tg(oxt:Gal4)* transgenic abolished food intake differences between isolated and non-isolated fish (Fig. 3.4.3C). Thus, OXT neuron activity may be particularly important for the modulation of food intake by social isolation.

OXT neurons also co-express glutamate, thus we asked if it was OXT, glutamate, or both molecules that mediated its appetite-suppressing effects. We first acutely treated larvae with OXT agonists and antagonists. We found that OXT agonists strongly suppressed food intake of fish in a group, but did not reduce food intake in isolated fish, suggesting that enhanced OXT signaling was key to the reduced appetite of larval zebrafish during social isolation (Fig. 3.4.3D). In contrast, OXT antagonists

strongly increased food intake in isolated fish, but not in a group (Fig. 3.4.3D). Thus, the neuropeptide OXT mediates social state-dependent regulation of appetite.

We next compared food intake between OXT null mutants and their heterozygous wildtype siblings, expecting a similar enhancement of food intake during isolation. As predicted, null mutants did not modulate their food intake based on social context. However, to our surprise, OXT null mutants had much lower low food intake in a group, matching instead the food intake during isolation (Fig. 3.4.3E).

There are a number of possible explanations for this phenomenon: first, OXT null mutants experience a much more severe loss in OXT than caused by ablation/silencing of OXT neurons, and second, this is a complete loss of OXT (but not glutamate) over the long-term. Since *Oxt* mutant mice show a failure in social recognition[274], *oxt* zebrafish mutants may likewise have deficits in detecting or processing social information, and thus the presence of conspecifics may be unable to enhance (or disinhibit) appetite. We have also considered the possibility that null mutants are unable to compete with heterozygous siblings for food in a group, although equally efficient at hunting when alone. However, we argue that this is unlikely given the excess of paramecia provided. More experiments will be needed to tease out the mechanisms behind the interesting behaviors of the OXT mutant, although the lack of regulation of food intake by social context in these mutants is still consistent with the idea that OXT is required for this socially modulated behavior.

Figure 3.4.3: Oxytocin mediate the social regulation of appetite (A) Images show oxytocin neurons labeled by *Tg(oxt:Gal4;UASnsfbCherry)* with or without treatment with 2.5mM MTZ (24 hrs). MTZ treatment successfully ablates OXT neurons. Scale bar = 50µm. **(B)** Cell-specific chemical ablation of OXT neurons specifically rescues effect of social isolation on appetite. Single control vs group control: *** $p = 1.931x10^{-5}$; Single ablated vs group ablated: p= 0.533, n = 65/59/57/56, Wilcoxon rank sum test. Data is from multiple sets of experiments normalized to food intake in a group of 3 fish. (**C)** Cell-specific genetic silencing of OXT neurons *using Tg(UAS:Botox-GFP)* specifically rescues effects of social isolation on appetite. Single control vs group control: *p = 0.0429, single Botox vs group Botox: p = 0.503, n = 30/39/23/22, Wilcoxon rank sum test. Data is from multiple sets of experiments normalized to food intake in a group of 3 fish. **(D)** OXT antagonists enhance appetite in isolated fish. OXT agonists suppress appetite in non-isolated fish. Asterisks show corrected $p < 0.05$, One –way ANOVA, Tukey Kramer correction, n =40/50/49/34/22/21. **(E)** Comparison of food intake of *oxt* null mutants (*oxt*-/-) and their heterozygous wild-type siblings (*oxt*+/-) in isolated and non-isolated contexts. n = 60/59/58/54. Heterozygous isolated vs group: **p = 0.0011, Null mutants isolated vs group: p = 0.293, Heterozygous group vs null mutant group: ** p= 0.0012.

Figure 3.4.3 (Continued):

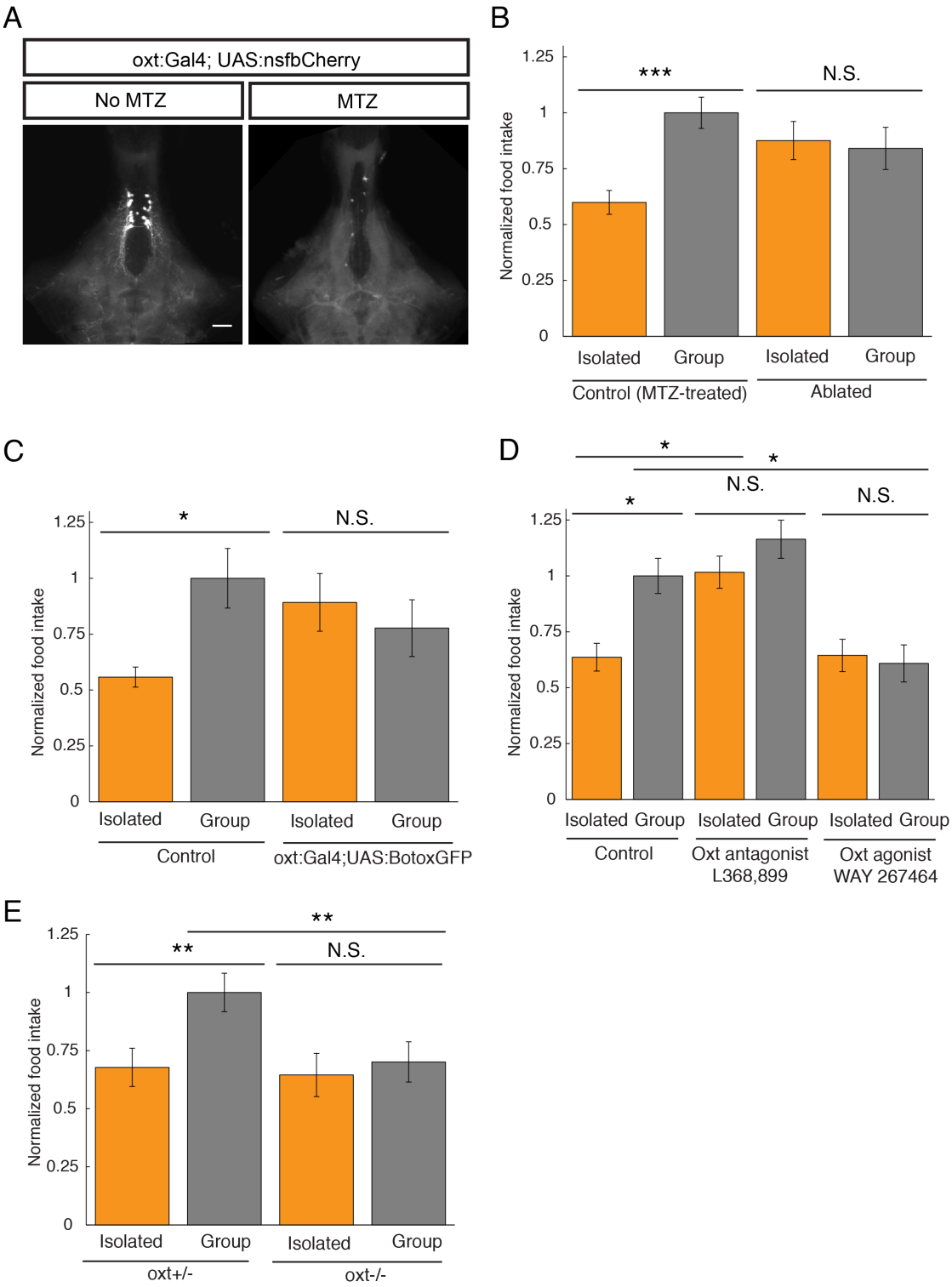

3.5 DISCUSSION

Neuromodulatory circuits are complex, but much progress has been made dissecting them in simpler models with smaller and more tractable brains. OXT/OXT-like peptides are expressed in nematodes, annelids, molluscs and arthropods, where they have been shown play important roles not only in reproductive behavior, but also other non-social behaviors such as aversive learning[206,255,256]. However, the OXT circuits of these invertebrate models look vastly different from those of mammals, making it difficult to generalize across or draw comparisons to higher organisms.

Here, we took advantage of a simple vertebrate model whose OXT circuitry is targetable, tractable (~50 neurons) and much more highly conserved, and which also has a small brain amenable to comprehensive characterization and manipulations. We show that even in the one-week-old larval zebrafish, which has previously been reported to lack social behaviors[188], OXT neurons encode social context, and many (both magnocellular and parvocellular) neurons increase their activity after short-term social isolation. Given that OXT neurons are also activated by painful stimuli, we propose that isolation and OXT activation represents a negative valence state. Thus, the OXT circuit forms a convergence point for both social isolation and pain stimuli, which can then be used to control divergent behaviors, such as pain avoidance or appetite (Fig. 3.5.1).

Figure 3.5.1: Model for oxytocinergic integration of social and non-social behaviors (A) OXT neurons respond to noxious external stimuli, and also integrate information concerning social context (i.e. the presence or absence of conspecifics). OXT neuron activation by noxious stimuli or isolation may drive a coordinated set of behavioral responses, such as the enhancement of defensive behaviors and the reduction of appetite, that overall promote survival. They may also drive other behaviors (such as conspecific approach). OXT neurons project to multiple effector regions, such as the hindbrain, spine and other hypothalamic regions, as well as the pituitary gland where OXT can be released into the circulation. **(B)** Oxytocin modulates multiple homeostatic survival circuits, such as circuits for defense, and appetite, and can shift the balance between the two drives. They do so by encoding both social and non-social sensory stimuli.

Figure 3.5.1 (Continued):

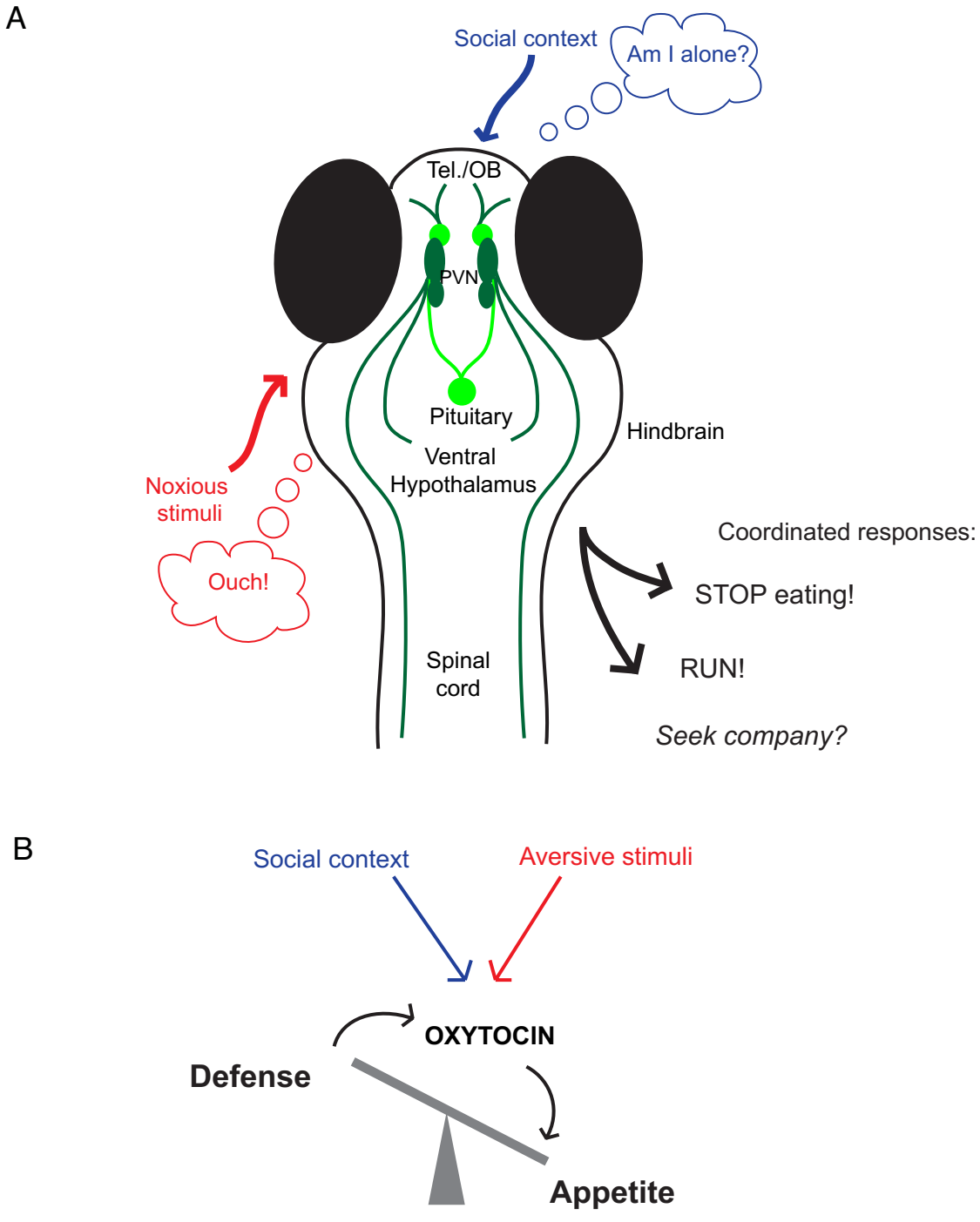

Notably, the sensory stimulus that drives these social state-dependent changes in OXT activity and behavior is olfactory, and not visual in nature. This raises the possibility that the reported lack of conspecific preference in larval zebrafish may partially be due to emphasis on vision in behavioral assays[188]. While we have not yet identified the exact cue(s) involved, we show that the prior consumption of food is necessary for production of the "social odor", suggesting that the odor may comprise excreted pheromones or digested food products. The olfactory stimuli from non-kin larvae were sufficient to restore normal behavior, suggesting that kin recognition information may not be pertinent for larval zebrafish at this current age. Interestingly, OXT has also been implicated in mediating olfactory social recognition behaviors in mammals[275], thus it is perhaps not surprising that zebrafish OXT neurons are similarly sensitive to social olfactory input.

We show that social isolation causes a suppression of appetite, which we demonstrate to be mediated by OXT signaling, either via secretion of OXT from the pituitary gland, or through intra-hypothalamic projections. It is interesting to speculate why appetite suppression may be an evolutionarily adaptive response to social isolation. A straightforward explanation would be that isolation, being a stressful state, might cause a shift in priorities from feeding to more immediate needs such as increasing vigilance, escaping the current environment, or seeking out conspecifics (Fig. 3.5.1). These changes in behavior make sense in the light of the fact that isolated fish are more susceptible to the risk of predation. We previously demonstrated that OXT neurons can drive locomotion and large angle tail bends, thus, even a small rise in their baseline activity in the isolated state would likely increase locomotor activity and/or escape

behavior, which would both enhance their survival prospects and increase their likelihood of leaving their current location for a safer and more favorable one. A second hypothesis is that the drive to eat competes with the drive to reproduce or, more broadly, to prioritize social interactions[276]. We speculate that high OXT signaling may also promote the seeking of conspecfiics. Certainly, larval zebrafish are not yet sexually differentiated or capable of reproducing, however it is possible that their OXT circuit is already set up for facilitating this decision-making process, by reducing the urgency of feeding to favor other more important behaviors.

Our results complement mammalian findings on the effect of OXT on appetite[277]. Atasoy et al. (2012) showed that acute inhibition of paraventricular OXT neurons could promote food intake, and that hunger-sensing neurons expressing Agouti-related protein (AGRP) can promote eating by inhibiting OXT neuron activity. In mammals, OXT receptors are especially dense in the ventromedial hypothalamus, an important satiety-promoting region[276]. Furthermore, lesions or suppression of the PVN, or mutations that affected OXT neuron development have been shown to cause hyperphagia and obesity[278,279]. We further add to these studies by highlighting the involvement of social context in the regulation of appetite by OXT. While it is unclear at this point if our findings generalize to mammals, a recent study in mice has looked at the role that social context (in this case dominance) plays in appetite regulation, and the involvement of OXT. The study showed that an OXT receptor antagonist could enhance sugar intake in a dominant mouse regardless of their social context, whereas in subordinate mice, the antagonist only enhanced appetite in the absence of cues of the dominant mouse[280]. While, the precise mechanism for this phenomenon, as well as its generalizability to

other social contexts remains unknown, it suggests that OXT may very well play a role in social-state-dependent control of appetite.

Finally, our results may also provide some insights into how OXT dysfunction in various genetic diseases may produce their diverse phenotypes spanning appetite regulation, pain responses and social behaviors. More specifically, the disease phenotypes associated with high or low OXT signaling can in generally be recapitulated in the larval zebrafish. Taken together with the previous chapter, we show that multiple social and non-social sensory stimuli converge onto hypothalamic OXT neurons to promote diverse behavioral responses, such as locomotion, pain avoidance and suppression of food intake (Fig. 3.5.1). This logic is reminiscent of the “hub-and-spoke” structure of C-elegans RMG neuron, which receive input from neurons encoding noxious stimuli, as well as pheromones, to coordinate social and non-socially-driven aggregation behavior[142,144].

We propose that dissecting the function of OXT neurons in the larval zebrafish brain should provide an entry point into our understanding of how the circuits controlling motivated behaviors interact across multiple stimuli to drive multiple behaviors. Our studies suggest a mechanistic framework for understanding OXT function – it can report behavioral state, over the timescale of minutes to hours, but also integrate other acute sensory input, such as painful stimuli, to drive decisions about behavioral output in a state-dependent manner.

3.6 FUTURE DIRECTIONS

There are many unanswered questions with regards to this story, and some experiments are already in the works to tackle some of these. We strongly suspect that this social modulation of appetite is experience-dependent, but still do not understand the time course/mechanisms underlying the development of this behavioral phenomenon. We are testing hypotheses for why *oxt* mutants have a distinct phenotype from our other manipulations. We also do not know how OXT may control other social behaviors, especially in older larvae that show strong social preferences (~3 weeks).

While I have focused mostly on how social state, represented by OXT, can modulate appetite, I have not neglected the very likely possibility that it also affects pain avoidance behavior, since both social and pain information converge on the exact same neuronal population. I hypothesize that OXT neurons could be important for "social buffering" of the pain response. Experiments are underway both at looking at the effects of social cues (in particular odor cues) on pain avoidance behavior, both in freely swimming fish and under the two-photon where we can correlate pain behavior with OXT neuron responses.

There are also plans in the works to directly assess the rewarding properties of social interactions in the larval zebrafish, by testing their preference in a preference chamber for proximity towards visual or olfactory cues of other fish. Other studies that have attempted this have only looked at visual cues, and did not see any preference[188]. Our results suggest that olfactory cues may be more salient. If successful this would be

a more direct readout of “social” behavior than the current behavioral assays we are using.

We would like to further dissect the circuit connecting social information to appetite control. OXT neurons extend their dendrites into the telencephalon, including the olfactory bulb. Could they be receiving direct social information from there, and if so, are these social odors detected by specific glomeruli that process reward-specific, or social-specific information? I would like to elucidate how it suppresses food intake downstream of OXT neurons. This may involve looking at whole brain network changes (probably using pERK) in response to OXT manipulations, including drugs, ablations, optogenetic activation or inhibition. It is unclear at this point whether circulating OXT or axonal release is mediating appetite suppression. Coupled with anatomical studies on OXT receptor expression, we may be able to identify hypothalamic (or other) nuclei that OXT acts on to suppress feeding, which will likely eventually intersect with appetite-regulating regions I have identified in Chapter 4.

Finally, we are exploring the role of other components of the HPA axis, such as CRF and AVP-expressing neurons. Is the activity of these neurons also upregulated during social isolation, and if so, what are the respective roles of these neurons in controlling appetite and other behaviors? Do they act in parallel, or interact with OXT neuron function? Our ultimate goal would be a complete understanding of the “social brain” network, and how OXT neurons play a role in the activity and function of this network.

3.7 EXPERIMENTAL PROCEDURES

Fish husbandry and transgenic lines

Larvae and adults were raised in facility water and maintained on a 14:10 hr light:dark cycle at 28°C. All protocols and procedures involving zebrafish were approved by the Harvard University/Faculty of Arts & Sciences Standing Committee on the Use of Animals in Research and Teaching (IACUC). Behavioral experiments were carried out mostly on fish of the WIK background, although other genotypes (e.g. AB, or mit1fa-/- (nacre) in the AB background) were also utilized as available. MAP-mapping experiments were performed *on Tg(oxt:GFP)* fish in then nacre background. Fish were raised at a density of ~40 fish per dish and fed from 5dpf till the day of the experiment (7 or 8dpf). Transgenic lines *Tg(oxt:GFP)*[219] and *Tg(UAS:nsfbCherry)*[263] had previously been published. *Tg(oxt:Gal4),* and OXT mutants were generated for work in Chapter 2. *Tg(UAS:Botox:GFP)* was generated by Koichi Kawakami.

MAP-mapping

7-8dpf larvae of the nacre background were either isolated or split into small groups (3, 5, 10). For groups of 10, a larger dish was used to prevent overcrowding. Paramecia was added to each dish to ensure that the fish were well-fed and had ample stimulation. After 2hrs, larvae were quickly funneled through a sieve, which was then quickly dropped into 4% paraformaldehyde, immunostained, imaged and analyzed as described in Randlett et al. (2015)[166]. For quantification of pERK/tERK ratios over individual OXT neurons, pERK experiments were performed on nacre *Tg(oxt:GFP)* fish, or dissected *Tg(oxt:GFP)* brains. Cellular-resolution imaging of the hypothalamus of dissected

brains was obtained using the LSM 700 Inverted and LSM 880 confocal microscopes. pERK/tERK intensities of individual GFP-positive neurons were measured using ImageJ and quantified using MATLAB.

Quantification of food intake

Paramecia were harvested and incubated with lipid dye (DiD' solid, D-7757, Thermo Fischer Scientific) for > 2hrs. They were then spun down gently (<3000 rpm) and reconstituted in deionized water, and an equal amount (100ul, ~500 paramecia) was pipetted into each dish of larvae. This method was adapted from Shimada et al (2012)[115]. After the experiment, larvae were immediately fixed, by pouring them through a sieve, and mounted on their sides on glass slides. They were then imaged using the AxioZoom V16 (Zeiss). In cases where identity of larvae needed to be maintained, for example, to correlate food intake with brain activity, larvae were imaged and subsequently stained individually in 96 well plates.

Acquired images were thresholded using custom ImageJ software, and total intensity calculated from the product of mean gut intensity and number of object voxels. Unless stated otherwise, food intake data was often combined across multiple datasets, though only for experiment of the same type (e.g. pharmacology, or ablations). For normalization purposes, the gut fluorescence of each individual fish within an experiment was divided by the mean gut fluorescence of the control (group of 3) fish. Thus, the mean of the control is always 1.

Behavioral experiments/sensory cues

Larvae that had been raised and fed in groups of ~40 were split into smaller (35mm) dishes containing one (isolated) or more (up to 5) fish. For experiments with 10 fish, a larger 55mm dish was used. After 2hrs, labeled paramecia was added as described above. After 30 minutes, larvae were immediately fixed and imaged as described above.

For generation of the “social odor” cue, sibling or non-sibling larvae that had been continuously fed with an excess of paramecia up to 7 or 8 dpf were transferred into a new 10cm petri dish (~40 fish per dish) that did not contain any paramecia. After a 2hr incubation, a syringe was used to very gently suck out the conditioned water, with great care taken not to disturb or stress the fish in the process. 700µl-1ml of the fish-conditioned water was then added immediately before labeled food is added. For providing visual access to conspecifics, the 35mm dishes containing single larvae were inserted into larger (55mm) dishes containing ~5 larvae that thus be surrounding but unable to interact with the single larva.

Pharmacological experiments

For pharmacology experiments, the OXT antagonist L-368,899 hydrochloride (Tocris Biosciences, 2641, 5µM) and agonist WAY 267464 dihydrochloride (Tocris Biosciences, 3933, 5µM) were added to each dish from the beginning of the isolation period (2hrs prior to adding labeled food).

OXT neuron ablation/inhibition experiments

Transgenic larvae expressing *Tg(oxt:Gal4;UAS:nsfbCherry)* or their non-transgenic siblings were incubated in 2.5mM Metronidazole (Sigma-Aldrich, M3761) from 5-6/6-7dpf. MTZ was subsequently washed out, and food intake was measured at 7 or 8dpf. For these experiments, the MTZ-treated siblings were used as the control group. For silencing of OXT neurons, food intake of fish co-expressing *Tg(oxt:Gal4)* and *Tg(UAS:Botox:GFP)* (from Koichi Kawakami) were compared to their non-expressor siblings in isolated or non-isolated conditions.

Oxytocin mutants

For experiments with OXT mutants, a heterozygous OXT mutant was crossed to a null mutant. All fish from the same clutch were raised together in the same dish and fed from 5dpf. On the day of the experiment (7 or 8dpf), the larvae were distributed into isolated or non-isolated conditions and fed labeled paramecia after 2hrs. They were fixed after 30 minutes, transferred into 96 well plates to keep track of experimental conditions and their gut fluorescence imaged. After imaging their genomic DNA was extracted and genotyped and their genotypes were matched to their experimental conditions (isolated or non-isolated).

Statistics

All error bars show mean ± SEM over fish. Significance was reported as follows: *p<0.05, **p<0.01, ***p<0.001. Significance was determined using the Paired Student's

T-test for paired data and the Wilcoxon rank sum test for independent samples. The two-sample Kolmogorov–Smirnov was used for comparing distributions of pERK/tERK ratios between control and treatment conditions. The Wilcoxon signed rank test was used in Fig. 3.4.1 for comparing the distribution of normalized OXT ROI signals across different behavioral stimuli to the null hypothesis of median 1. One-way ANOVA with Tukey-Kramer corrections were used when comparing fish using multiple parameters.

Chapter 4:

Satiation state-dependent control of appetite by zebrafish serotonergic networks

4.1 Intellectual Contributions

The following chapter will be written into a manuscript entitled “Satiation state-dependent control of appetite by zebrafish serotonergic networks” that has not yet been submitted for review. Data acquisition is still in progress and so this manuscript is not in its final form. I am first on the author list, but also an equal-contribution first author with Dr. Erin Song (ES) and Robert Johnson (RJ). Other authors include Dr. Owen Randlett (OR), James Bohnslav (JB), Maxim Nikitchenko (MN), Josua Jordi (JJ), Adam D. Douglass (ADD), Eva A. Naumann (EAN), Jared Wortzman (JW), Thomas Panier (TP), Koichi Kawakami (KK), Florian Engert (FE) and Samuel Kunes (SK).

ES, SK and I conceived of the project. ES and I designed most experiments together. SK and FE supervised the project. I carried out MAP-mapping and calcium imaging experiments, analyzed and plotted all data with help from ES, and wrote the manuscript with input from ES, SK and FE. ES developed the labeled dye-feeding assay, carried out all labeled dye-feeding and dissected brain imaging experiments, and also analyzed some data. RJ and TP built the high-resolution behavioral tracking setup that I discuss in 4.6 (Future Directions). RJ performed behavioral experiments on his setup with help from ES and myself, and analyzed all data acquired on his setup. OR advised MAP-mapping experiments. MN developed hardware and software for 2P

volumetric imaging/odor stimulation experiments and ran some of these experiments. JB, JJ, ADD, EAN and JW carried out preliminary experiments and contributed supporting data. In particular, ADD, EAN and JW performed bioluminescence imaging experiments, and ADD analyzed data and plotted Figure 4.4.9. KK generated and kindly provided the *Tg(116A:Gal4)* transgenic line through a gene trap screen.

4.2 SUMMARY

Appetite is controlled by phylogenetically old circuits that integrate internal hunger and satiety signals with external sensory cues to control food intake. However, many of these circuits are still poorly understood. For example, while the neuromodulator serotonin has long been implicated in appetite regulation, particularly in promoting satiety, there are numerous contradictory reports on whether it actually enhances or suppresses appetite, as well as on its precise mechanisms of action. In order to fully understand the hypothalamic circuits regulating appetite, it is necessary to adopt an integrative approach that combines large-scale activity mapping at cellular resolution with controlled pertubations. Here we demonstrate the utility of the larval zebrafish model for dissecting the role of serotonin circuits in appetite regulation. Using brain- and hypothalamic-wide activity mapping approaches, we identify neural populations that are differentially regulated during hunger, satiety and voracious feeding phases. We discover that many medially- and laterally-localized hypothalamic regions had anti-correlated activity patterns relative to each other, with strong activation of lateral hypothalamic regions (LH) during voracious feeding, and strong activation of medial regions during an energy deficit. In particular we identify a medially-situated locus, the serotonergic caudal periventricular hypothalamus (cH), that is important for regulating LH activity and food intake. A distinct serotonergic population, the superior raphe, responds to sensory cues of food and regulates food intake during satiety, also by acting on the LH. As predicted by the opposing activity patterns of these two serotonergic populations, we find that drugs that interfere with serotonergic signaling have opposite effects on hungry and satiated animals. Thus, by visualizing and

manipulating serotonergic neuron activity in the context of the entire hypothalamic network, we show how the internal state of an animal can influence serotonin function to exert flexible control of downstream feeding circuits.

4.3 INTRODUCTION

The hypothalamus is an evolutionarily ancient structure that is involved in numerous motivated behaviors, including the control of appetite. A number of pioneering studies in the 1950s demonstrated that the electrical stimulation or lesion of distinct hypothalamic regions in mammals could have dramatic effects on appetite. For example, while stimulation of medial hypothalamic loci reduced feeding, activation of more lateral regions strongly enhanced food search and consumption [23,24,28,30]. Conversely, medial hypothalamic lesions caused overeating, whereas lateral hypothalamic lesions led to starvation[28,29,31]. Thus, the lateral and medial hypothalamus were characterized as “hunger” and “satiety” centers respectively.

Over the past decades, more careful dissection of hypothalamic circuits has unveiled cell-type specific control of appetite by diverse neuronal subpopulations, which often express distinct neurotransmitters and modulators. Recent advances in optical and electrophysiology techniques have allowed in-vivo recordings of neural dynamics in small, genetically defined populations during appetitive and consummatory behaviors, using rodent models[83–85,281]. These studies have confirmed hypotheses derived from earlier stimulation and lesion studies – for example, GABAergic neurons in the lateral hypothalamus were found to be activated during feeding behavior and essential for driving food intake during hunger[281]. However, while unprecedented in resolution and timescale, these experiments still sample from a limited subset of hypothalamic neurons, and thus cannot be viewed in the context of the entire network – that is, other neurons in the same region, other hypothalamic areas, or even the entire brain. These

neuronal cell types or areas have to be specifically targeted, since an unbiased, large-scale mapping of appetite regulating loci is tedious to achieve in mammals.

The hypothalamic circuits that control appetite are furthermore poorly understood in the context of evolution, since the necessary comparative studies with non-mammalian vertebrates are lacking[11]. Here, we use the larval zebrafish, a vertebrate genetic model with a tractable and optically accessible brain, to identify evolutionarily conserved neuronal populations involved in the control of appetite. We adopted an integrative and unbiased approach that combined brain-wide activity mapping and controlled circuit perturbations to highlight similarities and differences between the hypothalamic control of appetite in zebrafish and mammals.

Larval zebrafish hunt paramecia, their natural prey, through a well-studied sequence of motor actions that has most often been conceptualized as a reflexive response triggered by external stimuli[185,282–284]. Our results demonstrate that their hunting behavior is flexible and controlled by satiation state. Using a brain-wide approach to identify neuron populations that are differentially regulated in fed and food-deprived fish, we present evidence consistent with mammalian studies that lateral and medial hypothalamic regions show opposing activity patterns during satiety, hunger and voracious feeding phases. Through a combination of imaging, ablation and behavioral studies, we establish that serotonergic neurons in the caudal periventricular zone of the medial hypothalamus (cH) are crucial regulators of lateral hypothalamic signaling. We subsequently discovered that a separate serotonergic population, the raphe nucleus, controls feeding in a distinct manner from the caudal hypothalamus. While serotonin is

largely believed to act as an appetite suppressant[101], our studies uncover a more complex role for serotonin that depends both on context and the activity patterns of functionally distinct populations. We propose that studying appetite in the larval zebrafish can provide insights into the evolutionary organization and logic of hypothalamic function during hunger and satiety.

4.4 RESULTS

Whole brain activity mapping of appetite-regulating regions

Hungry animals respond differently to food than satiated ones, but the neural circuits underlying this process are poorly understood[122]. We thus examined how the brain-wide activity response to the presentation of food differs between 7-day-old (7dpf) larval zebrafish that were food-deprived and those that were continuously fed (Fig. 4.4.1A). using the whole-brain phosphorylated ERK-based activity mapping (MAP-mapping) recently described by Randlett et al. (2015)[166]. In this experiment, animals were either continuously presented with a large excess of food ("Fed" condition) or removed from all food sources for 2-hours prior to the reintroduction of food ("Food-deprived" condition). We first used dye-labeled paramecia to confirm that food intake was higher in food-deprived fish, and the highest at the onset of food reintroduction, as we had previously reported (Fig. 4.4.1B)[115,186]. Since we were interested in identifying brain regions that were active during this phase of "voracious feeding", we fixed the food-deprived animals 15 minutes after food reintroduction, and compared their brain activity to continuously fed fish.

We identified multiple neuron populations that were either more or less active in food-deprived fish than fed fish, during the "voracious feeding" phase (Fig. 4.4.1C). Enhanced neural activity in food-deprived fish (after food) was observed in multiple regions and these could largely be grouped by their positions according to a hierarchy beginning with food detection and ending with behavioral output. For example, we found stronger activation in retinal Arborization Fields (AFs; optic tectum and AF7), as well as multiple downstream hindbrain loci including reticulospinal and oculomotor neurons, all

of which have been shown to be engaged during prey capture behavior[184,282,283]. In addition, we saw enhanced activation of the cerebellum, inferior olive, vagal sensory and motor neurons, area postrema and locus coeruleus, all of which have been implicated in feeding behaviors[285–288]. Regions of particular interest were those that appeared likely to perform a modulatory role. These included areas of strong activation in the hypothalamus (Fig. 4.4.1C, D), in particular the lateral region of the intermediate hypothalamus (LH). Note that this region is distinct from the LH in mammals in that it does not express melanin-concentrating hormone (MCH) and orexin, but similarly in that it express glutamatergic and GABAergic cell types[90] (Fig. 4.4.2).

In contrast to the enhanced activity of the LH, we also observed areas with decreased activity, which were located more medially. The most significant region of this kind was the caudal hypothalamus, which contains monoaminergic neurons (cH; Fig. 4.4.1C,D). In all nine independent MAP-mapping experiments that we performed, we found that cH activity was lower, and LH activity enhanced, in food-deprived fish after food (Fig. 4.4.1E).

Figure 4.4.1: Whole brain activity mapping of appetite regulating regions (**A)** Schematic of strategy for phosphorylated ERK-mediated activity mapping (MAP mapping) and food intake measurements. For measuring food intake, dye-labeled paramecia were added and larvae were fixed and imaged between 15 min and 2hrs after the experiment. For MAP-mapping, fish were either fed paramecia or food-deprived for 2 hours, before being presented with paramecia for 15 min, after which they were immediately fixed and stained for phosphorylated ERK. **(B)** Top: Comparison of gut fluorescence in fish that were fed and food-deprived, fixed after feeding with labeled paramecia. Bottom: Time course of absolute fluorescence increase for a single set of experiments. Groups of fed or food-deprived larvae were fixed at 1, 15, 30, 60 and 150 minutes after feeding of labeled paramecia (fed: n=7/18/19/17/17, food-deprived, n= 8/23/20/14/15). Food-deprived fish had significantly higher gut fluorescence than fed fish overall ($p = 7.5859x10^{-10}$, Two-way ANOVA) and at the 15, 30, 60 and 150 min time points (Corrected p-values<0.05). The rate of food intake was highest in the first 15 minutes (voracious feeding phase), thus we chose this time point for subsequent MAP-mapping experiments. **(C)** Representative MAP-map resulting from a single experiment described in (A). n = 12/17 (Food-deprived/Fed). In green are pixels that were significantly more active in food-deprived fish after food, and magenta represents pixels that were significantly suppressed. Activated regions include the telencephalon (Tel), Optic tectum (OTc), cerebellum (CB), hindbrain (HB), Vagal ganglion (VG) and Lateral lobe of the intermediate hypothalamus (LH). Suppression was observed in the caudal hypothalamus (cH) and some parts of the telencephalon. Scale bar = 100μm.

Figure 4.4.1 (Continued): (D) Z-projection of same MAP-map showing the hypothalamus, where lateral regions (i.e. LH) are strongly activated and medial regions (e.g. cH) are suppressed. The map is overlaid on an anatomy stack for the transgenic line *Tg(etVMAT:GFP),* in order to highlight the location of cH neurons. (**E)** ROI-specific analysis of LH and cH regions in 9 independent MAP-mapping experiments (10-20 fish per treatment per experiment). Food-deprived fish constantly had higher LH (***$p=8.2428x10^{-5}$) and lower cH (**p=0.0013) activity in response to food (paired Student's T-test). Images on right show respective Z-brain ROIs used for this analysis.

Figure 4.4.1 (Continued):

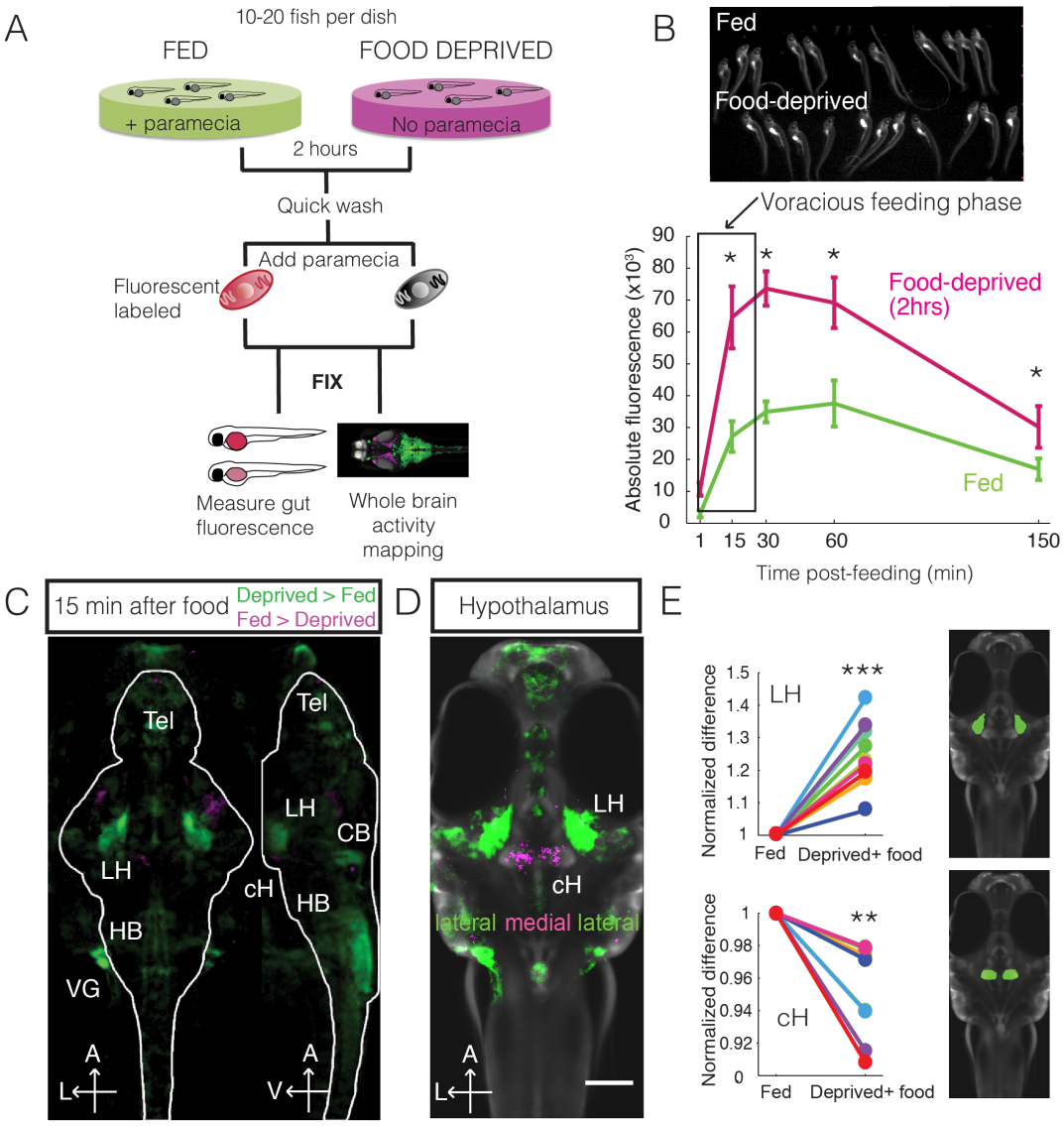

Figure 4.4.2: Neurotrasmitter identity of the LH. pERK-positive cells in LH overlap with glutamatergic and GABAergic cells. All fish were mounted ventral side up. Scale bar = 50μm. Inset scale bar = 20μm. **(A)** Glutamatergic cells, labeled by Tg(VGlut2a:dsRed), overlap with active neurons in both the lLH and outer rim of the mLH. **(i)** Overview of hypothalamus. **(ii)** Higher magnification images of LH. (**iii)** Inset showing overlap of lLH and outer rim of mLH with glutamatergic cells. **(B)** GABAergic cells, labeled by Tg(Gad1b:GFP), overlap with active neurons in the inner rim of the mLH but not the lLH. **(i)** Overview of hypothalamus. **(ii)** Higher magnification images of LH. (**iii)** Inset showing overlap of inner rim of mLH with GABAergic cells. White arrows point to examples of overlapping cells. **(C)** Antibody staining for melanin-concentrating hormone (MCH) shows expression in the rostral periventricular hypothalamus, that extends projections into the pituitary gland (pit). Note that MCH staining is absent from the LH. **(D)** Hypocretin/Orexin-positive cells, as labeled by the Tg(HCRT:RFP) transgenic line. Note that this is a Z-projection image and orexin cells are in fact dorsal to the LH and cH and would not actually be visible if focusing on the LH z-plane**. (E)** Diagram showing selected hypothalamic cell types and their localization along the medial-lateral axis of the larval zebrafish hypothalamus. Orexin and MCH are located more medially, whereas the LH comprises glutamatergic and GABAergic neurons. The cH, also more medially-located, comprises monoaminergic populations.

Figure 4.4.2 (Continued):

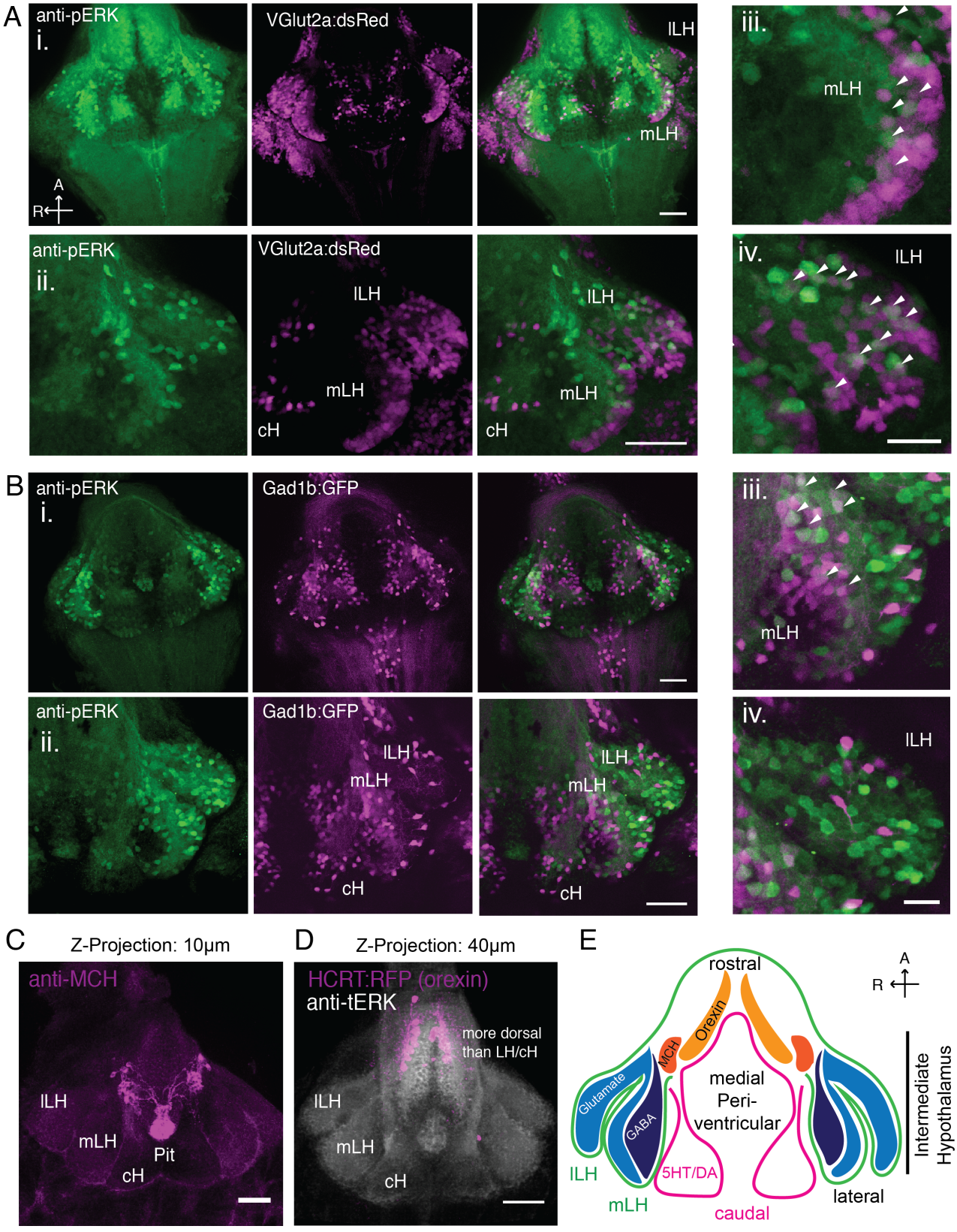

The LH and cH are activated by food presentation and removal respectively

We decided to investigate the functions of the LH and cH in more detail. Given its relatively strong activation during the voracious feeding phase, we hypothesized that the LH might be involved in the enhanced food intake following food deprivation. We characterized the LH at cellular resolution by confocal microscopy of dissected brains, and found that the number of active neurons in both the medial and lateral lobes of the LH (mLH and lLH respectively) was greater when food-deprived animals were provided with paramecia, as compared to when fed fish were given the same amount of food (Fig. 4.4.3A). Furthermore, this enhanced activity increased with increased food deprivation times. Correspondingly, the consumption of paramecia, as measured by the ingestion of fluorescently labeled paramecia[115], increased with the length of food deprivation (Fig. 4.4.3A). On the level of individual fish, LH activity also correlated with food intake (Fig. 4.4.3B). Thus, we observed that food deprivation modulates the activity response LH neurons to food, and that this activity is correlated with the behavioral output of prey capture and ingestion.

In contrast to the LH, which was activated by food, we found that the cH was activated by food removal. Food-deprived fish had higher cH activity (as measured by overall pERK fluorescence) than satiated fish (Fig. 4.4.3C). Activated cH neurons observed during food-deprivation overlapped extensively with antibody staining for 5-HT expression, and less with a transgenic reporter line that expresses in dopaminergic neurons (Fig. 4.4.4). To explore the activity of cH neurons at higher time resolution, we identified a Gal4 line *Tg(116A:Gal4)* from the gene/enhancer-trap database[289] of Koichi Kawakami and colleagues (National Institute of Genetics, Mishima, Japan), that

specifically labels serotonergic cH neurons (Fig. 4.4.4). We then expressed *Tg(UAS:GCaMPHS)* in these neurons, and measured calcium activity in this population over time (Fig. 4.4.3D). Consistent with our pERK results, we found that the absolute fluorescence of cH neurons was higher in food-deprived than fed fish and increased over time of imaging, as during this time they do not have access to food. The rate of increase of cH activity was highest in fed fish, plateauing at about 2hrs, which is consistent with our results showing a significant enhancement of food intake following 2hrs of food deprivation. Thus, the serotonergic cH neurons are robust reporters of an energy deficit in the hunger state.

Figure 4.4.3: The LH and cH are activated by food presentation and removal respectively (A) Food intake (top, n=10/17/13, corrected p-value < 0.05 for 2hr and 4hrs, one-way ANOVA) and LH activity (bottom, n = 6/5/7, corrected p-value < 0.05 for 2hrs and 4hrs, one-way ANOVA) increase with the duration of food-deprivation. In this panel, different sets of fish were used for behavior and imaging. Images: Dissected brains stained for pERK, for fish that were food-deprived for 30 min (top) or 2hrs (bottom) prior to food presentation. Scale bar = 50μm. Fish were mounted ventral side up. **(B)** (i) Food intake correlates with LH activity on the level of individual fish. mLH: R = 0.43, *p= 0.0013, lLH: R = 0.36, **p=0.0097 (Pearson's correlation) (ii) Time of food-deprivation and (iii) gut fluorescence mapped onto LH activity. Higher LH activity is associated with longer food-deprivation times and higher food intake. **(C)** The cH is activated by food removal. Bar plot show mean cH fluorescence and LH cell count during food-deprivation, after 30 minutes of feeding and after subsequent food removal. After 30 minutes of food, cH activity is significantly lower, and LH activity significantly lower, than during food deprivation and after 30 minutes of food removal. cH: *p = 0.0103, mLH: **p = 0.0002, **lLH: p = 0.0023, n = 6/3/3 (one-way ANOVA). Images: Representative images of different pERK-stained brains 0 min (top) and 30 min (bottom) after removal of food from continuously fed fish. Medial/caudal hypothalamic regions are strongly activated after food removal, whereas the LH is suppressed. Scale bar = 50μm. Fish were mounted ventral side up.

Figure 4.4.3 (Continued): (D) (i) Calcium imaging of cH neurons in Tg(116A:Gal4;UASGCamPHS) fish shows an increase in calcium indicator fluorescence with food-deprivation. (ii) The rate of fluorescence increase is much higher in the early stages of food deprivation (0.5hrs) than after a longer period of deprivation. (iii) Mean absolute calcium fluorescence plotted against time for 0.5hrs, 2hr, 4hr and 6.5hr food deprivation (n = 12/4/4/8). Absolute calcium fluorescence is lowest at the start of 0.5hr food deprivation, but increases rapidly over the course of 2hrs, whereas for fish that had already been food-deprived prior (2hr, 4hr, 6.5hr), absolute fluorescence is already high and does not increase further. (iv) Same data as in (iii) plotted in absolute time of food-deprivation.

Figure 4.4.3 (Continued):

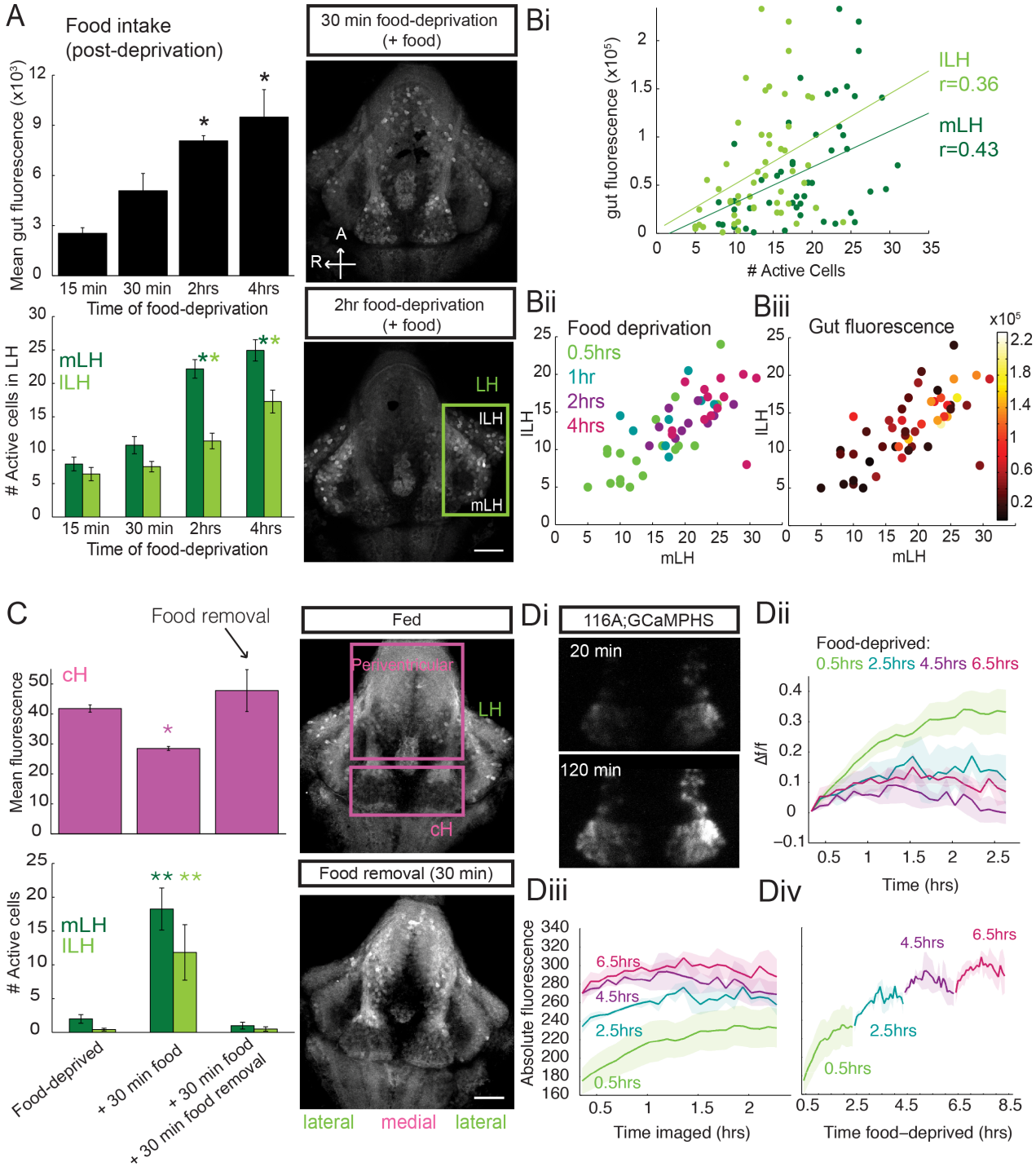

Figure 4.4.4: Identification of a transgenic Gal4 line that labels serotonergic caudal hypothalamic neurons (A) pERK-positive cH cells overlaps with anti-5-HT immunostaining and *Tg(116A:Gal4)* cells, and less with *Tg(TH2:GCaMP5)* cells. Scale bar = 20μm. White arrows point to examples of overlapping cells. **(B)** Z-projection images of whole mount *Tg(116A:Gal4;UASGFP)* fish at low (left) and high (right) intensities. cH neurons may extend neuritis into telencephalic areas. Scale bar = 100μm**. (C)** Overlap of *Tg(116A:Gal4;UASGFP)* with anti-5-HT immunostaining is seen in all layers of the caudal hypothalamus, and also the paraventricular organ (PVO). Each row shows a dfferent Z-plane, moving from more dorsal to more ventral. Dissected fish brains mounted ventral side up. Scale bar = 50μm. **(D*)*** Higher resolution images showing higher overlap of *Tg(116A:Gal4;UAS:nsfbCherry)* with anti-5HT immunostaining and minimal overlap with dopamine neurons, labeled by *Tg(TH2:GCaMP5).* Note that the *Tg(116A:Gal4;UAS:nsfbCherry)* transgenic, which is used in ablation experiments, shows sparser labeling than with *Tg(UAS:GFP).* Scale bar = 50μm.

Figure 4.4.4 (Continued):

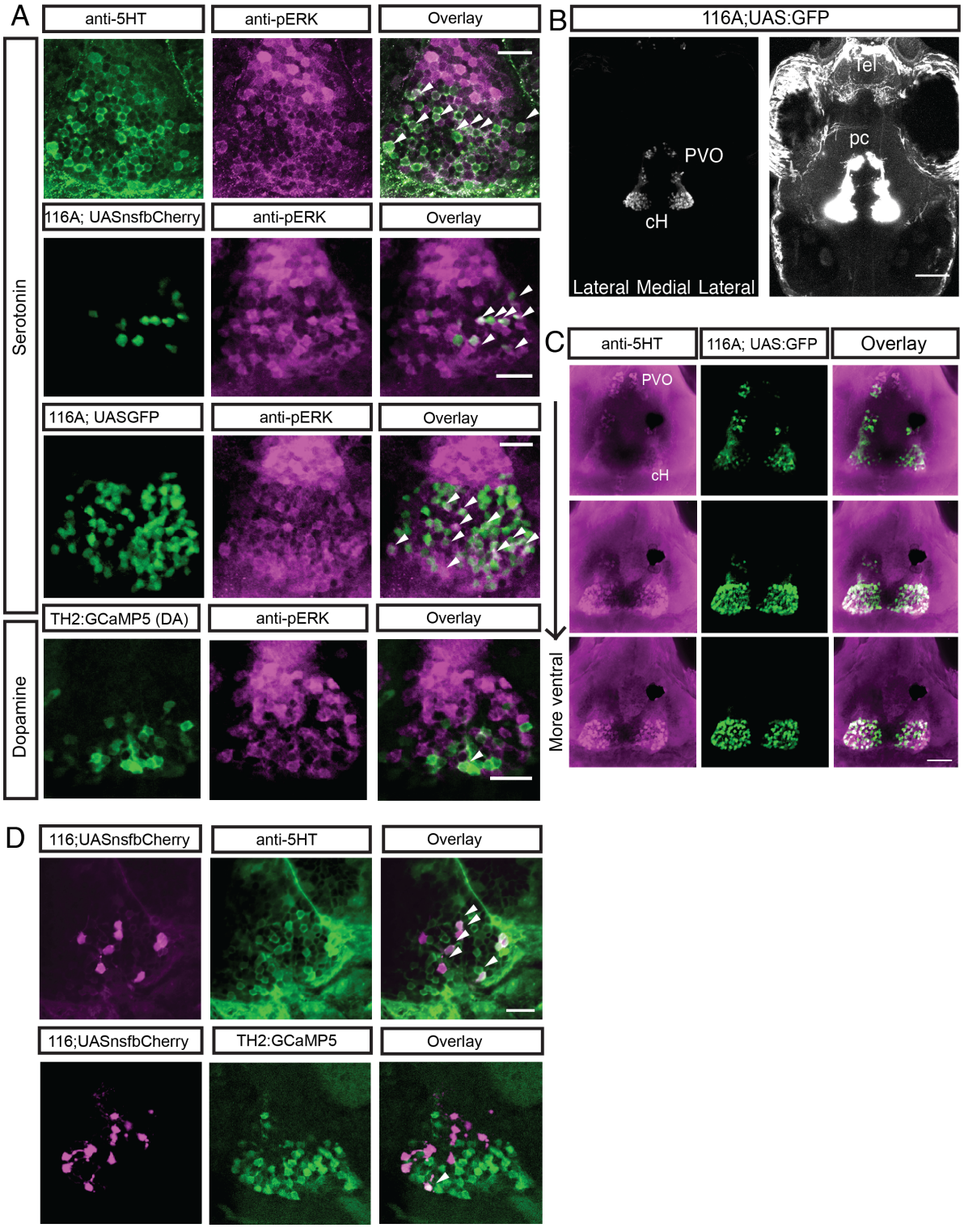

The LH and cH show anti-correlated activity patterns

The opposing activation patterns of the LH and cH by food and food removal respectively suggested that they might act in an anti-correlated manner. Using independent component analysis[166], a statistical technique used to identify putative functional connectivity between different brain regions, we found multiple (13/30) independent component networks (ICs) in which the LH and cH neurons had an inverse relationship to each other (Fig. 4.4.5A). 5/13 of these IC maps showed other medial hypothalamic regions being co-activated with the cH (e.g. IC#10, 18, 23), This analysis suggested to us that the lateral and medial/caudal hypothalamus may form a functionally interconnected appetite regulatory network.

We probed the relationship between cH and LH neuronal activity again by examining hypothalamic pERK staining at cellular resolution in isolated brains (Fig. 4.4.5B-C). As also shown in Figure 4.4.3, cH activity, as well as the activity other medial hypothalamic nuclei, is extremely high during food-deprivation, whereas the number of active LH cells was extremely low (Fig. 4.4.5B-C). Thus, high cH and low LH activity is associated with the state of hunger. However, as early as 5 minutes after food presentation to a hungry fish, the number of active cH cells was dramatically reduced, to even fewer than observed in continuously fed fish (Fig. 4.4.5B-C). This reduction of cH activity was accompanied by a corresponding strong increase in the number of active LH cells. Thus, cH activity is extremely low and LH activity extremely high, during voracious feeding in hungry fish.

In contrast, a satiated fish had cH and LH activity that was *in between* hunger and voracious feeding levels (Fig. 4.4.5B). Indeed, as a hungry fish continued to eat, LH activity slowly declined, and cH activity increased to baseline levels, with a time course consistent with the onset of satiation (Fig. 4.4.5C, 4.4.1B). Thus, the cH and LH activity are anti-correlated during hunger and voracious feeding phases, and a restoration of energy homeostasis (i.e. satiety) was marked by a return of both cH and LH activity to intermediate levels (Fig. 4.4.5D).

However, the picture started to look more complex once we explored the sensory cues that drive changes in cH and LH activity. We first used pERK immunostaining to investigate the sensory cues that were important for such a fast (~5 minutes) reversal of activity patterns once food was presented to a hungry fish. In particular, we asked whether it was food detection (e.g. visual or olfactory cues) or food consumption that caused the strong increase in LH activity as well as the phasic drop in cH activity. Interestingly, we found that non-visual cues of food (i.e. paramecia presented in darkness) were sufficient to activate the mLH in a food-deprived fish, whereas visual access to paramecia was not as effective (Fig. 4.4.5E). In addition presentation of artemia, a natural prey that larval fish actively hunt but which are too large to be consumed, could also enhance mLH activity. Thus, external sensory cues of food were already sufficient to activate the mLH, although not as strongly as with whole paramecia (Fig. 4.4.5E). In contrast, none of these external food cues (paramecia in darkness/artemia) was sufficient to reduce cH activity, or to increase lLH activity (Fig. 4.4.5E).

To confirm that the mLH could be activated by the sensory cues of food and precedes hunting behavior, we performed calcium imaging in food-deprived, paralyzed fish expressing pan-neuronal GCaMP6s. Since these fish would be unable to eat, but had visual and olfactory access to food cues, any activity observed would be caused by sensory cues of food, and upstream of actual food intake. We used both manual and automated segmentation approaches to distinguish between activity patterns of different hypothalamic regions. First, we hand-segmented the hypothalamus into medial (periventricular), and lateral (mLH and lLH) regions, which includes both neuropil and cell bodies, and compared activity patterns between these anatomically segregated regions (Fig. 4.4.5F). Indeed, consistent with our pERK results, we found that the mLH was strongly activated seconds after addition of a dense drop of paramecia (Fig. 4.4.5F-G). We also observed weaker and more transient responses of the lLH (Fig. 4.4.5F-G). Interestingly, the lLH also showed more spontaneous activity in the absence of food The periventricular hypothalamus also showed some weak responses to food, though this may be due activation of neuropil projecting to the mLH (Fig. 4.4.5F, 4.4.6).

Figure 4.4.5: Anti-correlated activity patterns of caudal and lateral hypothalamus across different stages of feeding (A) Six examples of independent component analysis (ICA) maps generated from a dataset of 904 fish. Voxels for each recovered independent component (IC) are shown as maximum projections, with intensity proportional to the z-score of the loadings of the ICA signal. IC#5, 9, 10, 18, 21 and 23 (out of 30) highlight LH and cH regions of opposite loadings, suggesting they may be part of a network with anti-correlated activity patterns. IC#10, 18 and 23 furthermore show segregation of activity between entire medial and lateral hypothalamus. **(B)** Higher resolution imaging of dissected brains stained with pERK during hunger (food-deprivation), satiety and voracious feeding phases. cH activity is higher and LH activity is lower in food-deprived (vs fed) fish. However in response to food, the opposite is true: food-deprived fish now have lower cH activity and but higher number of pERK-positive cells in the LH. Fed fish have intermediate cH and LH activity levels. Scale bar: 50μm. Inset: Higher magnification view of cH neurons. Scale bar: Scale bar = 20μm. Fish were mounted ventral side up. **(C)** Quantification of LH (mLH and lLH) activity (# pERK-positive cells) and cH activity (mean fluorescence intensity) in fed and food-deprived fish. Fed fish have lower LH and higher cH activity than food-deprived fish in response to food. cH activity decreased and LH activity increased within 5 minutes of feeding, but returned to baseline levels over the course of feeding (n = 8/5/3/5/3, asterisks represents corrected $p<0.05$ (one way ANOVA). **(D)** Schematic of inferred LH and cH activity patterns based on pERK experiments.

Figure 4.4.5 (Continued): (E) Effect of food sensory cues on cH and LH activity. Food sensory cues alone could neither reduce cH activity nor enhance lLH activity. However non-visual paramecia cues (food in darkness) significantly enhanced mLH activity, though not as strongly as with whole paramecia. Hatched artemia, which are actively hunted by 7-8dpf larval zebrafish but too large to consume, similarly enhanced mLH but not lLH activity. Notably, mLH activity in the presence of food sensory cues was still significantly lower than in the presence of whole paramecia (black asterisks). n = 39/34/9/12/18 fish combined over multiple experiments. Asterisks represent corrected $p<0.05$ (one way ANOVA). **(F)** Confocal calcium imaging of the hypothalamus, in food-deprived, paralyzed, agarose-embedded fish before and after addition of a dense drop of paramecia. Top image: Average intensity image from a representative hypothalamus of pan-neuronal GCaMP6s fish. Scale bar = 50μm. *Tg(HuC:GCaMP6s)* does not label the caudal hypothalamus, and labels both neuropil (np) and cell bodies (cb). Bottom image: ROIs used to delimit different hypothalamic areas spanning both neuropil and cell bodies. The trigeminal ganglion (TG) is not part of the hypothalamus and was used as a control. Traces: Mean calcium activity from both lobes of 10 fish. The mLH shows the strongest and most sustained responses to food. Scale bar = 0.2 Δf/f (vertical), 1 min (horizontal). **(G)** Rastor plots showing responses of individual lobes to food over time. Each row represents a single lobe (left and right alternating) from a single fish (20 rows, n=10 fish). Within-fish responses are highly correlated, and the mLH shows the strongest and most sustained responses to food. TG shows negligible responses to food.

Figure 4.4.5 (Continued):

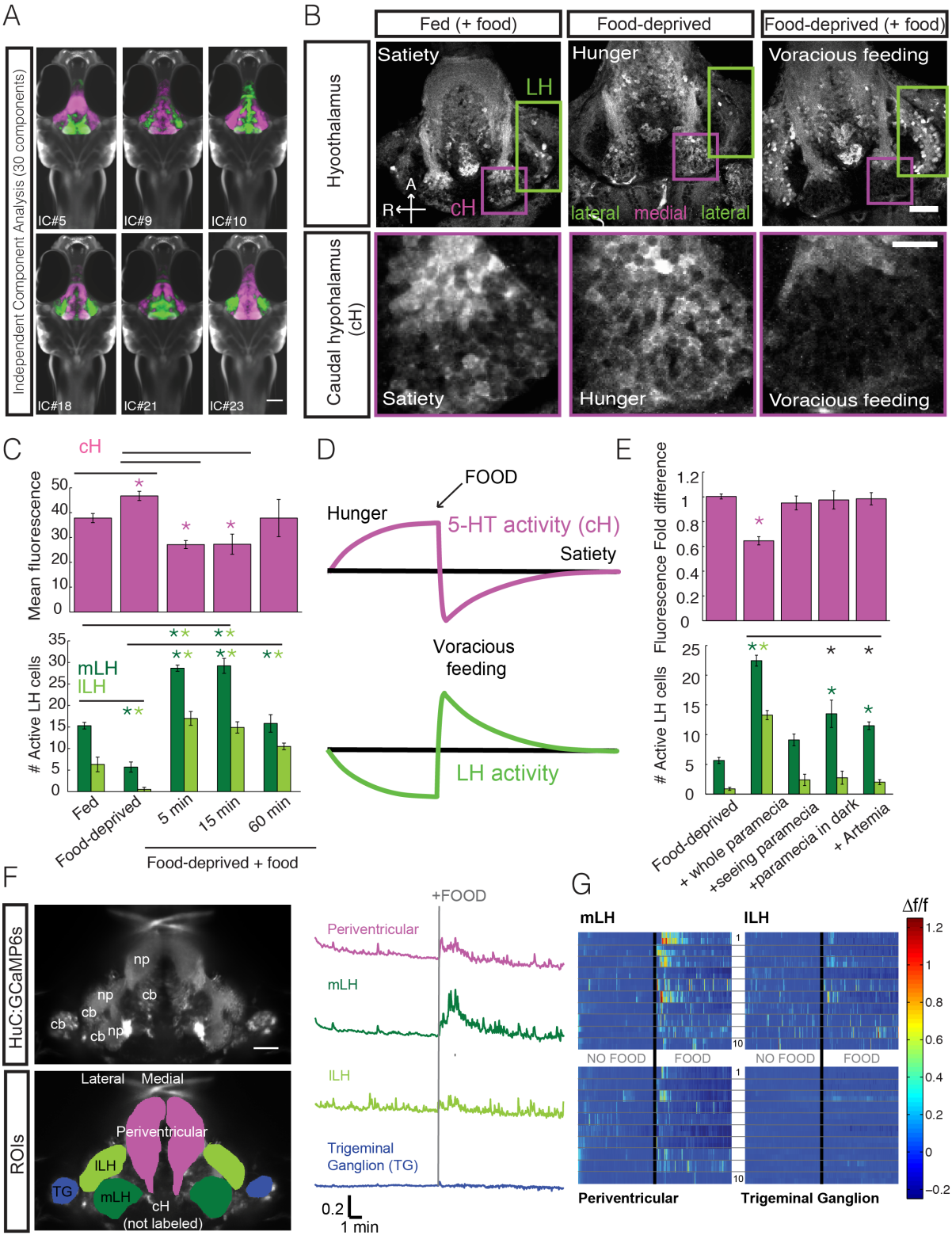

We also utilized k-means clustering to automatically segment neuronal responses within individual fish on a pixel-by-pixel basis (Fig. 4.4.6). This automated clustering method identified bilaterally symmetric clusters displaying correlated activity at higher spatial resolution. Pixels within the mLH showing the highest mean responses to food cues, and low baseline activity, and clustered within some periventricular fibers that may carry sensory information to that region (Fig. 4.4.6). The lLH formed a separate cluster with higher activity in the absence of food (Fig. 4.4.6). Thus, there appears to be a “sensory” phase in between when food is presented, and when it is consumed, where food cues are being conveyed to the hypothalamus, strongly activating the mLH but not the lLH or medial (periventricular) hypothalamic neurons. We were unable to visualize the cH using this transgenic line; however we similarly did not observe changes in cH activity in response to food sensory cues with *Tg(116A:Gal4;UASGCaMPHS)* (data not shown), consistent with the idea that only food consumption (and satiation state) can modulate cH signaling.

Taken together, our results suggest that while the mLH can be activated by the sensory cues of food, albeit not as strongly as when food is actually consumed. In contrast, the acute drop in cH activity, and rise of lLH activity can only occur post-food consumption. Whether this involves pregrastic (i.e. taste/tactile/swallowing), gastric (distention) or postgastric (absorption) cues remains to be explored. Thus, in addition to comprising distinct cell types (Fig. 4.4.2), the lLH and mLH are also selective for different food cues, raising the possibility that they could be specialized for different functions or controlled independently.

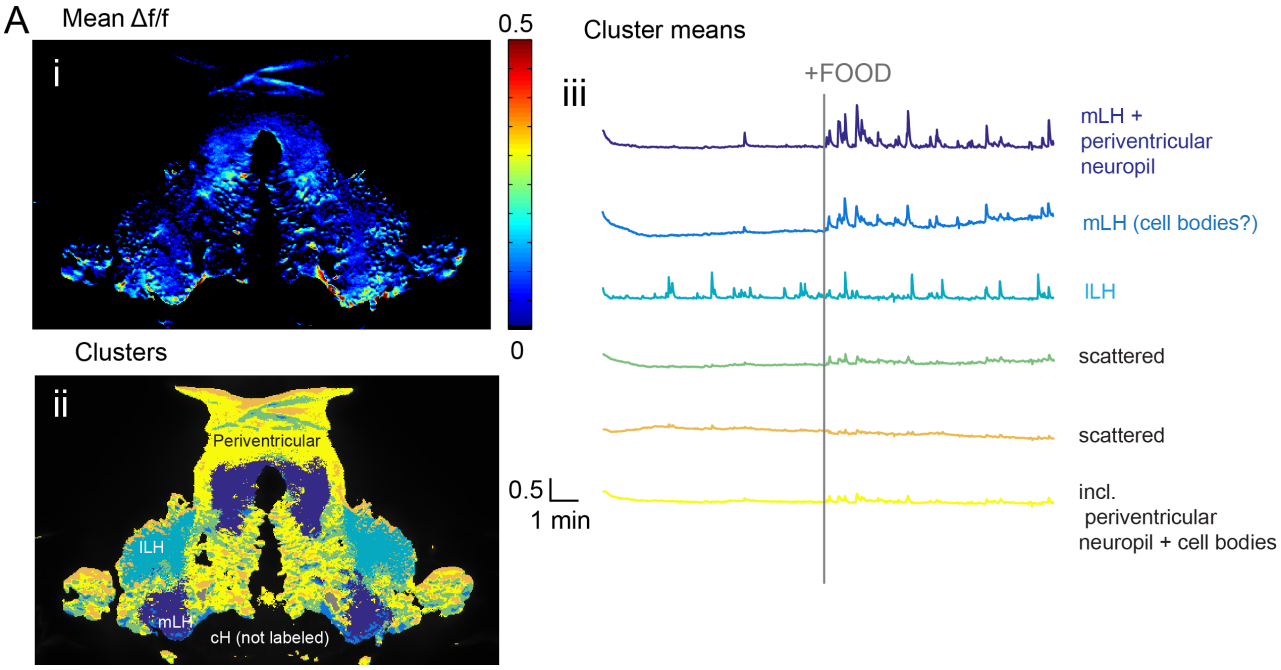

Figure 4.4.6: High resolution mapping of hypothalamic calcium activity

(A) Analysis of hypothalamic calcium activity from a single food-deprived fish. (i) Heat map showing mean Δf/f of entire post-food period of all pixels across entire hypothalamic plane. (ii) False-colored clusters identified from k-means clustering (k=6) of time series traces (both before and after food) from all pixels within the hypothalamus. (iii) Mean time series traces from all pixels within each cluster, with corresponding colors to (ii). The mLH cluster shows highest activation post food. The lLH shows higher activity during the baseline period. Other regions show relatively weaker responses to food. Scale bar: 0.5 Δf/f (vertical), 1 min (horizontal).

Circuit relationship of the caudal and lateral hypothalamus in appetite control

Given their anti-correlated activity patterns, we next explored whether there is a circuit relationship between serotonergic cH neurons and activity in the lateral hypothalamus (LH), in particular whether the cH could regulate LH activity. We performed chemical-genetic ablations of serotonergic cH neurons by incubating *Tg(116A:Gal4;UASnsfbCherry)* fish in the pro-drug Metronidazole from 4-6dpf, and compared LH responses to food at 7dpf to that of sibling controls also exposed to metronidazole (Fig. 4.4.7A). Since the labeling of cH neurons with nitroreductase-mCherry is relatively weak (Fig. 4.4.4), our ablations are only partial. Despite this, we found that ablating serotonergic cH neurons significantly increased the number of active mLH cells, in both food-deprived and fed fish after food exposure, whereas lLH activity was unaffected (Fig. 4.4.7B). Thus, the loss of cH neurons may lead to a disinhibition of mLH activity in the presence of food.

Since ablating serotonergic cH neurons increased mLH activity, we anticipated that this would also induce an enhancement of food intake. Indeed, chemical-genetic ablation of cH neurons significantly enhanced food intake during both fed and food-deprived states. (Fig. 4.4.7C). Thus, silencing/ablating cH neurons promotes eating through the disinhibition of both mLH and lLH activity, likely by leaving the animal perpetually in the “hungry” state, even if they had been previously well-fed.

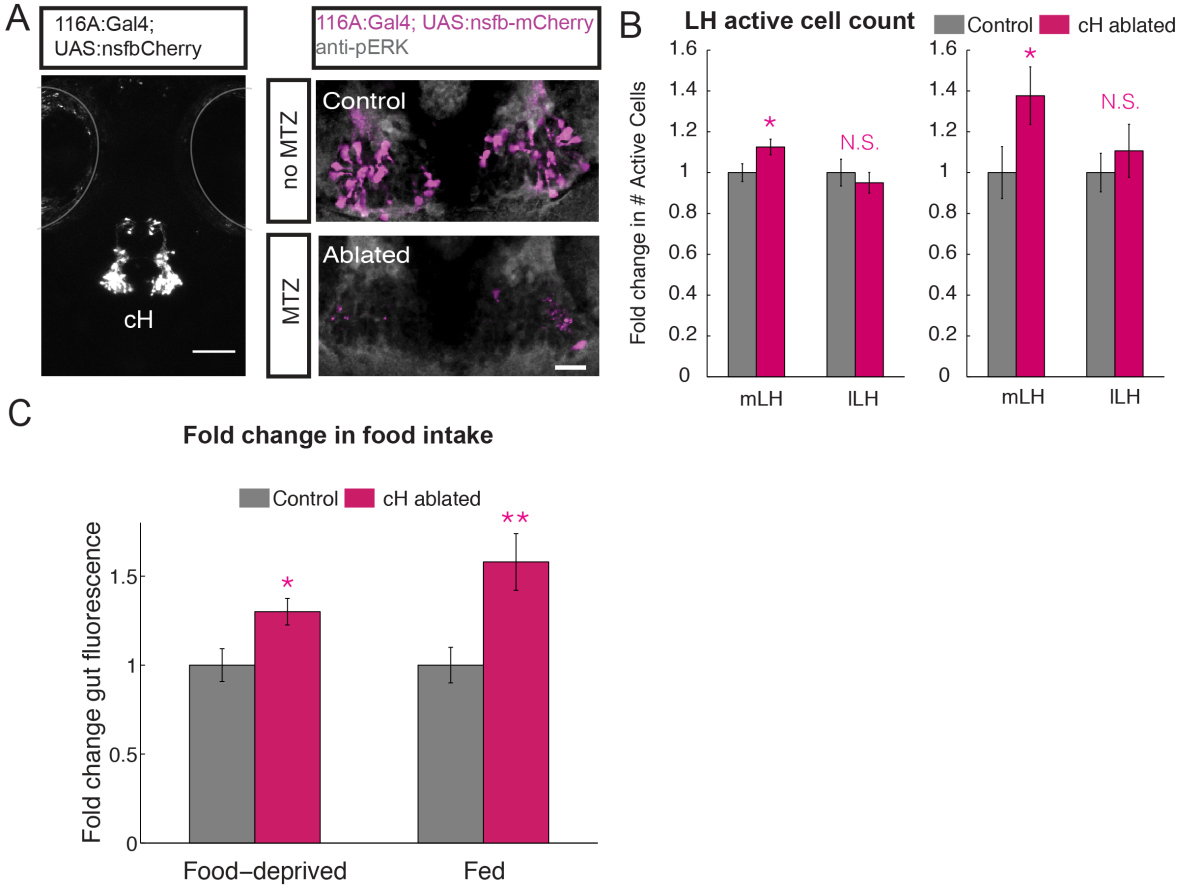

Figure 4.4.7: Circuit relationship of the caudal and lateral hypothalamus in appetite control **(A)** Left: Z-projection of *Tg(116A:Gal4;UAS:nsfbCherry)* fish showing labeling of the caudal hypothalamus. Eyes are outlined. Scale bar = 100μm. Right: MTZ treatment 2.5mM, 48 hours) successfully ablates nitroreductase-expressing cH neurons. Scale bar = 20μm. **(B)** Ablation of cH neurons increases the number of active mLH but not lLH neurons in both food-deprived (mLH: *p = 0.0384, lLH: p = 0.3744, n = 40 control/39 ablated) and fed conditions (mLH: p = 0.0322, lLH = 0.1867, n = 37control/27 ablated). **(C)** Ablation of cH neurons enhances food intake in food-deprived **(**p = 0.0165, n = 48 cont/50 ablated) and fed fish (**p= 0.0063, n = 48 cont/46 ablated). Wilcoxon rank sum test.

How could the cH affect mLH activity? We did not find any evidence of axonal projections of serotonergic cH neurons to the mLH; in fact, it is unclear if they send projections anywhere at all. Instead, given their close proximity to LH lobes, these neurosecretory cells could exert their effects through direct secretion of serotonin into the ventricles or perineuronal space. Whether they act directly on 5-HT receptors in the LH, or through other inhibitory interneurons remains to be explored.

Serotonergic neurons of the superior raphe respond to external food cues and promote food intake during satiety

Our experiments dissecting cH function pointed to a role of serotonin signaling in controlling appetite in larval zebrafish. However, the cH is not the only serotonergic source in the larval zebrafish – in fact, the larval zebrafish contains another prominent 5-HT population, the raphe nucleus, which is highly conserved and the sole source of 5-HT neurons in the mammalian brain. In zebrafish, the raphe projects extensively, including to the optic tectum and hypothalamus[290,291]. In fact, we found that the superior raphe of larval zebrafish sends axonal projections both to the cH and mLH (Fig. 4.4.8E), thus it is well-poised to regulate appetite by acting on these loci. While the raphe nucleus was not identified from our brain-wide MAP-mapping approach, we rationalized that its small size may make it susceptible to morphing errors, and thus decided to use alternative approaches to characterize raphe activity.

We first looked at raphe neuron activity in dissected brains, where we could monitor pERK activation at higher resolution (Fig. 4.4.8A). Interestingly, raphe pERK levels were significantly higher in the presence of food, which persisted even in darkness, suggesting that the raphe nucleus can be activated by food and food sensory

cues (Fig. 4.4.8A-B). In order to confirm our pERK results, we monitored calcium activity in the raphe nucleus using two complementary approaches – confocal-based calcium imaging in the presence of whole paramecia, and two-photon (2P) volumetric calcium imaging with food odor stimulation (whole paramecia scatter IR light and are unsuitable for use in 2P microscopy). To monitor superior raphe calcium activity we used a pan-neuronal GCaMP6s line with *Tg(tph2:nsfb-mCherry)* co-expressed in the background to identify 5-HT-positive neurons (Fig. 4.4.8C). We saw a sustained increase in calcium activity of the raphe in response to a dense drop of paramecia, using the same protocol we used for imaging the hypothalamus (Fig. 4.4.8C). We also observed higher raphe neuron activity in response to food odor stimulations as compared to control water stimulation, with peak differences in responses between odor and control stimuli occurred within the first 15 seconds of stimulation (Fig. 4.4.8D). However, we also found that raphe firing was highly variable and not exclusively locked to the initial presentation of the stimulus (Fig. 4.4.8D). Furthermore, spontaneous activity was high, especially in the dark and in dorsal regions (i.e. during 2P but not confocal microscopy, see Fig. 4.4.8D), consistent with the reported suppressive effects of light on dorsal raphe activity[292]. More experiments will be needed to elucidate how the raphe encodes food odors both in time and anatomical space (e.g. dorsal vs median raphe). Finally, similar activation of the raphe nucleus in response to food cues was observed by measuring bioluminescence[293] in freely-swimming, *Tg(pet1:GFPAequorin)* fish although this transgenic line labels both the superior and inferior raphe[290,293] (Fig. 4.4.9).

Figure 4.4.8: Serotonergic neurons of the superior raphe respond to external food cues and promote food intake during satiety (A) Left: Z-projection of *Tg(tph2-nsfb:Cherry)* fish. Eyes are outlined. Scale bar = 100μm. **(B)** Effect of food sensory cues on raphe pERK activity. Food-deprived fish had significantly higher pERK levels in the raphe nucleus after food was presented whether in light or darkness. Visual presentation of food did not increase raphe pERK signals. (n = 6/6/7/4, Uncorrected p-values = 0.0303/0.0221/0.5762 compared to no food condition, Wilcoxon rank sum test). **(C)** (i) Confocal calcium imaging in the raphe (HuC:GCamP6s with tph2nsfbCherry label in red channel) shows modulation of 5-HT neuron activity when a dense drop of paramecia is added close to the head of the fish. Scale bar: 20μm. Right: Δf/f traces show individual neuron responses to paramecia, from ROIs shown on left. The first stimulus is a water-only control. (ii) Rastor plot of 5-HT neuron responses (n=5 fish, bounded by grey lines, 64 neurons total) in response to a drop of water and a drop of paramecia. Neurons from the same fish show correlated activity. **(D)** Two-photon volumetric calcium imaging of the superior raphe nucleus in response to repeated presentations of conditioned paramecia water, alternating with unconditioned water as controls (i) An example of a single fish showing stronger responses during odor stimulation as compared to the control stimulus. Top: Rastor plot showing calcium activity of individual tph2-positive neurons sorted from ventral to dorsal. Dorsal-most neurons show high spontaneous activity. Raphe activity is in generally highly synchronous. Bottom: Mean responses from all neurons shown in (i). Note that the timing of the responses with respect to the stimulus varies, but more activity is seen during odor periods.

Figure 4.4.8 (Continued): (ii) Top: Mean calcium activity averaged over 192 neurons, from 5 fish. There was a significant difference between odor and control activity averaged over the first 15 seconds of the trial ($p= 2.7177x10^{-4}$). Botttom: Average traces from the same 5 fish but excluding the first control and stimulus period, to rule out the effect of novelty from the first stimulus ($p = 0.0043$). Wilcoxon rank sum test. **(E)** The raphe nucleus, labeled by *Tg(tph2:Gal4;UASnsfbCherry)* sends projections into the medial and caudal hypothalamus. Scale bar 50μm. (**F)** Raphe nucleus of a control and Metronidazole-treated (2.5mM, 48 hours) *Tg(tph2:nsfb-Cherry)* fish, double-labeled with anti-5-HT antibody. MTZ treatment successfully ablates raphe 5-HT neurons. (**G)** Nitroreductase-mediated ablation of raphe neurons reduces food intake in satiated fish (n = 80 control/73 ablated, ***$p= 5.097x10^{-4}$) but had no effect on food-deprived fish (n = 94 control/102 ablated, $p = 0.246$). Wilcoxon Rank Sum test. **(H)** Raphe ablation significantly reduces mLH activity in fed state (n = 18 control/19 ablated, mLH: *$p = 0.0372$ lLH: $p = 0.308$) but not in the food-deprived state (n = 27 control/26 ablated, mLH: $p = 0.7553$, lLH: $p = 0.2853$). The cH was also more active but only in the fed (n = 30 control/37 ablated, ***$p = 2.7598x10^{-5}$) and not food-deprived state (n = 27 control /28 ablated, $p = 1$). Wilcoxon rank sum test.

Figure 4.4.8 (Continued):

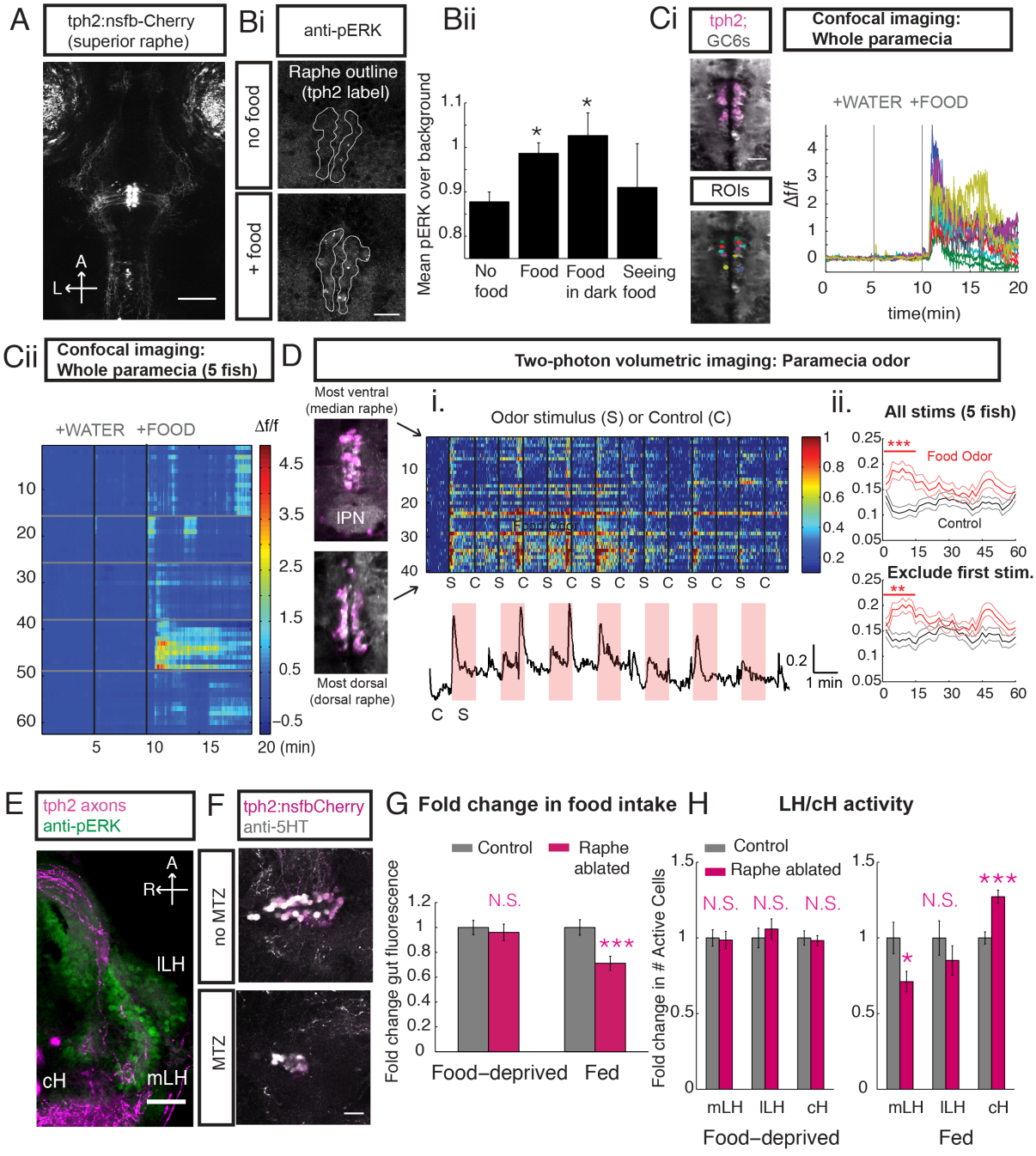

Figure 4.4.9: Serotonergic raphe neurons are activated by food (A) Transgenic zebrafish larvae expressing GFP-aequorin under the control of the *pet1* enhancer were treated with coelenterazine and bioluminescence signals were then monitored in free-swimming animals. Simultaneous bioluminescence (green trace, PMT photon counts per 167 ms) and behavior (black trace, mean single-frame per-pixel intensity change measured at the behavior camera) recordings for two representative fish. Red triangles indicate superthreshold peaks in the bioluminescence trace. Left and right panels depict recordings made in the absence and presence of paramecia, respectively. **(B)** Event-locked profiles of all bioluminescence spikes (top panels) and the corresponding behavior traces (bottom) in the absence or presence of food. 6.8 second segments of each trace centered on the positions of identified bioluminescence peaks (t=0) are plotted for single events (colored traces) and for the average across all segment. We found a larger frequency of bioluminescent spikes in the presence of paramecia, as compared to during baseline (Baseline: 0.0022 +/- 0.000799 bioluminescence spikes/s, Paramecia: 0.0081 +/- 0.0022 spikes/s, p=0.0191,one-tailed T-test). Motion was not time-locked to bioluminescent spikes. **(C)** As in panel B, but depicting the averaged bioluminescence and movement traces only. No event-triggered correlation was observed between normalized bioluminescence and behavior traces. (Baseline R =0 .1171, p=0.4659; Paramecia R =0 .2252, p=0.1568).

Figure 4.4.9 (Continued):

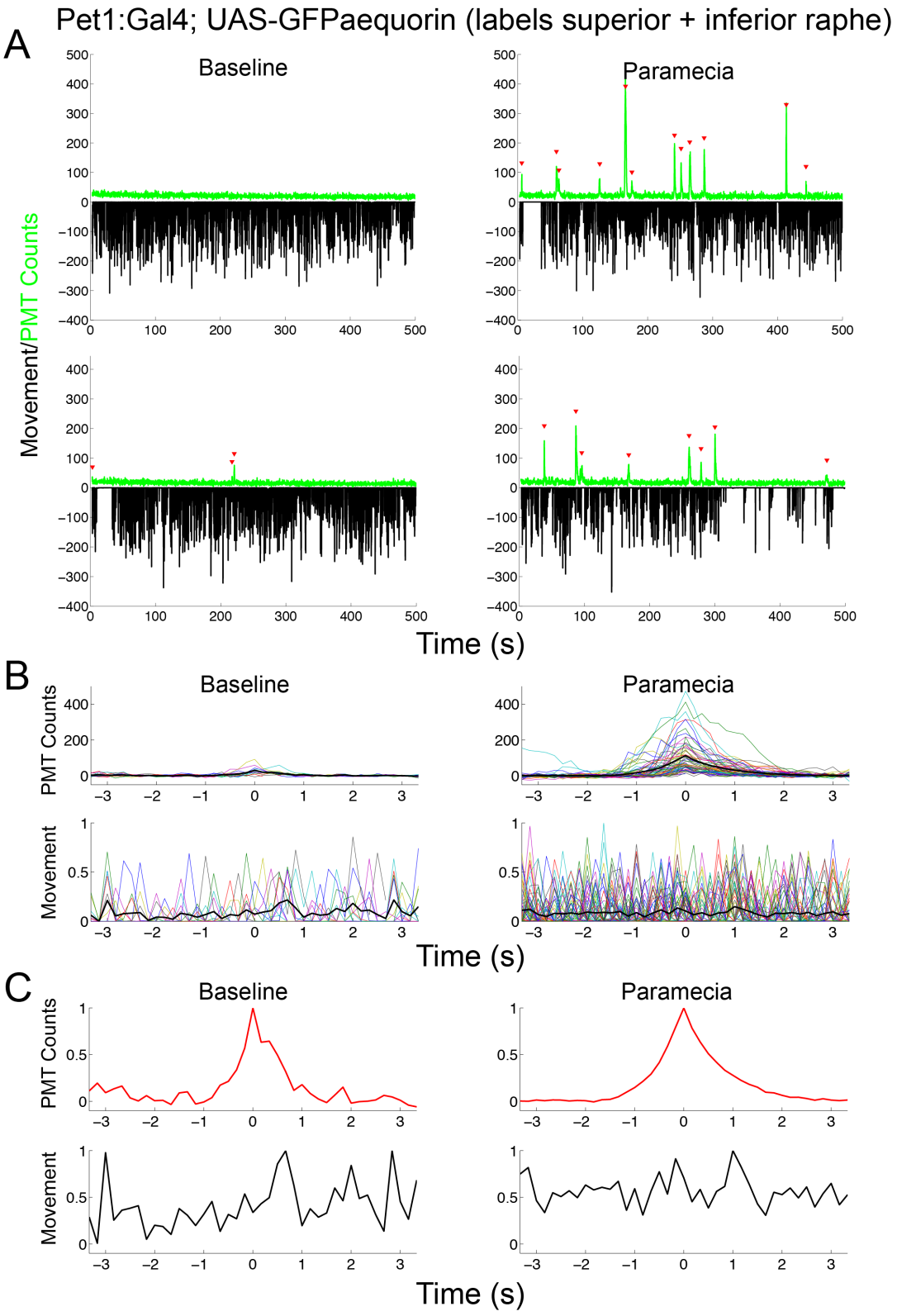

Since the superior raphe responds to food, we hypothesized that it may regulate food intake. To test this hypothesis, we ablated the raphe nucleus by exposing *Tg(tph2:nsfbCherry)* larvae to MTZ and comparing their food intake to MTZ-treated sibling controls (Fig. 4.4.8F). To our surprise, we found that while disruption of raphe signaling could suppress food intake, it only did so in fed fish (Fig. 4.4.8G). Thus, the raphe may be more important for regulating food intake during satiety.

How does the raphe control food intake? Since raphe neurons send axonal projections to the hypothalamus, including the cH and mLH (Fig. 4.4.8E), we quantified pERK-positive neurons in the hypothalamus of ablated and non-ablated fish. Consistent with our behavioral results, we found that ablating the raphe nucleus could reduce mLH, and enhance cH activity, but only during satiety suggesting that the raphe nucleus plays an important role in promoting food intake during the fed state (Fig. 4.4.8H). However, since the raphe projects to both these regions, it is unclear at this point whether the raphe is acting on both the mLH and cH in parallel, or if it is acting on one of these regions (e.g. cH) which then controls the other. Taken together, we have shown that while the raphe is responsive to food cues and may report the discovery of food; it has a satiation state-dependent role in the control of food intake. The lack of an effect of raphe ablation on hypothalamic activity and food intake during hunger suggests while it might play a modulatory role in appetite control, its activity is insufficient to dominate processes that control food intake during the hunger state.

Serotonin depletion has satiation state-dependent effects on food intake and hunting behavior

Our results so far have demonstrated that the serotonergic cH and raphe populations have opposing and satiation state-dependent effects on food intake; namely, while lowered cH activity post food-deprivation increases the drive to eat, increased raphe activity in a satiated animal can promote feeding. What would happen if functions of both these populations are disrupted simultaneously?

To explore this question we ablated both cH and raphe neurons using double transgenics expressing both *Tg(116A:Gal4;UASnsfbCherry)* and *Tg(tph2:nsfbCherry)*. Interestingly, while ablating both the cH and raphe led to enhanced food intake during hunger (similar to ablating the cH alone), we found that the double ablations reduced food intake during satiety (Fig. 4.4.10A). The latter effect was more surprising, given that cH ablation alone strongly enhances food intake, and demonstrate that raphe signaling may dominate in controlling food intake during satiation. Part of the reason is that our cH ablations are only partial, and thus raphe ablation could still suppress eating by activating other non-ablated cH neurons, or reducing mLH neuron activity downstream of the cH.

These double ablation results furthermore predict that systemic changes in serotonin signaling might have different effects on the zebrafish depending on whether it is hungry or satiated. To test this hypothesis, we depleted serotonin by either incubating the fish in pCPA 4 hours before the experiment, or treating the fish with the non-specific antagonist ketanserin 1 hr before the experiment, and subsequently quantified food intake and hunting behavior in both food-deprived and fed fish. We found that similar to

the double ablation results, serotonin depletion/antagonism enhanced food intake in food-deprived fish, but reduced intake in fed fish, confirming a state-dependent role of serotonin signaling (Fig. 4.4.10B). LH activity also changed in accordance with satiation state. Specifically, 5-HT depletion enhanced both mLH and lLH activity during hunger, but reduced their activity during satiation (Fig. 4.4.10C). Given that the effects of cH and raphe ablation appear to be concentrated on mLH activity, it is interesting that lLH activity is also affected. Whether this is a matter of differences in severity of the phenotype, or involvement of other mechanisms remain to be seen.

Overall, we propose a model in which reduced cH activity is crucial for promoting voracious eating during hunger, whereas the raphe features more prominently during satiety when cH activity is at baseline levels (Fig. 4.4.10D). We have shown that these two distinct 5-HT populations converge in the hypothalamus, particularly on the mLH, where they regulate food intake during different satiation states (Fig. 4.4.10D-E). The raphe is tuned to external sensory cues, whereas the cH sensitive both to energy status as well as to post-consumption (internal) cues of food. The coordinated actions of these neurons help to promote food intake in both hunger and satiated states, and disruption of these pathways can leads to state-dependent dysregulation of appetite.

Figure 4.4.10: Satiation state-dependent effects of serotonergic drugs (A) Effect of double ablation of both cH and raphe simultaneously on food intake in food-deprived and fed states. Double ablation enhanced food intake in the food-deprived state (*p = 0.0296, n = 16 control/6 ablated) but reduced food intake in the fed state (***p = $9.2252x10^{-5}$, n = 16 control/35 ablated). Wilcoxon rank sum test. **(B)** Effect of serotonergic depletion/antagonists on food intake, relative to controls. Food-deprived fish treated with the 5-HT antagonists pCPA (5um, 4hrs) and Ketanserin (5um, 30min) had enhanced gut fluorescence relative to control in the food-deprived state, but reduced gut fluorescence relative to controls in the satiated state. pCPA: n = 46/30, ***p = $3.8987x10^{-5}$/ *p = 0.035; Ketanserin: n = 29/23, *p = 0.035/ **p = $4.1464x10^{-4}$ (Wilcoxon signed rank test, significantly different from median of 1). **(C)** Effect of serotonergic depletion on LH activity. Serotonin depletion increased active LH cell counts in the food deprived (mLH: *p = 0.0238, *lLH = 0.026, n = 6 control/6 pCPA) condition but reduced overall activity in the fed condition (mLH: *p = 0.0171, **lLH = 0.0078, n = 8 controls, 7 pCPA).

Figure 4.4.10 (Continued): (D) Model for how raphe and cH serotonergic populations control food intake during hunger and satiety. While cH and LH activity are normally balanced, an energy deficit shifts the network to a state in which cH signaling is high, and LH signaling low. Once food is added, the balance “flops” to the opposite direction, with high LH and low cH activity. When satiety (energy balance) is finally achieved, the network returns to a homeostatic state. The raphe nucleus, which reports food intake, plays a role in pushing the balance towards enhanced food intake (i.e. low cH and high LH activity). Its effects are thus most pronounced during satiety. High cH activity (and low LH) may promote food seeking/foraging behavior, whereas high LH activity would promote food consumption. **(E)** Serotonin from the raphe and cH act on the LH (particularly the mLH) to control food intake. The raphe (also mLH) responds to external cues of food. The cH is activated by an energy deficit, but also rapidly inhibited by food consumption. Its periventricular position allows it access to circulating nutrients and hormones, but it may also receive sensory input about food consumption from peripheral sensory neurons.

Figure 4.4.10 (Continued):

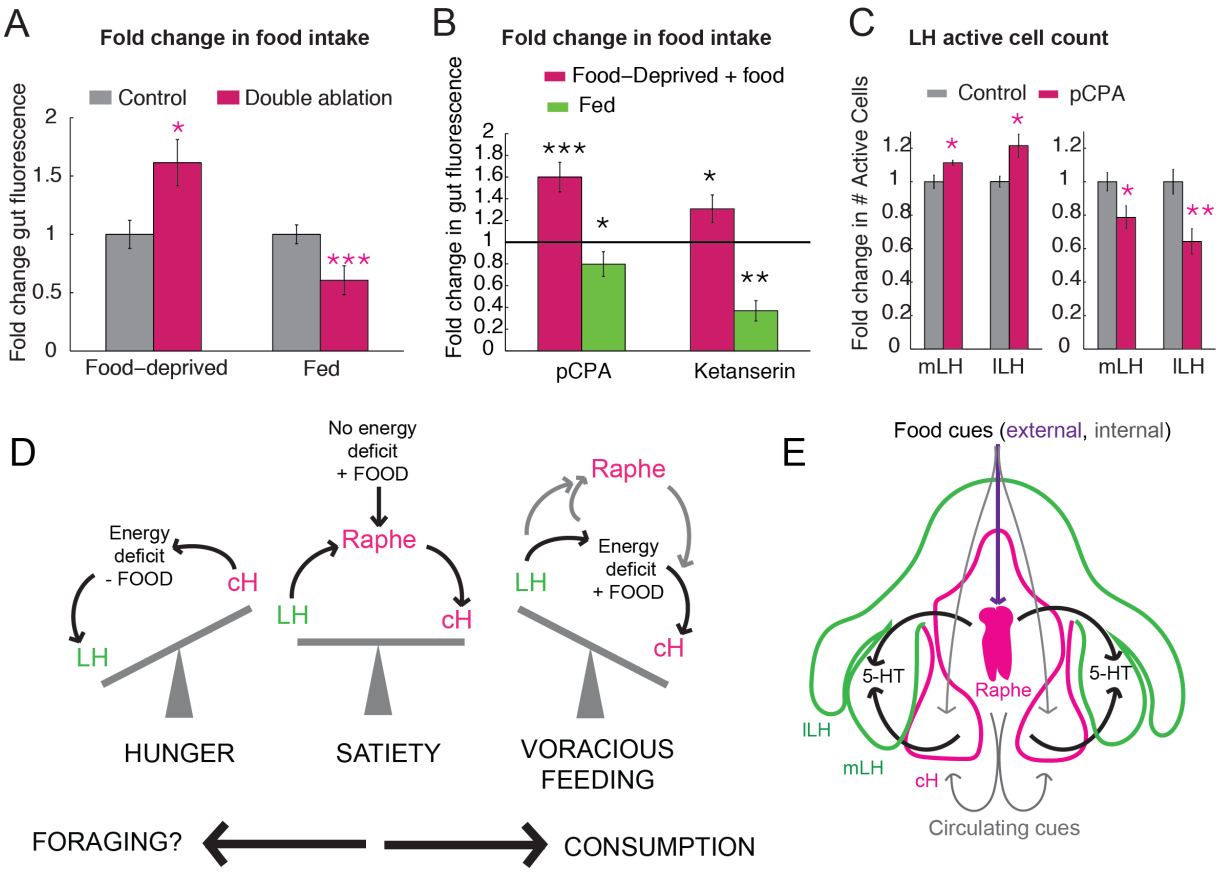

4.5 DISCUSSION

Mutually opposing hypothalamic networks control appetite

Is there an evolutionary logic behind the circuits controlling appetite in vertebrate species? Older studies suggested modular, functional hypothalamic units that work to suppress or motivate food intake respectively. Here, we show that the larval zebrafish hypothalamic network can similarly be functionally divided into medial and lateral units, which show anti-correlated activity patterns during various stages of ingestive behavior, that is, hunger, voracious eating, and satiety. However, within these broad units lies a diversity of neurons that encode specific stimuli and perform distinct functions.

The medial hypothalamic zone in the zebrafish comprises numerous neuromodulatory populations, including 5-HT and DA neurons of the PVO and cH, as well as a number of feeding peptides including AgRP, NPY, POMC as well as MCH and orexin, which are not as laterally-situated as in mammals. In this paper, we focused only on serotonergic cH neurons, although many medially localized neurons may show similar activity patterns. We found in particular that 5-HT neurons in the cH were strongly activated during food-deprivation, but strongly suppressed during voracious eating, on the timescale of minutes. In contrast, the LH, which contains GABAergic and glutamatergic neurons, is strongly inhibited in the absence of food and most strongly activated during voracious eating. Interestingly, a satiated fish had intermediate activity levels of both hypothalamic regions – thus a restoration of energy homeostasis is paralleled by homeostastis of the entire hypothalamic network.

Their opposing activity patterns suggest that medial and lateral networks may mutually inhibit each other, similar to a “flip-flop” circuit design. In the absence of food, medial hypothalamic activity is driven to a “high” state, whereas lateral hypothalamic activity is kept “low”. Once food becomes available (but when energy deficit is still high), a state change occurs, and LH activity is strongly enhanced while medial hypothalamic activity is strongly suppressed. Thus, the medial and lateral hypothalamic nuclei are inversely regulated by the presence or absence of food, but only when there is an energy deficit. A challenge to this model occurs when a hungry fish is presented with the sensory cues of food. In this “sensory” stage, cH/medial hypothalamic activity remains high, but the mLH is already strongly activated, which may reflect an enhanced sensitivity to food cues during hunger. However, our results also suggest that mLH activation during this sensory stage is not as strong as post-food consumption, thus a reduction in cH activity may still further promote mLH disinhibtion. The “flip flop” circuit analogy is completely consistent between the cH and lLH, although the exact function of the lLH remains to be elucidated.

In mammals, electrical or optogenetic stimulation of lateral hypothalamic neurons triggers voracious eating, thus consistent with our findings that the LH is highly activated during the voracious eating phase in hungry fish. While we do not currently have the genetic tools to optogenetically stimulate these neurons, electrical stimulation of the homologous region (lateral recess nuclei) in adult cichlids and bluegills[294,295] can elicit feeding behavior, consistent with our hypothesis. Interestingly, while stimulating some of these regions induced food intake, other induced behaviors, such as the “snapping of gravel”, were reminiscent of food search or procurement. Furthermore, the

neurotransmitter identities of these LH lobes (especially the GABAergic mLH) are consistent with the population of mammalian LH neurons that have been shown to stimulate food intake[281]. We have shown that distinct lobes of the lateral hypothalamus are sensitive to different food cues, with the mLH lobe being activated by the sensory cues of food (prior to eating), whereas the lLH is activated by consumption. Overall, it is conceivable that stimulation of mLH and lLH would produce distinct behaviors, for example the mLH might drive food approach, while the lLH might promote consumption or report food intake to downstream circuits. Certainly, the causal relationship between LH activity and food intake remains to be proven.

On the other hand, the medial periventricular hypothalamus, which includes serotonergic cH, appears to encode energy deficit in the absence of food. This function seems logical given that cH neurons are cerebral spinal fluid- contacting and thus have access to circulatory information[291,296]. These neurons may also respond to sensory information regarding food detection or consumption; for example, they also appear to extend dendrites to olfactory regions in the telencephalon (Fig. 4.4.4). At first glance, the fact that the medial hypothalamus encodes hunger in zebrafish may seem contradictory to the original idea that it is a satiety-promoting center. However, our results suggest that high medial hypothalamic activity may in fact suppress LH activity, which would reduce food intake. Similarly, ablating these medial populations, for example the cH serotonergic cells, would enhance food intake, which is again consistent with mammalian lesion studies of medial hypothalamic areas. Thus, the medial-lateral logic of hypothalamic function may be conserved even in non-mammalian vertebrates.

What is the function of high cH/medial hypothalamic activity during food-deprivation? One possibility is that it may represent a negative valence state or teaching signal, which is relieved when food is presented, as has been demonstrated for hunger-reporting agouti-releasing protein (AgRP) neurons in rodents[85]. Furthermore, the high cH activity during food-deprivation may serve to enhance responsiveness specifically to food cues, or to promote foraging behavior prior to food consumption. Such food-seeking/foraging/exploratory behavior, which happens during hunger in the *absence of food* needs to be suppressed once food actually arrives, which may explain the abrupt switch in signaling states.

Functionally distinct serotonergic circuits mediate flexible control of appetite

Ingestive behavior comprises distinct temporal stages and involves more than simply food consumption[297,298]. In particular, the presence of external sensory cues may be sufficient, even in the absence of hunger, to promote the initiation/procurement phases, in which the animal turns its attention to food, and/or begins to forage[297]. These stages are distinct from the consummatory phase, which involves a more stereotyped motor program. An animals' energy status is sensed internally and may influence both the initiation/procurement and consummatory stages of ingestive behavior. Thus, a hungry animal will be more aware of food cues, seek it more persistently and also eat it more voraciously.

Our studies indicate that 5-HT may have distinct, if not opposing roles in each of these stages. The cH, as already described, has multifaceted roles during hunger in the presence or absence of food. High cH activity during hunger may promote foraging

behavior, which is the initiation/procurement stage. Interestingly, food-deprivation also induces high 5-HT turnover (reflecting release/activity) in mammalian lateral hypothalamic areas[299]. However, once food is presented, the animal transitions through a brief sensory stage to a consummatory phase, which in the case of hunger is characterized by voracious eating. Once food is consumed, cH activity is heavily suppressed, to a level even lower than during satiety. This allows the disinhibition of LH activity, which could increase the drive to eat. Thus, in this consummatory phase, high 5-HT activity would in fact suppress food intake, in line with numerous studies that found appetite-suppressing effects of serotonin and its agonists[101]. In short, the cH regulates different stages of feeding by signaling in opposite directions over both long and short timescales, reporting energy deficit over hours, but acutely depressing its activity, within minutes, post food consumption.

To add to the complexity of the system, a second 5-HT population, the superior raphe nucleus, also acts on the hypothalamus to regulate feeding behavior. Whereas enhanced cH activity is correlated with food-deprivation, an increase in raphe activity is correlated with the presence of food. In particular, we have demonstrated that the raphe nucleus can be activated by external sensory cues of food, prior to food consumption. This is consistent with previous studies in mammals demonstrating that extracellular 5-HT in the hypothalamus, a major target region of raphe neurons, rose both transiently after food intake[300] and also during food anticipation, where only sensory cues of food are present[301]. We show that function of the raphe in alerting animals to food cues may be especially important during satiety, when the cH is at baseline levels. In particular it may promote feeding through its projections to the hypothalamus, especially the cH and

mLH. In addition, since the raphe is widely projecting, it may simultaneously modulate activity in other regions involved in hunting prey such as the optic tectum and hindbrain.

While our study implicates the raphe in feeding behavior, it is clear from the literature that the raphe nucleus has many roles beyond the control of food intake. However, our findings are consistent with other characterized raphe functions in at least two respects. First, it supports the idea that the raphe could be involved in reward anticipation, for example, in encoding the value of a reward[120]. Given that the raphe responds to the sensory cues of food, it is likely that it plays an important role in motivating the decision to begin to eat. Second, numerous studies have implicated the raphe in mediating arousal, that is, the enhancement of an organism's sensory responsiveness to incoming stimuli. Interestingly, in larval zebrafish, the superior raphe was previously shown to enhance visual sensitivity to moving grating during arousal[184]. It is tempting to speculate that this enhanced sensitivity may extend to food-like sensory cues, which may promote hunting behavior. Thus, the superior raphe nucleus may promote feeding by enhancing the animal's attentiveness or sensitivity towards food cues (i.e. the salience of food stimuli) as well as general arousal in response to food stimuli, and in addition also play a motivational role by signaling incoming food reward. To our knowledge, this study is the first to show that distinct serotonergic populations can be regulated independently to allow for differential responsiveness to food cues and flexible control of downstream behaviors.

The influence of internal state on serotonin function

The role of serotonin in appetite has long been a subject of debate. Multiple studies have demonstrated that selective 5-HT re-uptake inhibitors (SSRIs) or microinjection of 5-HT and its agonists into the hypothalamus reduces food intake[302–307], whereas depletion of 5-HT by P-chlorophenylalanine (pCPA) causes hyperphagia and weight gain[308]. This and a large body of cumulative evidence[101] led to the generally-accepted model that enhanced 5-HT signaling may signal satiety, reduce appetite and result in weight loss.

However, it has become increasingly apparent that 5-HT's effects on appetite are not as straightforward as previously believed. For example, many patients treated with SSRIs show paradoxical weight gain, instead of the weight loss expected from enhanced 5-HT signaling[309–312]. Across mammalian models[313–316], as well as the animal kingdom[111,317,112,318,113,319,114,115,320,321,116–119,322], there have been many contradictory reports of whether 5-HT promotes or suppresses food intake. The difficulty of converging on a common phenotype indicate that the mechanisms underlying 5-HT's effects on appetite are complex, and likely involve divergent responses depending on satiation state, downstream targets, and interactions with 5-HT's numerous other functions like reward anticipation, attention, anxiety, and arousal[101,102,120].

Here, we demonstrate that system-wide disruption or enhancement of 5-HT signaling using pharmacology has completely opposite effects depending on whether the animal is hungry or full, which may be due to the contrasting activity patterns of distinct 5-HT populations in the zebrafish. It is tempting to speculate that some of the

paradoxical effects of SSRI treatments in mammals could be at least partially explained by divergent serotonin functions during hunger and satiety, similar to what we have found in the larval zebrafish. While mammals do not have an equivalent of the caudal hypothalamus, the mammalian raphe nucleus projects to the hypothalamus, and it has been proposed that the functions of non-raphe 5-HT populations may have been centralized to the raphe over the course of evolution[291]. Thus, understanding the diverse roles of different 5-HT populations in the zebrafish could provide insights into the functional origins of the mammalian 5-HT system. It is also possible that some of the effects of serotonin depletion may be due to pertubations of other serotonin populations in the zebrafish[291,323], or in gut serotonin signaling[102,109,110]. Further investigations into distinct 5-HT pathways in the larval zebrafish may refine our model for how it controls food intake during hunger and satiety.

Our work on the role of serotonin in zebrafish appetite highlights how the internal state of an animal can dictate a neuromodulator's effects on its behavior. Furthermore, we have shown using brain-wide and hypothalamus–wide mapping approaches how serotonin neurons act in the context of other anatomically-segregated hypothalamic networks to control appetite. While in this study we focused only on subset of these neurons, the serotonergic and lateral hypothalamic populations, we propose the larval zebrafish as a promising vertebrate model for studying appetite-related circuitry. Continued efforts in this area should provide valuable insights into both the specific circuits underlying appetite control and the general principles governing hypothalamic evolution and function.

4.6 FUTURE DIRECTIONS

I have argued in this chapter that satiation state exerts a strong impact on larval zebrafish behavior, and that 5-HT drugs could differentially affect these behaviors due to satiation state. In collaboration with Robert Johnson (R.J), a PhD student in the Engert lab, we have used high-resolution behavioral tracking and machine-driven analysis techniques to more carefully dissect the impact of satiation state on zebrafish behavioral kinematics (Fig. 4.6.1). These experiments were performed in a very large arena where food density was sparser than in standard conditions. His data confirms results from our fluorescent dye assay, showing that food-deprived fish strongly upregulate their hunting related behaviors (J-turns, pursuits, strikes, and to a smaller degree, hunt aborts) and downregulate non-hunting behaviors, as compared to fed fish. He also observed satiation state-dependent effects of serotonin depletion, though of a different time course than with our fluorescent-labeled dyes. Namely, while fed fish treated with pCPA showed a strong suppression of all hunting behaviors, consistent with our data, food-deprived fish treated with pCPA increased their hunting over time relative to non-treated controls, starting off lower but exceeding the controls by the 1hr time point. It is not clear why their hunting behavior was initially suppressed, but it is likely due to the differences in arena size and food density. Overall, his data corroborates our findings that serotonin depletion differentially affects food intake during hunger and satiated states.

Figure 4.6.1: High-resolution analysis of hunting dynamics We developed a system schematized in **(A)** in which a high speed infrared camera moves on motorized rails to automatically track a zebrafish larvae in a large pool (300 x 300 x 4mm). A single fish is recruited to the arena center with motion cues delivered from a projector to initiate each trial. Paramecia are dispersed throughout the middle of the pool by loading them through a plastic C-shaped port (a single port is labeled in the diagram). A composite view of the arena is shown with swim paths from three trials overlaid. For analysis **(B),** 60 Hz image frames are centered and aligned. In every frame, the tail is skeletonized to 24 x-y points and the gaze angle of each eye is calculated. The eyes can each move from around zero degrees (parallel to body-axis) to 40 degrees (converged for hunting). **(C)** The distributions of mean convergence angle across bouts (n = 6600 bouts per group) are bimodal and the peak centered at ~30 degrees corresponds to hunting bouts. Each bout can be represented as a point in 500-dimensional space by collecting the skeleton and eye angle measurements across 10 image frames (~167 ms) from the beginning of each bout, such as the “j-turn” bout shown in **(B).** Food-deprived fish show more eye convergences than fed fish. Food-deprived fish treated with pCPA have the highest proportion of eye convergences across the entire 2hr experimental period, whereas fed fish treated with pCPA have the lowest eye convergences.

Figure 4.6.1 (Continued): (D) All bouts are mapped to a 2-D space with t-distributed stochastic neighbor embedding (t-SNE), as shown in. Four major hunting bout types can be identified from this embedding. Hunts begin with the “j-turn”, and fish follow and advance toward prey objects with “pursuit” bouts. Hunts end with an “abort” or a “strike”. When the fish is not actively involved in a hunt, it explores the arena with “meander” bouts. Within each group, the fraction of bouts assigned to each of these 5 bout types is calculated. These bout type fractions can be compared across groups in 15-minute time bins over an hour, as shown in the panels of **(E)** Food-deprived control fish upregulate hunting bouts compared to fed control fish, increasing strikes the most and aborts the least. Food-deprived fish incubated in pCPA gradually increase their food intake relative to food-deprived controls. Fed fish incubated in pCPA reduce all aspects of hunting behavior relative to controls.

Figure 4.6.1 (Continued):

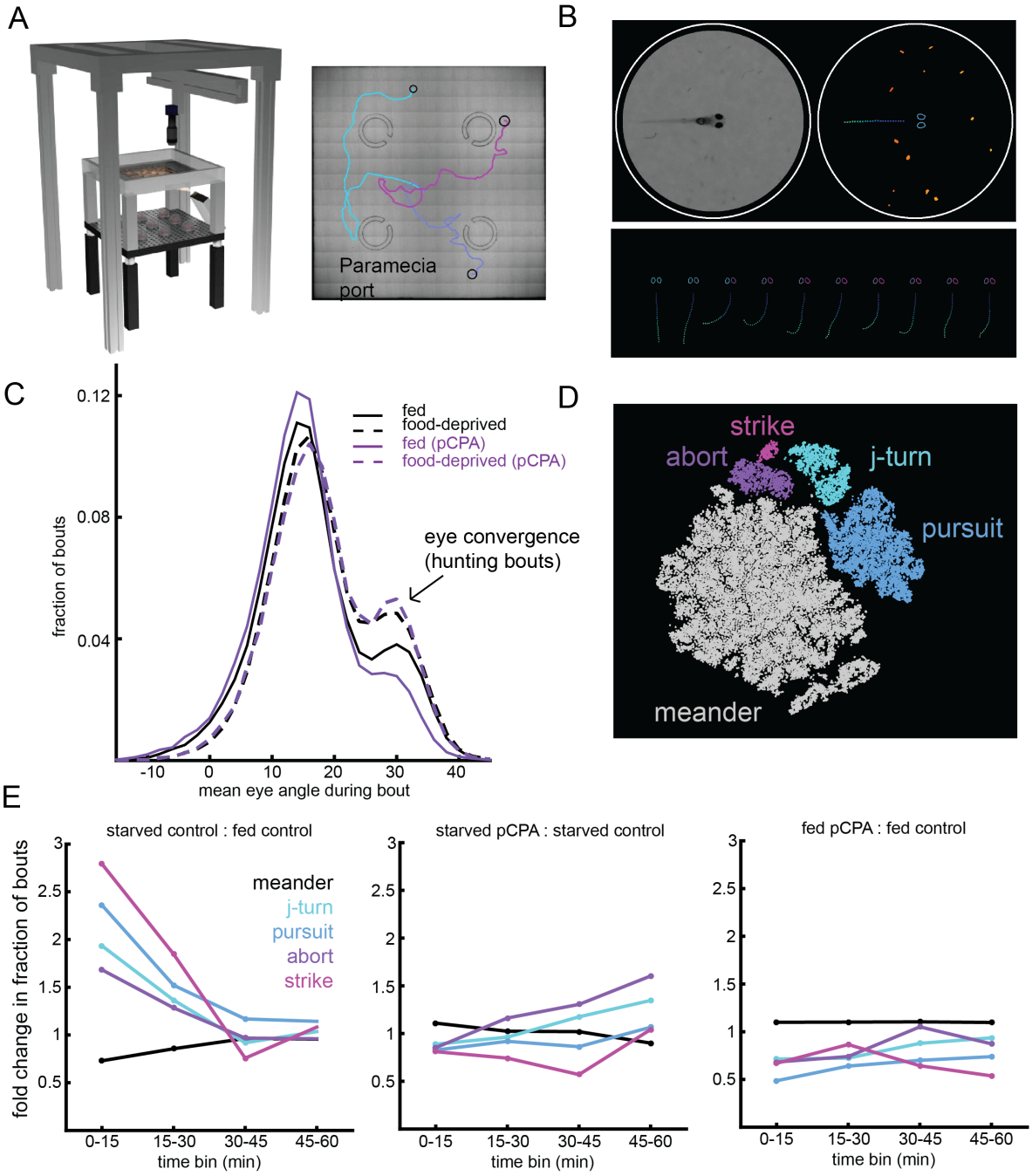

In addition, we have (again in collaboration with R.J) begun to characterize the hunting kinematics of fish that have had the cH or raphe ablated. Of particular interest is the function of high cH signaling during hunger in the absence of food. I put forth a number of hypotheses in the discussion – it could represent a negative valence state, it could promote food-seeking behavior, or it could potentially be a homeostatic mechanism to allow for more suppressed activity once food arrives, to permit a larger disinhibition of the LH. These behavioral experiments could help home in on some of the above hypotheses.

While we have relied on ablation experiments to draw most of our conclusions, I am attempting to expand the set of pertubations, including using more temporary-controlled methods and also to allow artificial activation of these neurons, especially the cH. Optogenetic experiments are now in process, hampered mostly by the poor expression of optogenetic channels especially in the cH. I am also hoping to implement a new TRP-based chemical activation method to explore the effect of enhancing cH activity both in the presence and absence of food, which should produce very distinct behaviors. Furthermore, activation and inhibition of the caudal hypothalamus would likely be aversive and rewarding respectively, and thus may have reinforcing properties which I would be very interested in exploring.

Next, I would like to further explore the interaction between raphe and caudal cH populations, by probing their functional and physical connectivity through perturbation experiments. For example, we could optogenetically stimulate or inhibit the raphe and

then carry out calcium imaging in the caudal hypothalamus (and vice versa), or use pERK as a secondary readout of activity.

At the current moment our ability to dissect hypothalamic circuits in zebrafish are limited mostly by the lack of specific transgenic lines to label and perturb the activity of interesting cell types. We are currently searching for transgenic lines that label the lobes of the lateral hypothalamus. Pertubation of these neurons would be the litmus test in our ability to draw parallels between mammalian and zebrafish circuits. We strongly hypothesize that activating these neurons should drive voracious eating, and removing or inhibiting them should abolish eating even in a starved animal. Furthermore, activation of these neurons should be positively reinforcing. I believe that demonstrating this in the larval zebrafish, even if it has already been shown in mammals, will be a huge stepping stone in our understanding of appetite control across species, and the beginning of many more interesting follow-up questions.

In addition, I am interested in exploring the role of dorsal raphe beyond food detection. Given its role in encoding reward, punishment and reward anticipation in mammals, it clearly serves a purpose beyond what currently we know of its function. I would also love to follow up on the numerous other modulatory populations identified by our whole brain mapping endeavor, which will likely expand our understanding of appetite-regulating circuits in the larval zebrafish, and ultimately also in mammals.

4.7 EXPERIMENTAL PROCEDURES

Fish husbandry and transgenic lines

Larvae and adults were raised in facility water and maintained on a 14:10 hr light:dark cycle at 28°C. All protocols and procedures involving zebrafish were approved by the Harvard University/Faculty of Arts & Sciences Standing Committee on the Use of Animals in Research and Teaching (IACUC). mit1fa-/- (nacre) larvae in the AB background, raised at a density of ~40 fish per 10 cm petri dish, were used for pharmacological and MAP-mapping experiments.

Transgenic lines *Tg(tph2:NfsB-mCherry)y226*[184] (referred to as tph2:nsfbCherry), *Tg(tph2:Gal4ff)y228)*[184] (referred to as tph2:Gal4), *Tg(UAS-E1b:NTR-mCherry)*[263] (referred to as UAS:nsfbCherry), *Tg(UAS:GCaMPHS)*[324], *Tg(UAS:ChR2-YFP)*[171], *Tg(Vglut2a:dsRed)*[261], *Tg(Gad1b:loxP-dsRed-loxP-GFP)*[325], *Tg(Gad1b:GFP)*[325], *Tg(TH2:GCamP5)*[242], *Tg(HCRT:RFP)*[326] and Tg*(etVMAT:GFP)* [327] have all been previously described and characterized. *Tg(pGal4FF:116A)* (referred to as *116A:Gal4*) was isolated from a gene trap screen by the Kawakami group[289]. *Tg(HuC:GCaMP6s)* was made by Ahbinav Grama and David G.C.Hildebrand from the Engert lab.

MAP-mapping of appetite regions

More details on the MAP-mapping procedure can be found in Randlett et al (2015)[166]. From 5-6dpf, mit1fa-/- (nacre) larvae in the AB background larvae were fed

an excess of paramecia once daily. On the day of the experiment (at 7dpf), the larvae were distributed randomly into two treatment groups: 1) FOOD-DEPRIVED, where larvae were transferred into a clean petri dish of facility water, taking care to rinse out all remaining paramecia or 2) FED, where after washing and transferring they were fed again with an excess of paramecia. After two hours, larvae in both groups were fed with paramecia. After 15 minutes, larvae were quickly funnelled through a fine-mesh sieve, and the sieve was then immediately dropped into 4% paraformaldehyde (PFA) in PBS + 0.25% Triton (PBT). Fish were then immunostained with procedures as reported below (see Immunostaining methods). The rabbit anti-pERK antibody (Cell Signaling, #4370) and mouse anti-ERK (p44/42 MAPK (Erk1/2) (L34F12) (Cell Signaling, #4696) were used at 1:500 dilution. Secondary antibodies conjugated with alexa-fluorophores (Life Technologies) were diluted 1:500. For imaging, fish were mounted dorsal-up in 2% (w/v) low melting agarose (Invitrogen) and imaged at ~0.8/0.8/2um voxel size (x/y/z) using an upright confocal microscope (Olympus FV1000), using a 20x 1.0NA water dipping objective. All fish to be analyzed in a MAP-Mapping experiment were mounted together on a single imaging dish, and imaged in a single run, alternating between treatment groups.

Immunostaining

24 hours after fixation (4% paraformaldehyde (PFA) in PBS + 0.25% Triton (PBT)), fish were washed in PBT, incubated in 150mM Tris-HCl at pH 9 for 15min at 70°C (antigen retrieval), washed in PBT, permeabilized in 0.05% Trypsin-EDTA for 45min on ice, washed in PBT, blocked in blocking solution (10% Goat Serum, 0.3%

Triton in BSS) for at least an hour and then incubated in primary and secondary antibodies for up to 3 days at 4°C diluted in blocking solution. In between primary and secondary antibodies, fish were washed in PBT and blocked for an hour. The protocol was similar for dissected brains, except that the brains were dissected in PBS after 24 hours of fixation, and the Tris-HCL antigen retrieval/permeabilization step in Trypsin-EDTA was omitted. Dissected brains were mounted on slides in 70% glycerol prior to imaging.

The following antibodies were used: rabbit anti-pERK antibody (Cell Signaling, #4370, 1:500 dilution), mouse anti-ERK (p44/42 MAPK (Erk1/2) (L34F12) (Cell Signaling, #4696, 1:500 dilution). Two anti-5-HT antbodies were used, rabbit anti-5-HT (Sigma-Aldrich, S5545, 1:500) and goat anti-5-HT (AbCam, ab66047, 1:500). The rabbit anti-MCH antibody was from Phoenix Pharmaceuticals (h-070-47). For this antibody, 5% Goat Serum in PBS was used as the blocking solution. Most confocal images of dissected brains were obtained using an inverted confocal (Zeiss LSM 700) except for the high resolution pERK imaging of the raphe, which was imaged using the Zeiss LSM 880 with Airy Scan.

Data analysis of dissected brains

To count cells in the lateral hypothalamus, custom cell counting software was used whenever possible, however the large variations in staining quality precluded its usage for all data sets. Blind manual cell counting using Image J point picker software was used as an alternative. cH activity was measured in ImageJ by drawing an ROI

over each of the caudal hypothalamic nuclei over the same plane across all samples. Any further analyses were performed using custom MATLAB software.

Quantification of food intake

Paramecia were harvested and incubated with lipid dye (DiD' solid, D-7757, Thermo Fischer Scientific) for > 2hrs. They were then spun down gently (<3000 rpm) and reconstituted in deionized water, and an equal amount (100ul, ~500 paramecia) was pipetted into each dish of larvae. This method was adapted from Shimada et al (2012)[115]. After the experiment, larvae were fixed and mounted on their sides on glass slides. They were then imaged using the AxioZoom V16 (Zeiss). In cases where identity of larvae needed to be maintained, for example, to correlate food intake with brain activity, larvae were imaged and subsequently stained individually in 96 well plates.

Pharmacology

Food intake in fed and food-deprived conditions were compared between control fish and fish treated with serotonergic drugs. The following drugs were used: Ketanserin tartrate, 5uM, 1hr prior to feeding (Tocris Biosciences, 0908) and p-chlorophenylalanine (pCPA), 5uM), 3 to 12 hours prior to feeding (Tocris Biosciences, 0938),

Nitroreductase-mediated ablations

Larvae expressing *Tg(tph2:nsfb-Cherry)* or *Tg(116A:Gal4;UAS:nsfb-Cherry)*, or their non-transgenic siblings were incubated in 2.5mM Metronidazole (Sigma-Aldrich, M3761) from 4-6dpf. MTZ was subsequently washed out, and food intake was

measured at 7 or 8dpf. For these experiments, the MTZ-treated siblings were used as the control group. Each control or ablated group was food-deprived or fed for 2hrs, and labeled food was added to quantify food intake. In the case of fed fish, unlabeled food was very gently washed out 15 mins before the experiment, and the food-deprived fish were also agitated slightly to simulate a short washout.

Calcium imaging and analysis

For calcium imaging of the caudal hypothalamus, 4 to 6 food-deprived (2-6hrs) or fed larvae expressing *Tg(116A:Gal4)*, were embedded in 1.5% agarose on a large petri dish, and a z-stack covering the entire caudal hypothalamus imaged using multi-area timelapse imaging every 5 minutes for 2hrs. Maximum projection images from the timelapse series were aligned to the first image of the series and total fluorescence of both caudal hypothalamic nuclei was subsequently measured using manually-drawn ROIs in ImageJ, to obtain the average calcium activity for each fish at each time point.

For confocal calcium imaging of the raphe nucleus a *Tg(HuC:GCaMP6s)*, *Tg(tph2:nsfbCherry)* double transgenic fish was paralyzed in bungarotoxin (Invitrogen,1mg/ml) and embedded in 1.5% agarose, with their eyes/nostrils were released. GCaMP activity from a single z-plane (where the most raphe neurons, labeled by tph2:nsfbCherry could be seen seen) was imaged using a confocal microscope. After a 5 min habituation period and a 10 min baseline period, a dense drop of paramecia was pipetted into the dish. Due to paramecia phototaxis, most of the paramecia moved into close vicinity of the fish's head under the laser, allowing for strong visual/olfactory exposure to paramecia. For analysis, hand-drawn ROIs were selected using the red

channel and total fluorescence within the ROI was calculated for the corresponding green channel. A similar protocol was used for calcium imaging of the hypothalamus.

For two-photon calcium imaging of the raphe nucleus with food odor, non-paralyzed *Tg(HuC:GCaMP6s) , Tg(tph2:nsfbCherry)* double transgenic fish were embedded in 1.5% agarose, with their nostrils released. An electrically tunable lens (Edmund Optics, 83-922) was installed in the light path before the galvanometers and controlled with custom LabView software. This allows for fast axial refocusing of the two-photon excitation spot. Alternating 60µl drops of filtered (0.45 µm filter) conditioned (>2hr) paramecia water or water without any paramecia was presented directly towards the head of the fish. The tunable lens repeatedly scanned through five z-frames spanning the ventral to dorsal-most regions of at 282 ms/frame, thus the entire superior raphe was imaged at ~1.5Hz.

Bioluminescence recordings

For bioluminescence recordings, double-transgenic larvae carrying the Tg(*pet1:gal4-vp16*) and Tg(*uas:egfp-aequorin*) alleles were screened for strong reporter expression in the raphe and reared in 40 µM Coelentrazine (CLZN-h, Biotium USA) for 24-48 hours prior to the experiment (all stock solutions at 10 mM dissolved in 45% 2-hydroxypropyl-b-cyclodextrin (Invitrogen, USA) were kept at −80°C to minimize auto-oxidation). At 7 dpf larvae were removed from CLZN and rinsed immediately prior to the experiment.

Single animals were placed in a 1 cm diameter (circular arena and allowed to swim freely while being illuminated from all sides with an infrared LED ring light. Behavior was imaged at 50 frames/second using an AVT Pike camera and the maximum single-frame pixel intensity change was measured in a difference image computed online. Bioluminescence was detected using a large active area PMT (H7360-02, Hamamatsu, Japan) abutting the arena, with a bandpass filter to eliminate infrared background. The experimental apparatus was situated in two nested blackout enclosures to block ambient light. Acquisition was carried out using custom software written in LabView and C++; analysis was performed using custom MATLAB (Natick, MA) scripts.

Statistics

All error bars show mean ± SEM over fish. Significance was reported as follows: *p<0.05, **p<0.01, ***p<0.001. Significance was determined using the Paired Student's T-test for paired data and the Wilcoxon rank sum test for independent samples, except for drug treatments, where the Wilcoxon signed rank test was used for analysis of 5-HT drug effects. One-way ANOVA with Tukey-Kramer corrections were used when comparing fish using multiple parameters.

Chapter 5: Conclusions

The work of a scientist is never truly complete. As described in each of these chapters, there are experiments still in progress, as well as future directions I am hoping to achieve, and I have highlighted those that I believe are the most pertinent. From these semi-finished works though there are already a number of insights that we can begin to draw.

First, I hope I have convinced the reader of the utility of the larval zebrafish model in studying behaviors beyond simple sensorimotor or reflexive actions. The small and simple, yet anatomically homologous brain of the larval zebrafish makes it a potent model for the large-scale dissection of neural circuits controlling behavior. So far it has been underutilized in the study of motivated behaviors, especially given its relatively large hypothalamus with many conserved neuromodulatory populations. While there are, understandably, differences between zebrafish and mammalian neural circuits, this vertebrate model will likely bridge a massive gap in our understanding of the evolution of circuits controlling our basic homeostatic drives.

Next, there are a number of underlying principles that we can derive from this research. None of these is uniquely novel, but they may resonate as recurring biological themes in research across different species. I have attempted to summarize these themes below:

Single neuromodulator, convergent inputs

I have presented a few examples of how a single modulatory circuit can integrate multiple inputs of diverse sensory modalities and also valences. Hypothalamic OXT neurons not only respond to a range of noxious stimuli, from heat and also damage-sensing neurons, but also olfactory and possible other stimuli encoding social state. These stimuli of opposite valence -- noxious stimuli are aversive, and social input generally rewarding -- drive the activity of OXT neurons in opposite directions. At the same time, different subpopulations (e.g. magnocellular or parvocellular) of OXT neurons, which project to diverse areas of the brain, may respond differentially to different types of stimuli. Thus the OXT network, while capable of integrating multiple inputs, may also be able to discriminate between them through cell-type specific responses. Volumetric imaging of the entire OXT network in response to distinct stimuli will be crucial in helping elucidate the function of these sub-circuits.

We have demonstrated that the serotonergic raphe nucleus receives sensory input reporting the presence of food. These results are interesting given the numerous other stimuli that the zebrafish raphe has been reported to respond to, including water flow, electric shock and light (which suppresses its activity). Is there a general underlying principle with regards to raphe function, or could different neurons within the network encode different stimuli of positive and negative valence? Again, volumetric imaging of the raphe network in response to numerous positive and negative stimuli may be key to help understand how diverse inputs are encoded in the raphe.

Single neuromodulator, multiple behaviors

We have now also encountered examples of how a single neuromodulator, either released from the same region, or by anatomically segregated populations, can control diverse downstream behaviors. Hypothalamic OXT neurons in the zebrafish preoptic area not only receive input from multiple stimuli but also control multiple downstream circuits such as those for defense and appetite. Our results suggest that driving OXT neurons can generate a pain avoidance response. At the same time, both the literature and our current data support a role for OXT neurons in suppressing food intake. We suggest that OXT neurons mediate these distinct behaviors through different projection patterns. Pain avoidance is likely mediated by hindbrain/spinal circuits, whereas appetite suppression could be mediated by hypothalamic projections or the release of OXT into the circulation. Since both of these behaviors are somewhat complementary – in a stressful situation both more readily escaping and reducing feeding would generally be a beneficial strategy for defending oneself against immediate harm – it is not inconceivable that the exact same neurons/neuron population could respond to the same inputs but mediate these different but complementary behaviors via different output pathways.

We have found that 5-HT signaling in the larval zebrafish is also very complex. Unlike in mammals, larval zebrafish contain multiple 5-HT populations, which may then have been centralized to the raphe over evolution. An increase in raphe firing appears to promote feeding by reporting the discovery of food. As we have previously discussed, it likely plays a role in many other behaviors, including arousal, reward, punishment and

learning. However, its role in a hungry fish appears to be dominated by that of the caudal hypothalamus (cH), whose reduction in activity is what releases lateral hypothalamic activity to drive food intake. At the same time, high cH 5-HT signaling during food-deprivation may very well play a role in driving food-seeking behavior in the absence of food, or at least reporting a negative valence, energy deficit state. Thus, even within the same 5-HT population, 5-HT signaling may serve multiple functions.

We have presented evidenced that the raphe and cH 5-HT neurons may converge on lateral hypothalamic loci. Furthermore, the raphe sends extensive projections to the cH and inhibits its activity. Thus, these anatomically distinct 5-HT populations may not only interact with downstream targets, but possibly also with each other, again highlighting the complex roles of a single neuromodulator in controlling brain function.

Single neuromodulator, multiple timescales

It is also clear that neuromodulators and their secreting neurons can act on different timescales. OXT neurons respond at short latencies to acute input from TRPA1 pain receptors. At the same time, they integrate social information, over minutes or hours, to influence the animal's behavior. Our mutant studies suggest the possibility that long-term inhibition of OXT signaling may have additional effects on social behavior, over the time course of development, which will be explored further. It is possible that OXT may be required for experience-dependent modulation of social behavior, but may also affect social behavior on a more rapid timescale.

The cH also signals on multiple timescales. As a reporter of satiation state, it gradually increases its activity over the course of food deprivation, plateauing after more than hour. However, within 5 minutes of food presentation, its activity is completely reversed. Thus, the cH can encode long-term information about energy status, and short-term information about food availability.

Single cell-type, multiple chemical transmitters

In our study of modulatory circuits we have encountered the phenomenon of co-transmission, for example, the co-expression of glutamate in OXT neurons. We show that while OXT is sufficient to drive large angle tail bends, it is not necessary for this behavior, since stimulation of OXT-depleted neurons can still drive tail bends. However, the absence of OXT reduces the frequency of large-angle tail bends elicited by OXT neuron stimulation, suggesting that OXT may serve to boost the effect of glutamate on locomotor drive. It is possible that while glutamate may provide some spatial temporal precision in signaling to downstream neurons, OXT may be able to diffuse farther or exert longer-term effects on downstream circuits (plasticity, pain relief, wound healing etc). Since peptide-containing vesicles tend to be released only when firing rates are extremely high, OXT may only be released during very strong activation of OXT neurons, to synergistically enhance pain avoidance responses.

In contrast, the effect of OXT neurons on appetite appears to be more dependent on the neuropeptide itself, since OXT antagonists and agonists are sufficient change affect food intake, and OXT mutants show an interesting modulation in behavior. Thus

depending on the downstream targets, the relative importance of different chemical transmitters may vary to add more flexibility to behavior.

State-dependent control of brain activity and behavior

My thesis work furthermore provides examples of how brain activity and behavior can be modulated by context or internal state. Since OXT neuron activity is modulated by social cues, it integrates information about the animal's social context. This information is then used to modulate the animal's response to other sensory cues, such as painful stimuli, or food. Thus, OXT neurons exert social state-dependent effects on multiple behaviors.

I have also shown that the activity of the serotonergic cH is modulated by satiation state. In the states of hunger, satiety, and voracious eating, cH neurons signal at different activity levels (high, medium and low respectively) and in doing so shape an animal's behavioral responses. Furthermore, the raphe nucleus may play a more important role in controlling food intake in a satiated animal, but is more dispensable in a hungry fish. Thus, the effects of these distinct serotonergic populations on behavior are satiation state-dependent, and as a consequence, opposite effects from systemic 5-HT manipulations are observed depending on whether the animal is hungry or full. Indeed, our interpretation of an animal's brain activity and behavior cannot be complete without taking into consideration its external context and internal state.

Mutually opposing activity states

For every group of neurons that performs one function, we can usually find another that acts in an opposite manner. This is a mechanism for homeostasis, and also allows efficient switching between different behavioral states. A prominent example would be the opposing signaling states of the lateral and medial hypothalamus during hunger, satiety and voracious feeding. When the lateral hypothalamus is active, the medial hypothalamus is inhibited, and vice versa, and these populations likely mutually inhibit each other, permitting the “flip-flopping” between two states.

These opposing activity states furthermore map onto behavioral states. For example, the activity patterns during hunger and voracious eating are opposite of one another, even though in both phases the fish is technically “hungry”. This suggests that hunger in the *absence* of food and hunger in the *presence* of food are in fact distinct and may control non-overlapping sets of behaviors. There is support for this idea in the literature, and our work on larval zebrafish appetite circuits has lent support for this model.

Motivated behaviors interact

Finally, as highlighted in the introduction, there is overlap and interactions between circuits controlling different motivated behaviors. The raphe nucleus, which we implicate in the regulation of feeding, has also been implicated in arousal, reward and aversive learning behaviors, and it will be interesting to explore its role within each of these intersecting circuits. I have also demonstrated an interaction between defense,

appetite, and an animal's social context, which intersect (albeit not exclusively) at the level of OXT neurons. A painful stimulus that activates OXT neurons would likely suppress appetite, and social isolation, which also activates OXT neurons, would likely enhance pain responses. This combinatorial assortment of interactions allows for specific but conditional control of behavior.

Conclusion

The above is just a taste of the motifs we might expect to find as we comb the animal world for insights into the human mind. While general principles such as those described can be derived from any and all species; the larval zebrafish, being amenable to circuit dissection across multiple conserved brain regions, sensory stimuli and behaviors, will hopefully continue to provide novel insights into how our brains perform the homeostatic tasks necessary for survival in a complex environment.

Bibliography

1. Bargmann, C. I. & Marder, E. From the connectome to brain function. *Nat. Methods* **10,** 483–490 (2013).

2. Marder, E. Neuromodulation of neuronal circuits: back to the future. *Neuron* **76,** 1–11 (2012).

3. Bargmann, C. I. Beyond the connectome: how neuromodulators shape neural circuits. *Bioessays* **34,** 458–65 (2012).

4. Nadim, F. & Bucher, D. Neuromodulation of neurons and synapses. *Curr. Opin. Neurobiol.* **29,** 48–56 (2014).

5. Nusbaum, M. The roles of co-transmission in neural network modulation. *Trends Neurosci.* **24,** 146–154 (2001).

6. Inagaki, H. K. *et al.* Visualizing Neuromodulation In Vivo: TANGO-Mapping of Dopamine Signaling Reveals Appetite Control of Sugar Sensing. *Cell* **148,** 583–595 (2012).

7. Fields, H. State-dependent opioid control of pain. *Nat. Rev. Neurosci.* **5,** 565–75 (2004).

8. Miles, G. B. & Sillar, K. T. Neuromodulation of vertebrate locomotor control networks. *Physiology (Bethesda).* **26,** 393–411 (2011).

9. Hoffman, P. L., Rabe, C. S., Moses, F. & Tabakoff, B. N-methyl-D-aspartate receptors and ethanol: inhibition of calcium flux and cyclic GMP production. *J. Neurochem.* **52,** 1937–1940 (1989).

10. Sternson, S. M. Hypothalamic survival circuits: blueprints for purposive behaviors. *Neuron* **77,** 810–24 (2013).

11. LeDoux, J. Rethinking the emotional brain. *Neuron* **73,** 653–76 (2012).

12. Swaab, D. F. Neuropeptides in hypothalamic neuronal disorders. *Int. Rev. Cytol.* **240,** 305–75 (2004).

13. DiLeone, R. J., Georgescu, D. & Nestler, E. J. Lateral hypothalamic neuropeptides in reward and drug addiction. *Life Sci.* **73,** 759–68 (2003).

14. Dileone, R. J., Taylor, J. R. & Picciotto, M. R. The drive to eat: comparisons and distinctions between mechanisms of food reward and drug addiction. *Nat. Neurosci.* **15,** 1330–1335 (2012).

15. Berridge, K. C. Motivation concepts in behavioral neuroscience. *Physiol. Behav.*

81, 179–209 (2004).

16. Pearson, C. A. & Placzek, M. Development of the medial hypothalamus: forming a functional hypothalamic-neurohypophyseal interface. *Curr. Top. Dev. Biol.* **106,** 49–88 (2013).

17. Saper, C. B. & Lowell, B. B. The hypothalamus. *Curr. Biol.* **24,** R1111–6 (2014).

18. Bard, P. A diencephalic mechanism for the expression of rage with special reference to the sympathetic nervous system. *Am. J. Physiol.* **84,** 490–515 (1928).

19. Canteras, N. S. The medial hypothalamic defensive system: Hodological organization and functional implications. *Pharmacol. Biochem. Behav.* **71,** 481–491 (2002).

20. Brown, J., Hunsperger, R. & Rosvold, H. E. Defence, attack, and flight elicited by electrical stimulation of the hypothalamus of the cat. *Exp. Brain Res.* **8,** (1969).

21. WASMAN, M. & FLYNN, J. P. Directed Attack Elicited from Hypothalamus. *Arch. Neurol.* **6,** 220–227 (1962).

22. Nakao, H. Emotional Behavior Produced by Hypothalamic Stimulation. *Am J Physiol -- Leg. Content* **194,** 411–418 (1958).

23. DELGADO, J. M. R. & ANAND, B. K. Increase of food intake induced by electrical stimulation of the lateral hypothalamus. *Am. J. Physiol.* **172,** 162–8 (1953).

24. BROBECK, J. R., LARSSON, S. & REYES, E. A study of the electrical activity of the hypothalamic feeding mechanism. *J. Physiol.* **132,** 358–64 (1956).

25. Mogenson, G. J. & Stevenson, J. A. Drinking induced by electrical stimulation of the lateral hypothalamus. *Exp. Neurol.* **17,** 119–27 (1967).

26. Mendelson, J. Lateral Hypothalamic Stimulation: Inhibition of Aversive Effects by Feeding, Drinking, and Gnawing. *Science (80-.).* **166,** 1431–1433 (1969).

27. Woodworth, C. H. Attack elicited in rats by electrical stimulation of the lateral hypothalamus. *Physiol. Behav.* **6,** 345–53 (1971).

28. ANAND, B. K. & BROBECK, J. R. Hypothalamic control of food intake in rats and cats. *Yale J. Biol. Med.* **24,** 123–40 (1951).

29. TEITELBAUM, P. & EPSTEIN, A. N. The lateral hypothalamic syndrome: recovery of feeding and drinking after lateral hypothalamic lesions. *Psychol. Rev.* **69,** 74–90 (1962).

30. Krasne, F. B. General Disruption Resulting from Electrical Stimulus of

Ventromedial Hypothalamus. *Science* **138,** 822–3 (1962).

31. Hoebel, B. G. Hypothalamic Lesions by Electrocauterization: Disinhibition of Feeding and Self-Stimulation. *Science* **149,** 452–3 (1965).

32. MARGULES, D. L. & OLDS, J. Identical 'feeding' and 'rewarding' systems in the lateral hypothalamus of rats. *Science* **135,** 374–5 (1962).

33. HOEBEL, B. G. & TEITELBAUM, P. Hypothalamic control of feeding and self-stimulation. *Science* **135,** 375–7 (1962).

34. Bentham, J. *An Introduction to the Principles of Morals and Legislation.* (Oxford: Clarendon Press., 1907).

35. Gross, C. T. & Canteras, N. S. The many paths to fear. *Nat. Rev. Neurosci.* **13,** 651–8 (2012).

36. Kunwar, P. S. *et al.* Ventromedial hypothalamic neurons control a defensive emotion state. *eLife* (2015). at <http://authors.library.caltech.edu/56065/1/e06633.full.pdf>

37. Wang, L., Chen, I. Z. & Lin, D. Collateral Pathways from the Ventromedial Hypothalamus Mediate Defensive Behaviors. *Neuron* **85,** 1344–1358 (2015).

38. Clarke, R. W. & Harris, J. The organization of motor responses to noxious stimuli. *Brain Res. Brain Res. Rev.* **46,** 163–72 (2004).

39. Ossipov, M. H., Dussor, G. O. & Porreca, F. Central modulation of pain. *J. Clin. Invest.* **120,** 3779–87 (2010).

40. Bolles, R. C. & Fanselow, M. S. A perceptual-defensive-recuperative model of fear and pain. *Behav. Brain Sci.* **3,** 291 (2010).

41. Siegfried, B., Frischknecht, H.-R. & Nunes de Souza, R. L. An ethological model for the study of activation and interaction of pain, memory and defensive systems in the attacked mouse. Role of endogenous opioids. *Neurosci. Biobehav. Rev.* **14,** 481–490 (1990).

42. Condés-Lara, M., Rojas-Piloni, G., Martínez-Lorenzana, G. & Rodríguez-Jiménez, J. Paraventricular hypothalamic oxytocinergic cells responding to noxious stimulation and projecting to the spinal dorsal horn represent a homeostatic analgesic mechanism. *Eur. J. Neurosci.* **30,** 1056–63 (2009).

43. Lumb, B. M. Hypothalamic and Midbrain Circuitry That Distinguishes Between Escapable and Inescapable Pain. *News Physiol. Sci.* **19,** 22–26 (2004).

44. Lumb, B. M. & Lovick, T. A. The rostral hypothalamus: an area for the integration of autonomic and sensory responsiveness. *J Neurophysiol* **70,** 1570–1577 (1993).

45. Condés-Lara, M. *et al.* Hypothalamic paraventricular nucleus stimulation enhances c-Fos expression in spinal and supraspinal structures related to pain modulation. *Neurosci. Res.* **98,** 59–63 (2015).

46. Amit, Z. & Galina, Z. H. Stress-induced analgesia: adaptive pain suppression. *Physiol Rev* **66,** 1091–1120 (1986).

47. Fields, H. L., Heinricher, M. M. & Mason, P. Neurotransmitters in nociceptive modulatory circuits. *Annu. Rev. Neurosci.* **14,** 219–45 (1991).

48. Rojas-Piloni, G. *et al.* Oxytocin, but not vassopressin, modulates nociceptive responses in dorsal horn neurons. *Neurosci. Lett.* **476,** 32–5 (2010).

49. DeLaTorre, S. *et al.* Paraventricular oxytocinergic hypothalamic prevention or interruption of long-term potentiation in dorsal horn nociceptive neurons: electrophysiological and behavioral evidence. *Pain* **144,** 320–8 (2009).

50. Rojas-Piloni, G., Martínez-Lorenzana, G., DelaTorre, S. & Condés-Lara, M. Nociceptive spinothalamic tract and postsynaptic dorsal column neurons are modulated by paraventricular hypothalamic activation. *Eur. J. Neurosci.* **28,** 546–58 (2008).

51. Eliava, M. *et al.* A New Population of Parvocellular Oxytocin Neurons Controlling Magnocellular Neuron Activity and Inflammatory Pain Processing. *Neuron* **89,** 1291–304 (2016).

52. STRATAKIS, C. A. & CHROUSOS, G. P. Neuroendocrinology and Pathophysiology of the Stress System. *Ann. N. Y. Acad. Sci.* **771,** 1–18 (1995).

53. Charmandari, E., Tsigos, C. & Chrousos, G. Endocrinology of the stress response. *Annu. Rev. Physiol.* **67,** 259–84 (2005).

54. Berridge, C. W. & Waterhouse, B. D. The locus coeruleus–noradrenergic system: modulation of behavioral state and state-dependent cognitive processes. *Brain Res. Rev.* **42,** 33–84 (2003).

55. Rodrigues, S. M., LeDoux, J. E. & Sapolsky, R. M. The influence of stress hormones on fear circuitry. *Annu. Rev. Neurosci.* **32,** 289–313 (2009).

56. Korte, S. . Corticosteroids in relation to fear, anxiety and psychopathology. *Neurosci. Biobehav. Rev.* **25,** 117–142 (2001).

57. Sapolsky, R. M., Romero, L. M. & Munck, A. U. How do glucocorticoids influence stress responses? Integrating permissive, suppressive, stimulatory, and preparative actions. *Endocr. Rev.* **21,** 55–89 (2000).

58. Rash, J. A., Aguirre-Camacho, A. & Campbell, T. S. Oxytocin and pain: a systematic review and synthesis of findings. *Clin. J. Pain* **30,** 453–62 (2014).

59. Piekut, D. T., Pretel, S. & Applegate, C. D. Activation of oxytocin-containing neurons of the paraventricular nucleus (PVN) following generalized seizures. *Synapse* **23,** 312–20 (1996).

60. Onaka, T. Neural pathways controlling central and peripheral oxytocin release during stress. *J. Neuroendocrinol.* **16,** 308–12 (2004).

61. Jezova, D., Skultetyova, I., Tokarev, D. I., Bakos, P. & Vigas, M. Vasopressin and oxytocin in stress. *Ann. N. Y. Acad. Sci.* **771,** 192–203 (1995).

62. Neumann, I. D. *Vasopressin and Oxytocin: From Genes to Clinical Applications*. *Progress in Brain Research* **139,** (Elsevier, 2002).

63. Neumann, I. D. Involvement of the brain oxytocin system in stress coping: interactions with the hypothalamo-pituitary-adrenal axis. *Prog. Brain Res.* **139,** 147–62 (2002).

64. Knobloch, H. S. *et al.* Evoked axonal oxytocin release in the central amygdala attenuates fear response. *Neuron* **73,** 553–66 (2012).

65. Maslow, A. H. A theory of human motivation. *Psychol. Rev.* **50,** 370–396 (1943).

66. Gao, Q. & Horvath, T. L. Neurobiology of feeding and energy expenditure. *Annu. Rev. Neurosci.* **30,** 367–98 (2007).

67. Cone, R. D. Anatomy and regulation of the central melanocortin system. *Nat. Neurosci.* **8,** 571–578 (2005).

68. Yaswen, L., Diehl, N., Brennan, M. B. & Hochgeschwender, U. Obesity in the mouse model of pro-opiomelanocortin deficiency responds to peripheral melanocortin. *Nat. Med.* **5,** 1066–70 (1999).

69. Huszar, D. *et al.* Targeted disruption of the melanocortin-4 receptor results in obesity in mice. *Cell* **88,** 131–41 (1997).

70. Ollmann, M. M. *et al.* Antagonism of central melanocortin receptors in vitro and in vivo by agouti-related protein. *Science* **278,** 135–8 (1997).

71. Qian, S. *et al.* Neither agouti-related protein nor neuropeptide Y is critically required for the regulation of energy homeostasis in mice. *Mol. Cell. Biol.* **22,** 5027–35 (2002).

72. Gropp, E. *et al.* Agouti-related peptide-expressing neurons are mandatory for feeding. *Nat. Neurosci.* **8,** 1289–91 (2005).

73. Luquet, S., Perez, F. A., Hnasko, T. S. & Palmiter, R. D. NPY/AgRP neurons are essential for feeding in adult mice but can be ablated in neonates. *Science* **310,** 683–5 (2005).

74. Flier, J. S. AgRP in energy balance: Will the real AgRP please stand up? *Cell Metab.* **3,** 83–5 (2006).

75. Cowley, M. A. *et al.* Leptin activates anorexigenic POMC neurons through a neural network in the arcuate nucleus. *Nature* **411,** 480–4 (2001).

76. Krashes, M. J. *et al.* Rapid, reversible activation of AgRP neurons drives feeding behavior in mice. *J. Clin. Invest.* **121,** 1424–8 (2011).

77. Aponte, Y., Atasoy, D. & Sternson, S. M. AGRP neurons are sufficient to orchestrate feeding behavior rapidly and without training. *Nat. Neurosci.* **14,** 351–5 (2011).

78. Atasoy, D., Betley, J. N., Su, H. H. & Sternson, S. M. Deconstruction of a neural circuit for hunger. *Nature* **488,** 172–7 (2012).

79. Betley, J. N., Cao, Z. F. H., Ritola, K. D. & Sternson, S. M. Parallel, redundant circuit organization for homeostatic control of feeding behavior. *Cell* **155,** 1337–50 (2013).

80. Williams, K. W. & Elmquist, J. K. From neuroanatomy to behavior: central integration of peripheral signals regulating feeding behavior. *Nat. Neurosci.* **15,** 1350–5 (2012).

81. Ibrahim, N. *et al.* Hypothalamic proopiomelanocortin neurons are glucose responsive and express K(ATP) channels. *Endocrinology* **144,** 1331–40 (2003).

82. Yang, Y., Atasoy, D., Su, H. H. & Sternson, S. M. Hunger states switch a flip-flop memory circuit via a synaptic AMPK-dependent positive feedback loop. *Cell* **146,** 992–1003 (2011).

83. Chen, Y., Lin, Y.-C., Kuo, T.-W. & Knight, Z. A. Sensory Detection of Food Rapidly Modulates Arcuate Feeding Circuits. *Cell* **160,** 829–841 (2015).

84. Mandelblat-Cerf, Y. *et al.* Arcuate hypothalamic AgRP and putative POMC neurons show opposite changes in spiking across multiple timescales. *Elife* **4,** e07122 (2015).

85. Betley, J. N. *et al.* Neurons for hunger and thirst transmit a negative-valence teaching signal. *Nature* **521,** 180–185 (2015).

86. Dietrich, M. O., Zimmer, M. R., Bober, J. & Horvath, T. L. Hypothalamic Agrp neurons drive stereotypic behaviors beyond feeding. *Cell* **160,** 1222–32 (2015).

87. Balthasar, N. *et al.* Leptin receptor signaling in POMC neurons is required for normal body weight homeostasis. *Neuron* **42,** 983–91 (2004).

88. Dhillon, H. *et al.* Leptin directly activates SF1 neurons in the VMH, and this action

by leptin is required for normal body-weight homeostasis. *Neuron* **49,** 191–203 (2006).

89. Sternson, S. M., Shepherd, G. M. G. & Friedman, J. M. Topographic mapping of VMH --> arcuate nucleus microcircuits and their reorganization by fasting. *Nat. Neurosci.* **8,** 1356–63 (2005).

90. Stuber, G. D. & Wise, R. A. Lateral hypothalamic circuits for feeding and reward. *Nat. Neurosci.* **19,** 198–205 (2016).

91. Berthoud, H.-R. & Münzberg, H. The lateral hypothalamus as integrator of metabolic and environmental needs: from electrical self-stimulation to opto-genetics. *Physiol. Behav.* **104,** 29–39 (2011).

92. Wise, R. A. Lateral hypothalamic electrical stimulation: does it make animals 'hungry'? *Brain Res.* **67,** 187–209 (1974).

93. Brown, J. A., Woodworth, H. L. & Leinninger, G. M. To ingest or rest? Specialized roles of lateral hypothalamic area neurons in coordinating energy balance. *Front. Syst. Neurosci.* **9,** 9 (2015).

94. Ono, T., Nakamura, K., Nishijo, H. & Fukuda, M. Hypothalamic neuron involvement in integration of reward, aversion, and cue signals. *J. Neurophysiol.* **56,** 63–79 (1986).

95. Jennings, J. H. *et al.* Visualizing Hypothalamic Network Dynamics for Appetitive and Consummatory Behaviors. *Cell* **160,** 516–527 (2015).

96. Nieh, E. H. *et al.* Decoding neural circuits that control compulsive sucrose seeking. *Cell* **160,** 528–41 (2015).

97. Jennings, J. H., Rizzi, G., Stamatakis, A. M., Ung, R. L. & Stuber, G. D. The inhibitory circuit architecture of the lateral hypothalamus orchestrates feeding. *Science* **341,** 1517–21 (2013).

98. Harris, G. C., Wimmer, M. & Aston-Jones, G. A role for lateral hypothalamic orexin neurons in reward seeking. *Nature* **437,** 556–9 (2005).

99. Adamantidis, A. R., Zhang, F., Aravanis, A. M., Deisseroth, K. & de Lecea, L. Neural substrates of awakening probed with optogenetic control of hypocretin neurons. *Nature* **450,** 420–4 (2007).

100. Hara, J. *et al.* Genetic ablation of orexin neurons in mice results in narcolepsy, hypophagia, and obesity. *Neuron* **30,** 345–54 (2001).

101. Lam, D. D., Garfield, A. S., Marston, O. J., Shaw, J. & Heisler, L. K. Brain serotonin system in the coordination of food intake and body weight. *Pharmacol. Biochem. Behav.* **97,** 84–91 (2010).

102. Voigt, J.-P. & Fink, H. Serotonin controlling feeding and satiety. *Behav. Brain Res.* **277,** 14–31 (2015).

103. Xu, Y. *et al.* A serotonin and melanocortin circuit mediates D-fenfluramine anorexia. *J. Neurosci.* **30,** 14630–4 (2010).

104. Xu, Y. *et al.* 5-HT2CRs expressed by pro-opiomelanocortin neurons regulate energy homeostasis. *Neuron* **60,** 582–9 (2008).

105. Heisler, L. K. *et al.* Serotonin reciprocally regulates melanocortin neurons to modulate food intake. *Neuron* **51,** 239–49 (2006).

106. Heisler, L. K. *et al.* Activation of central melanocortin pathways by fenfluramine. *Science* **297,** 609–11 (2002).

107. Collin, M., Bäckberg, M., Onnestam, K. & Meister, B. 5-HT1A receptor immunoreactivity in hypothalamic neurons involved in body weight control. *Neuroreport* **13,** 945–51 (2002).

108. Muraki, Y. *et al.* Serotonergic regulation of the orexin/hypocretin neurons through the 5-HT1A receptor. *J. Neurosci.* **24,** 7159–66 (2004).

109. Fletcher, P. J. & Burton, M. J. Effects of manipulations of peripheral serotonin on feeding and drinking in the rat. *Pharmacol. Biochem. Behav.* **20,** 835–40 (1984).

110. Pollock, J. D. & Rowland, N. Peripherally administered serotonin decreases food intake in rats. *Pharmacol. Biochem. Behav.* **15,** 179–83 (1981).

111. Gaudry, Q. & Kristan, W. B. Decision points: the factors influencing the decision to feed in the medicinal leech. *Front. Neurosci.* **6,** 101 (2012).

112. Horvitz, H. R., Chalfie, M., Trent, C., Sulston, J. E. & Evans, P. D. Serotonin and octopamine in the nematode Caenorhabditis elegans. *Science* **216,** 1012–4 (1982).

113. Sze, J. Y., Victor, M., Loer, C., Shi, Y. & Ruvkun, G. Food and metabolic signalling defects in a Caenorhabditis elegans serotonin-synthesis mutant. *Nature* **403,** 560–4 (2000).

114. Gasque, G., Conway, S., Huang, J., Rao, Y. & Vosshall, L. B. Small molecule drug screening in Drosophila identifies the 5HT2A receptor as a feeding modulation target. *Sci. Rep.* **3,** srep02120 (2013).

115. Shimada, Y., Hirano, M., Nishimura, Y. & Tanaka, T. A high-throughput fluorescence-based assay system for appetite-regulating gene and drug screening. *PLoS One* **7,** e52549 (2012).

116. Weinberger, J. & Klaper, R. Environmental concentrations of the selective

serotonin reuptake inhibitor fluoxetine impact specific behaviors involved in reproduction, feeding and predator avoidance in the fish Pimephales promelas (fathead minnow). *Aquat. Toxicol.* **151,** 77–83 (2014).

117. Pérez Maceira, J. J., Mancebo, M. J. & Aldegunde, M. The involvement of 5-HT-like receptors in the regulation of food intake in rainbow trout (Oncorhynchus mykiss). *Comp. Biochem. Physiol. C. Toxicol. Pharmacol.* **161,** 1–6 (2014).

118. Elipot, Y., Hinaux, H., Callebert, J. & Rétaux, S. Evolutionary shift from fighting to foraging in blind cavefish through changes in the serotonin network. *Curr. Biol.* **23,** 1–10 (2013).

119. Elipot, Y. *et al.* A mutation in the enzyme monoamine oxidase explains part of the Astyanax cavefish behavioural syndrome. *Nat. Commun.* **5,** 3647 (2014).

120. Nakamura, K. The role of the dorsal raphé nucleus in reward-seeking behavior. *Front. Integr. Neurosci.* **7,** 60 (2013).

121. Cohen, J. Y., Amoroso, M. W. & Uchida, N. Serotonergic neurons signal reward and punishment on multiple timescales. *Elife* **4,** (2015).

122. Sternson, S. M., Nicholas Betley, J. & Cao, Z. F. H. Neural circuits and motivational processes for hunger. *Curr. Opin. Neurobiol.* **23,** 353–60 (2013).

123. Bromberg-Martin, E. S., Matsumoto, M. & Hikosaka, O. Dopamine in motivational control: rewarding, aversive, and alerting. *Neuron* **68,** 815–834 (2010).

124. Cohen, J. Y., Haesler, S., Vong, L., Lowell, B. B. & Uchida, N. Neuron-type-specific signals for reward and punishment in the ventral tegmental area. *Nature* (2012). doi:10.1038/nature10754

125. Watabe-Uchida, M., Zhu, L., Ogawa, S. K., Vamanrao, A. & Uchida, N. Whole-brain mapping of direct inputs to midbrain dopamine neurons. *Neuron* **74,** 858–73 (2012).

126. Domingos, A. I. *et al.* Leptin regulates the reward value of nutrient. *Nat. Neurosci.* **14,** 1562–8 (2011).

127. Hommel, J. D. *et al.* Leptin receptor signaling in midbrain dopamine neurons regulates feeding. *Neuron* **51,** 801–10 (2006).

128. Berridge, K. C. 'Liking' and 'wanting' food rewards: brain substrates and roles in eating disorders. *Physiol. Behav.* **97,** 537–50 (2009).

129. Volkow, N. D., Wang, G.-J. & Baler, R. D. Reward, dopamine and the control of food intake: implications for obesity. *Trends Cogn. Sci.* **15,** 37–46 (2011).

130. Berridge, K. C. & Robinson, T. E. What is the role of dopamine in reward: hedonic

impact, reward learning, or incentive salience? *Brain Res. Rev.* **28,** 309–369 (1998).

131. Smith, K. S. & Berridge, K. C. The ventral pallidum and hedonic reward: neurochemical maps of sucrose 'liking' and food intake. *J. Neurosci.* **25,** 8637–49 (2005).

132. Navratilova, E. & Porreca, F. Reward and motivation in pain and pain relief. *Nat. Neurosci.* **17,** 1304–12 (2014).

133. Gerber, B. *et al.* Pain-relief learning in flies, rats, and man: basic research and applied perspectives. *Learn. Mem.* **21,** 232–52 (2014).

134. Budygin, E. A. *et al.* Aversive stimulus differentially triggers subsecond dopamine release in reward regions. *Neuroscience* **201,** 331–7 (2012).

135. Maniam, J. & Morris, M. J. The link between stress and feeding behaviour. *Neuropharmacology* **63,** 97–110 (2012).

136. Bazhan, N. & Zelena, D. Food-intake regulation during stress by the hypothalamo-pituitary-adrenal axis. *Brain Res. Bull.* **95,** 46–53 (2013).

137. Arase, K., York, D. A., Shimizu, H., Shargill, N. & Bray, G. A. Effects of corticotropin-releasing factor on food intake and brown adipose tissue thermogenesis in rats. *Am. J. Physiol.* **255,** E255–9 (1988).

138. Gyengesi, E. *et al.* Corticosterone regulates synaptic input organization of POMC and NPY/AgRP neurons in adult mice. *Endocrinology* **151,** 5395–402 (2010).

139. Wanat, M. J., Hopf, F. W., Stuber, G. D., Phillips, P. E. M. & Bonci, A. Corticotropin-releasing factor increases mouse ventral tegmental area dopamine neuron firing through a protein kinase C-dependent enhancement of Ih. *J. Physiol.* **586,** 2157–70 (2008).

140. Ambroggi, F. *et al.* Stress and addiction: glucocorticoid receptor in dopaminoceptive neurons facilitates cocaine seeking. *Nat. Neurosci.* **12,** 247–9 (2009).

141. Nelson, D. L. & Gehlert, D. R. Central nervous system biogenic amine targets for control of appetite and energy expenditure. *Endocrine* **29,** 49–60 (2006).

142. Macosko, E. Z. *et al.* A hub-and-spoke circuit drives pheromone attraction and social behaviour in C. elegans. *Nature* **458,** 1171–5 (2009).

143. Ramdya, P. *et al.* Mechanosensory interactions drive collective behaviour in Drosophila. *Nature* **519,** 233–6 (2015).

144. Sokolowski, M. B. Social interactions in 'simple' model systems. *Neuron* **65,** 780–

94 (2010).

145. Kikusui, T., Winslow, J. T. & Mori, Y. Social buffering: relief from stress and anxiety. *Philos. Trans. R. Soc. Lond. B. Biol. Sci.* **361,** 2215–28 (2006).

146. DeVries, A. C., Glasper, E. R. & Detillion, C. E. Social modulation of stress responses. *Physiol. Behav.* **79,** 399–407 (2003).

147. D'Amato, F. R. Kin interaction enhances morphine analgesia in male mice. *Behav. Pharmacol.* **9,** 369–73 (1998).

148. Panksepp, J. & Bishop, P. An autoradiographic map of (3H)diprenorphine binding in rat brain: effects of social interaction. *Brain Res. Bull.* **7,** 405–10 (1981).

149. Dobzhansky, T. Nothing in biology makes sense except in the light of evolution. *Am. Biol. Teach.* (1973).

150. Friedrich, R. W., Jacobson, G. A. & Zhu, P. Circuit neuroscience in zebrafish. *Curr. Biol.* **20,** R371–81 (2010).

151. Matsumoto, M. & Hikosaka, O. Representation of negative motivational value in the primate lateral habenula. *Nat. Neurosci.* **12,** 77–84 (2009).

152. Matsumoto, M. & Hikosaka, O. Lateral habenula as a source of negative reward signals in dopamine neurons. *Nature* **447,** 1111–1115 (2007).

153. Amo, R. *et al.* The Habenulo-Raphe Serotonergic Circuit Encodes an Aversive Expectation Value Essential for Adaptive Active Avoidance of Danger. *Neuron* **84,** 1034–48 (2014).

154. Lee, A. *et al.* The habenula prevents helpless behavior in larval zebrafish. *Curr. Biol.* **20,** 2211–2216 (2010).

155. Tay, T. L., Ronneberger, O., Ryu, S., Nitschke, R. & Driever, W. Comprehensive catecholaminergic projectome analysis reveals single-neuron integration of zebrafish ascending and descending dopaminergic systems. *Nat. Commun.* **2,** 171 (2011).

156. Panula, P. *et al.* The comparative neuroanatomy and neurochemistry of zebrafish CNS systems of relevance to human neuropsychiatric diseases. *Neurobiol. Dis.* **40,** 46–57 (2010).

157. Renninger, S. L. & Orger, M. B. Two-photon imaging of neural population activity in zebrafish. *Methods* **62,** 255–67 (2013).

158. Yang, W. *et al.* Simultaneous Multi-plane Imaging of Neural Circuits. *Neuron* **89,** 269–284 (2016).

159. Watson, B. O. *et al.* Two-photon microscopy with diffractive optical elements and spatial light modulators. *Front. Neurosci.* **4,** (2010).

160. Grewe, B. F., Langer, D., Kasper, H., Kampa, B. M. & Helmchen, F. High-speed in vivo calcium imaging reveals neuronal network activity with near-millisecond precision. *Nat. Methods* **7,** 399–405 (2010).

161. Ahrens, M. B., Orger, M. B., Robson, D. N., Li, J. M. & Keller, P. J. Whole-brain functional imaging at cellular resolution using light-sheet microscopy. *Nat. Methods* **10,** 413–20 (2013).

162. Keller, P. J. & Ahrens, M. B. Visualizing Whole-Brain Activity and Development at the Single-Cell Level Using Light-Sheet Microscopy. *Neuron* **85,** 462–483 (2015).

163. Panier, T. *et al.* Fast functional imaging of multiple brain regions in intact zebrafish larvae using selective plane illumination microscopy. *Front. Neural Circuits* **7,** 65 (2013).

164. Prevedel, R. *et al.* Simultaneous whole-animal 3D imaging of neuronal activity using light-field microscopy. *Nat. Methods* **11,** 727–30 (2014).

165. Ahrens, M. B. *et al.* Brain-wide neural dynamics at single-cell resolution during rapid motor adaptation in larval zebrafish . *Nature* (2011).

166. Randlett, O. *et al.* Whole-brain activity mapping onto a zebrafish brain atlas. *Nat. Methods* **12,** 1039–1046 (2015).

167. Curado, S., Stainier, D. Y. & Anderson, R. M. Nitroreductase-mediated cell/tissue ablation in zebrafish: a spatially and temporally controlled ablation method with applications in developmental and regeneration studies. *Nat. Protoc.* **3,** 948–954 (2008).

168. Portugues, R., Severi, K. E., Wyart, C. & Ahrens, M. B. Optogenetics in a transparent animal: circuit function in the larval zebrafish. *Curr. Opin. Neurobiol.* **23,** 119–26 (2013).

169. Chen, S., Chiu, C. N., McArthur, K. L., Fetcho, J. R. & Prober, D. A. TRP channel mediated neuronal activation and ablation in freely behaving zebrafish. *Nat. Methods* **13,** 147–50 (2015).

170. Huang, K.-H., Ahrens, M. B., Dunn, T. W. & Engert, F. Spinal projection neurons control turning behaviors in zebrafish. *Curr. Biol.* **23,** 1566–73 (2013).

171. Lacoste, A. M. B. *et al.* A convergent and essential interneuron pathway for Mauthner-cell-mediated escapes. *Curr. Biol.* **25,** 1526–34 (2015).

172. Asakawa, K. *et al.* Genetic dissection of neural circuits by Tol2 transposon-mediated Gal4 gene and enhancer trapping in zebrafish. *Proc. Natl. Acad. Sci. U.*

S. A. **105,** 1255–60 (2008).

173. Gagnon, J. A. *et al.* Efficient mutagenesis by Cas9 protein-mediated oligonucleotide insertion and large-scale assessment of single-guide RNAs. *PLoS One* **9,** e98186 (2014).

174. Biran, J., Tahor, M., Wircer, E. & Levkowitz, G. Role of developmental factors in hypothalamic function. *Front. Neuroanat.* **9,** 47 (2015).

175. Kim, C. K. *et al.* Simultaneous fast measurement of circuit dynamics at multiple sites across the mammalian brain. *Nat. Methods* **advance on,** (2016).

176. Yao, Y. *et al.* Visual Cue-Discriminative Dopaminergic Control of Visuomotor Transformation and Behavior Selection. *Neuron* (2016). doi:10.1016/j.neuron.2015.12.036

177. Mu, Y., Li, X., Zhang, B. & Du, J. Visual input modulates audiomotor function via hypothalamic dopaminergic neurons through a cooperative mechanism. *Neuron* **75,** 688–99 (2012).

178. Prober, D. A. *et al.* Zebrafish TRPA1 channels are required for chemosensation but not for thermosensation or mechanosensory hair cell function. *J. Neurosci.* **28,** 10102–10 (2008).

179. Gau, P. *et al.* The zebrafish ortholog of TRPV1 is required for heat-induced locomotion. *J. Neurosci.* **33,** 5249–60 (2013).

180. Haesemeyer, M., Robson, D. N., Li, J. M., Schier, A. F. & Engert, F. The structure and timescales of heat perception in larval zebrafish. *Cell Syst.* **1,** 338–348 (2015).

181. Vom Berg-Maurer, C. M., Trivedi, C. A., Bollmann, J. H., De Marco, R. J. & Ryu, S. The Severity of Acute Stress Is Represented by Increased Synchronous Activity and Recruitment of Hypothalamic CRH Neurons. *J. Neurosci.* **36,** 3350–62 (2016).

182. Ziv, L. *et al.* An affective disorder in zebrafish with mutation of the glucocorticoid receptor. *Mol. Psychiatry* **18,** 681–91 (2013).

183. Griffiths, B. B. *et al.* A zebrafish model of glucocorticoid resistance shows serotonergic modulation of the stress response. *Front. Behav. Neurosci.* **6,** 68 (2012).

184. Yokogawa, T., Hannan, M. C. & Burgess, H. a. The dorsal raphe modulates sensory responsiveness during arousal in zebrafish. *J. Neurosci.* **32,** 15205–15 (2012).

185. Bianco, I. H., Kampff, A. R. & Engert, F. Prey capture behavior evoked by simple

visual stimuli in larval zebrafish. *Front. Syst. Neurosci.* **5,** 101 (2011).

186. Jordi, J. *et al.* A high-throughput assay for quantifying appetite and digestive dynamics. *Am. J. Physiol. Regul. Integr. Comp. Physiol.* ajpregu.00225.2015 (2015). doi:10.1152/ajpregu.00225.2015

187. Buske, C. & Gerlai, R. Shoaling develops with age in Zebrafish (Danio rerio). *Prog. Neuropsychopharmacol. Biol. Psychiatry* **35,** 1409–15 (2011).

188. Dreosti, E., Lopes, G., Kampff, A. R. & Wilson, S. W. Development of social behavior in young zebrafish. *Front. Neural Circuits* **9,** 39 (2015).

189. Hinz, F. I., Aizenberg, M., Tushev, G. & Schuman, E. M. Protein synthesis-dependent associative long-term memory in larval zebrafish. *J. Neurosci.* **33,** 15382–7 (2013).

190. Valente, A., Huang, K. H., Portugues, R. & Engert, F. Ontogeny of classical and operant learning behaviors in zebrafish. *Learn. Mem.* **19,** 170–177 (2012).

191. Onaka, T. *et al.* Medullary A1 noradrenergic neurones may mediate oxytocin release after noxious stimuli. *Neuroreport* **12,** 2499–502 (2001).

192. Grillon, C. *et al.* Oxytocin increases anxiety to unpredictable threat. *Mol. Psychiatry* **18,** 958–60 (2013).

193. Zhu, L. & Onaka, T. Involvement of medullary A2 noradrenergic neurons in the activation of oxytocin neurons after conditioned fear stimuli. *Eur. J. Neurosci.* **16,** 2186–98 (2002).

194. Kubota, N., Amemiya, S., Yanagita, S., Nishijima, T. & Kita, I. Emotional stress evoked by classical fear conditioning induces yawning behavior in rats. *Neurosci. Lett.* **566,** 182–7 (2014).

195. Yan, Y. *et al.* Effect of oxytocin on the behavioral activity in the behavioral despair depression rat model. *Neuropeptides* **48,** 83–9 (2014).

196. Braida, D. *et al.* Neurohypophyseal hormones manipulation modulate social and anxiety-related behavior in zebrafish. *Psychopharmacology (Berl).* **220,** 319–30 (2012).

197. Juif, P.-E. *et al.* Long-lasting spinal oxytocin analgesia is ensured by the stimulation of allopregnanolone synthesis which potentiates GABA(A) receptor-mediated synaptic inhibition. *J. Neurosci.* **33,** 16617–26 (2013).

198. Neumann, I. D. & Landgraf, R. Balance of brain oxytocin and vasopressin: implications for anxiety, depression, and social behaviors. *Trends Neurosci.* **35,** 649–59 (2012).

199. Tracy, L. M., Georgiou-Karistianis, N., Gibson, S. J. & Giummarra, M. J. Oxytocin and the modulation of pain experience: Implications for chronic pain management. *Neurosci. Biobehav. Rev.* **55,** 53–67 (2015).

200. Petersson, M., Eklund, M. & Uvnäs-Moberg, K. Oxytocin decreases corticosterone and nociception and increases motor activity in OVX rats. *Maturitas* **51,** 426–33 (2005).

201. Gong, L. *et al.* Oxytocin-induced membrane hyperpolarization in pain-sensitive dorsal root ganglia neurons mediated by Ca(2+)/nNOS/NO/KATP pathway. *Neuroscience* **289,** 417–28 (2015).

202. Jiang, C.-Y., Fujita, T. & Kumamoto, E. Synaptic modulation and inward current produced by oxytocin in substantia gelatinosa neurons of adult rat spinal cord slices. *J. Neurophysiol.* **111,** 991–1007 (2014).

203. Pearson, S. a, Mouihate, A., Pittman, Q. J. & Whelan, P. J. Peptidergic activation of locomotor pattern generators in the neonatal spinal cord. *J. Neurosci.* **23,** 10154–63 (2003).

204. Barrière, G., Bertrand, S. & Cazalets, J.-R. Peptidergic neuromodulation of the lumbar locomotor network in the neonatal rat spinal cord. *Peptides* **26,** 277–86 (2005).

205. Dose, F., Zanon, P., Coslovich, T. & Taccola, G. Nanomolar oxytocin synergizes with weak electrical afferent stimulation to activate the locomotor CpG of the rat spinal cord in vitro. *PLoS One* **9,** e92967 (2014).

206. Garrison, J. L. *et al.* Oxytocin/vasopressin-related peptides have an ancient role in reproductive behavior. *Science* **338,** 540–3 (2012).

207. Wagenaar, D. a, Hamilton, M. S., Huang, T., Kristan, W. B. & French, K. a. A hormone-activated central pattern generator for courtship. *Curr. Biol.* **20,** 487–95 (2010).

208. Oumi, T. *et al.* Annetocin, an annelid oxytocin-related peptide, induces egg-laying behavior in the earthworm, Eisenia foetida. *J. Exp. Zool.* **276,** 151–6 (1996).

209. van Kesteren, R. E. *et al.* A novel G protein-coupled receptor mediating both vasopressin- and oxytocin-like functions of Lys-conopressin in Lymnaea stagnalis. *Neuron* **15,** 897–908 (1995).

210. Gwee, P.-C., Amemiya, C. T., Brenner, S. & Venkatesh, B. Sequence and organization of coelacanth neurohypophysial hormone genes: evolutionary history of the vertebrate neurohypophysial hormone gene locus. *BMC Evol. Biol.* **8,** 93 (2008).

211. Venkatesh, B. & Brenner, S. Structure and organization of the isotocin and

vasotocin genes from teleosts. *Adv. Exp. Med. Biol.* **395,** 629–38 (1995).

212. Godwin, J. & Thompson, R. Nonapeptides and social behavior in fishes. *Horm. Behav.* **61,** 230–8 (2012).

213. O'Connell, L. A., Matthews, B. J. & Hofmann, H. A. Isotocin regulates paternal care in a monogamous cichlid fish. *Horm. Behav.* **61,** 725–33 (2012).

214. Oldfield, R. G. & Hofmann, H. A. Neuropeptide regulation of social behavior in a monogamous cichlid fish. *Physiol. Behav.* **102,** 296–303 (2011).

215. Knobloch, H. S. & Grinevich, V. Evolution of oxytocin pathways in the brain of vertebrates. *Front. Behav. Neurosci.* **8,** 31 (2014).

216. Herget, U., Wolf, A., Wullimann, M. F. & Ryu, S. Molecular neuroanatomy and chemoarchitecture of the neurosecretory preoptic-hypothalamic area in zebrafish larvae. *J. Comp. Neurol.* **522,** 1542–64 (2014).

217. Sawchenko, P. E. & Swanson, L. W. Immunohistochemical identification of neurons in the paraventricular nucleus of the hypothalamus that project to the medulla or to the spinal cord in the rat. *J. Comp. Neurol.* **205,** 260–72 (1982).

218. Swanson, L. W. & Sawchenko, P. E. Paraventricular nucleus: a site for the integration of neuroendocrine and autonomic mechanisms. *Neuroendocrinology* **31,** 410–7 (1980).

219. Coffey, C. M. *et al.* Novel oxytocin gene expression in the hindbrain is induced by alcohol exposure: transgenic zebrafish enable visualization of sensitive neurons. *PLoS One* **8,** e53991 (2013).

220. Saito, D., Komatsuda, M. & Urano, A. Functional organization of preoptic vasotocin and isotocin neurons in the brain of rainbow trout: central and neurohypophysial projections of single neurons. *Neuroscience* **124,** 973–984 (2004).

221. Ludwig, M. & Leng, G. Dendritic peptide release and peptide-dependent behaviours. *Nat. Rev. Neurosci.* **7,** 126–36 (2006).

222. Swanson, L. W. & Sawchenko, P. E. Hypothalamic integration: organization of the paraventricular and supraoptic nuclei. *Annu. Rev. Neurosci.* **6,** 269–324 (1983).

223. Fujimoto, E., Stevenson, T. J., Chien, C. B. & Bonkowsky, J. L. Identification of a dopaminergic enhancer indicates complexity in vertebrate dopamine neuron phenotype specification. *Dev. Biol.* **352,** 393–404 (2011).

224. Gutierrez-Triana, J. A., Herget, U., Lichtner, P., Castillo-Ramírez, L. A. & Ryu, S. A vertebrate-conserved cis-regulatory module for targeted expression in the main hypothalamic regulatory region for the stress response. *BMC Dev. Biol.* **14,** 41

(2014).

225. Koivisto, A. *et al.* TRPA1: a transducer and amplifier of pain and inflammation. *Basic Clin. Pharmacol. Toxicol.* **114,** 50–5 (2014).

226. Kokel, D. *et al.* Photochemical activation of TRPA1 channels in neurons and animals. *Nat. Chem. Biol.* **9,** 257–63 (2013).

227. Herget, U. & Ryu, S. Coexpression analysis of nine neuropeptides in the neurosecretory preoptic area of larval zebrafish. *Front. Neuroanat.* **9,** 2 (2015).

228. Patapoutian, A., Tate, S. & Woolf, C. J. Transient receptor potential channels: targeting pain at the source. *Nat. Rev. Drug Discov.* **8,** 55–68 (2009).

229. Bautista, D. M., Pellegrino, M. & Tsunozaki, M. TRPA1: A Gatekeeper for Inflammation. (2013). at <http://www.annualreviews.org/doi/abs/10.1146/annurev-physiol-030212-183811>

230. Kang, K. *et al.* Analysis of Drosophila TRPA1 reveals an ancient origin for human chemical nociception. *Nature* **464,** 597–600 (2010).

231. Kang, K. *et al.* Modulation of TRPA1 thermal sensitivity enables sensory discrimination in Drosophila. *Nature* **481,** 76–80 (2012).

232. Peng, G., Shi, X. & Kadowaki, T. Evolution of TRP channels inferred by their classification in diverse animal species. *Mol. Phylogenet. Evol.* **84,** 145–57 (2015).

233. Venkatachalam, K., Luo, J. & Montell, C. Evolutionarily conserved, multitasking TRP channels: lessons from worms and flies. *Handb. Exp. Pharmacol.* **223,** 937–62 (2014).

234. Pogorzala, L. A., Mishra, S. K. & Hoon, M. A. The cellular code for mammalian thermosensation. *J. Neurosci.* **33,** 5533–41 (2013).

235. Douglass, A. D., Kraves, S., Deisseroth, K., Schier, A. F. & Engert, F. Escape behavior elicited by single, channelrhodopsin-2-evoked spikes in zebrafish somatosensory neurons. *Curr. Biol.* **18,** 1133–1137 (2008).

236. Umeda, K. *et al.* Targeted expression of a chimeric channelrhodopsin in zebrafish under regulation of Gal4-UAS system. *Neurosci. Res.* **75,** 69–75 (2013).

237. Monesson-Olson, B. D., Browning-Kamins, J., Aziz-Bose, R., Kreines, F. & Trapani, J. G. Optical stimulation of zebrafish hair cells expressing channelrhodopsin-2. *PLoS One* **9,** e96641 (2014).

238. Fajardo, O., Zhu, P. & Friedrich, R. W. Control of a specific motor program by a small brain area in zebrafish. *Front. Neural Circuits* **7,** 67 (2013).

239. Kimura, Y. *et al.* Hindbrain V2a neurons in the excitation of spinal locomotor circuits during zebrafish swimming. *Curr. Biol.* **23,** 843–9 (2013).

240. Schoonheim, P. J., Arrenberg, A. B., Del Bene, F. & Baier, H. Optogenetic localization and genetic perturbation of saccade-generating neurons in zebrafish. *J. Neurosci.* **30,** 7111–20 (2010).

241. Wyart, C. *et al.* Optogenetic dissection of a behavioural module in the vertebrate spinal cord. *Nature* **461,** 407–10 (2009).

242. McPherson, A. D. *et al.* Motor Behavior Mediated by Continuously Generated Dopaminergic Neurons in the Zebrafish Hypothalamus Recovers after Cell Ablation. *Curr. Biol.* **26,** 263–269 (2016).

243. Hrabovszky, E. & Liposits, Z. Novel aspects of glutamatergic signalling in the neuroendocrine system. *J. Neuroendocrinol.* **20,** 743–51 (2008).

244. Stoop, R. Neuromodulation by oxytocin and vasopressin. *Neuron* **76,** 142–59 (2012).

245. Kupfermann, I. Modulatory actions of neurotransmitters. *Annu. Rev. Neurosci.* **2,** 447–65 (1979).

246. Dose, F., Zanon, P., Coslovich, T. & Taccola, G. Nanomolar oxytocin synergizes with weak electrical afferent stimulation to activate the locomotor CpG of the rat spinal cord in vitro. *PLoS One* **9,** e92967 (2014).

247. Lieberwirth, C. & Wang, Z. Social bonding: regulation by neuropeptides. *Front. Neurosci.* **8,** 171 (2014).

248. Anacker, A. M. J. & Beery, A. K. Life in groups: the roles of oxytocin in mammalian sociality. *Front. Behav. Neurosci.* **7,** 185 (2013).

249. Carter, C. S. Oxytocin pathways and the evolution of human behavior. *Annu. Rev. Psychol.* **65,** 17–39 (2014).

250. Choe, H. K. *et al.* Oxytocin Mediates Entrainment of Sensory Stimuli to Social Cues of Opposing Valence. *Neuron* **87,** 152–163 (2015).

251. Guzmán, Y. F. *et al.* Fear-enhancing effects of septal oxytocin receptors. *Nat. Neurosci.* **16,** 1185–7 (2013).

252. Beery, A. K. Antisocial oxytocin: complex effects on social behavior. *Curr. Opin. Behav. Sci.* **6,** 174–182 (2015).

253. Shamay-Tsoory, S. G. & Abu-Akel, A. The social salience hypothesis of oxytocin. *Biol. Psychiatry* (2015). doi:10.1016/j.biopsych.2015.07.020

254. Harari-Dahan, O. & Bernstein, A. A general approach-avoidance hypothesis of oxytocin: accounting for social and non-social effects of oxytocin. *Neurosci. Biobehav. Rev.* **47,** 506–19 (2014).

255. Gruber, C. W. Physiology of invertebrate oxytocin and vasopressin neuropeptides. *Exp. Physiol.* **99,** 55–61 (2014).

256. Beets, I. *et al.* Vasopressin/oxytocin-related signaling regulates gustatory associative learning in C. elegans. *Science* **338,** 543–5 (2012).

257. Bardou, I., Leprince, J., Chichery, R., Vaudry, H. & Agin, V. Vasopressin/oxytocin-related peptides influence long-term memory of a passive avoidance task in the cuttlefish, Sepia officinalis. *Neurobiol. Learn. Mem.* **93,** 240–7 (2010).

258. Smith, A. S. & Wang, Z. Hypothalamic oxytocin mediates social buffering of the stress response. *Biol. Psychiatry* **76,** 281–8 (2014).

259. Bagnall, M. W. & McLean, D. L. Modular organization of axial microcircuits in zebrafish. *Science* **343,** 197–200 (2014).

260. Ben Fredj, N. *et al.* Synaptic activity and activity-dependent competition regulates axon arbor maturation, growth arrest, and territory in the retinotectal projection. *J. Neurosci.* **30,** 10939–51 (2010).

261. Miyasaka, N. *et al.* From the olfactory bulb to higher brain centers: genetic visualization of secondary olfactory pathways in zebrafish. *J. Neurosci.* **29,** 4756–67 (2009).

262. Scott, E. K. *et al.* Targeting neural circuitry in zebrafish using GAL4 enhancer trapping. *Nat. Methods* **4,** 323–6 (2007).

263. Goll, M. G., Anderson, R., Stainier, D. Y. R., Spradling, A. C. & Halpern, M. E. Transcriptional silencing and reactivation in transgenic zebrafish. *Genetics* **182,** 747–55 (2009).

264. Del Bene, F. *et al.* Filtering of visual information in the tectum by an identified neural circuit. *Science* **330,** 669–73 (2010).

265. Montague, T. G., Cruz, J. M., Gagnon, J. A., Church, G. M. & Valen, E. CHOPCHOP: a CRISPR/Cas9 and TALEN web tool for genome editing. *Nucleic Acids Res.* **42,** W401–7 (2014).

266. Altstein, M. & Gainer, H. Differential biosynthesis and posttranslational processing of vasopressin and oxytocin in rat brain during embryonic and postnatal development. *J. Neurosci.* **8,** 3967–77 (1988).

267. Thisse, C. & Thisse, B. High-resolution in situ hybridization to whole-mount zebrafish embryos. *Nat. Protoc.* **3,** 59–69 (2008).

268. Leng, G., Pineda, R., Sabatier, N. & Ludwig, M. 60 YEARS OF NEUROENDOCRINOLOGY: The posterior pituitary, from Geoffrey Harris to our present understanding. *J. Endocrinol.* **226,** T173–85 (2015).

269. Grinevich, V., Desarménien, M. G., Chini, B., Tauber, M. & Muscatelli, F. Ontogenesis of oxytocin pathways in the mammalian brain: late maturation and psychosocial disorders. *Front. Neuroanat.* **8,** 164 (2014).

270. Dai, L. *et al.* Oxytocin and vasopressin are dysregulated in Williams Syndrome, a genetic disorder affecting social behavior. *PLoS One* **7,** e38513 (2012).

271. Francis, S. M. *et al.* Oxytocin and vasopressin systems in genetic syndromes and neurodevelopmental disorders. *Brain Res.* **1580,** 199–218 (2014).

272. Haas, B. W. & Smith, A. K. Oxytocin, vasopressin, and Williams syndrome: epigenetic effects on abnormal social behavior. *Front. Genet.* **6,** 28 (2015).

273. Gosch, A. & Pankau, R. Personality characteristics and behaviour problems in individuals of different ages with Williams syndrome. *Dev. Med. Child Neurol.* **39,** 527–533 (2008).

274. Winslow, J. T. & Insel, T. R. The social deficits of the oxytocin knockout mouse. *Neuropeptides* **36,** 221–229 (2002).

275. Winslow, J. T. & Insel, T. R. The social deficits of the oxytocin knockout mouse. *Neuropeptides* **36,** 221–9

276. Leng, G. *et al.* Oxytocin and appetite. *Prog. Brain Res.* **170,** 137–51 (2008).

277. Sabatier, N., Leng, G. & Menzies, J. Oxytocin, feeding, and satiety. *Front. Endocrinol. (Lausanne).* **4,** 35 (2013).

278. Xi, D., Gandhi, N., Lai, M. & Kublaoui, B. M. Ablation of Sim1 neurons causes obesity through hyperphagia and reduced energy expenditure. *PLoS One* **7,** e36453 (2012).

279. Tolson, K. P. *et al.* Inducible neuronal inactivation of Sim1 in adult mice causes hyperphagic obesity. *Endocrinology* **155,** 2436–44 (2014).

280. Olszewski, P. K., Allen, K. & Levine, A. S. Effect of oxytocin receptor blockade on appetite for sugar is modified by social context. *Appetite* **86,** 81–7 (2015).

281. Jennings, J. H. *et al.* Visualizing Hypothalamic Network Dynamics for Appetitive and Consummatory Behaviors. *Cell* **160,** 516–527 (2015).

282. Bianco, I. H. & Engert, F. Visuomotor Transformations Underlying Hunting Behavior in Zebrafish. *Curr. Biol.* **25,** 831–46 (2015).

283. Semmelhack, J. L. *et al.* A dedicated visual pathway for prey detection in larval zebrafish. *Elife* **4,** (2015).

284. Trivedi, C. A. & Bollmann, J. H. Visually driven chaining of elementary swim patterns into a goal-directed motor sequence: a virtual reality study of zebrafish prey capture. *Front. Neural Circuits* **7,** 86 (2013).

285. Zhu, J.-N. & Wang, J.-J. The cerebellum in feeding control: possible function and mechanism. *Cell. Mol. Neurobiol.* **28,** 469–78 (2008).

286. Dockray, G. J. The versatility of the vagus. *Physiol. Behav.* **97,** 531–6 (2009).

287. Ammar, A. A., Södersten, P. & Johnson, A. E. Locus coeruleus noradrenergic lesions attenuate intraoral intake. *Neuroreport* **12,** 3095–9 (2001).

288. Ahima, R. S. & Antwi, D. A. Brain regulation of appetite and satiety. *Endocrinol. Metab. Clin. North Am.* **37,** 811–23 (2008).

289. Kawakami, K. *et al.* zTrap: zebrafish gene trap and enhancer trap database. *BMC Dev. Biol.* **10,** 105 (2010).

290. Lillesaar, C., Stigloher, C., Tannhauser, B., Wullimann, M. F. & Bally-Cuif, L. Axonal projections originating from raphe serotonergic neurons in the developing and adult zebrafish, Danio rerio, using transgenics to visualize raphe-specific pet1 expression. *J. Comp. Neurol.* **512,** 158–182 (2009).

291. Lillesaar, C. The serotonergic system in fish. *J. Chem. Neuroanat.* **41,** 294–308 (2011).

292. Cheng, R.-K., Krishnan, S. & Jesuthasan, S. Activation and inhibition of tph2 serotonergic neurons operate in tandem to influence larval zebrafish preference for light over darkness. *Sci. Rep.* **6,** 20788 (2016).

293. Naumann, E. A., Kampff, A. R., Prober, D. A., Schier, A. F. & Engert, F. Monitoring neural activity with bioluminescence during natural behavior. *Nat. Neurosci.* **13,** 513–20 (2010).

294. Demski, L. S. Feeding and aggressive behavior evoked by hypothalamic stimulation in a cichlid fish. *Comp. Biochem. Physiol. Part A Physiol.* **44,** 685–692 (1973).

295. Demski, L. S. & Knigge, K. M. The telencephalon and hypothalamus of the bluegill (Lepomis macrochirus): evoked feeding, aggressive and reproductive behavior with representative frontal sections. *J. Comp. Neurol.* **143,** 1–16 (1971).

296. Pérez, M. R. *et al.* Relationships between radial glial progenitors and 5-HT neurons in the paraventricular organ of adult zebrafish - potential effects of serotonin on adult neurogenesis. *Eur. J. Neurosci.* **38,** 3292–301 (2013).

297. Berthoud, H.-R. Multiple neural systems controlling food intake and body weight. *Neurosci. Biobehav. Rev.* **26,** 393–428 (2002).

298. Watts, A. G. Understanding the neural control of ingestive behaviors: helping to separate cause from effect with dehydration-associated anorexia. *Horm. Behav.* **37,** 261–83 (2000).

299. Kantak, K. M., Wayner, M. J. & Stein, J. M. Effects of various periods of food deprivation on serotonin turnover in the lateral hypothalamus. *Pharmacol. Biochem. Behav.* **9,** 529–534 (1978).

300. Schwartz, D. H., McClane, S., Hernandez, L. & Hoebel, B. G. Feeding increases extracellular serotonin in the lateral hypothalamus of the rat as measured by microdialysis. *Brain Res.* **479,** 349–54 (1989).

301. Schwartz, D. H., Hernandez, L. & Hoebel, B. G. Serotonin release in lateral and medial hypothalamus during feeding and its anticipation. *Brain Res. Bull.* **25,** 797–802 (1990).

302. Heal, D. J., Cheetham, S. C., Prow, M. R., Martin, K. F. & Buckett, W. R. A comparison of the effects on central 5-HT function of sibutramine hydrochloride and other weight-modifying agents. *Br. J. Pharmacol.* **125,** 301–8 (1998).

303. Heisler, L. K., Kanarek, R. B. & Gerstein, A. Fluoxetine decreases fat and protein intakes but not carbohydrate intake in male rats. *Pharmacol. Biochem. Behav.* **58,** 767–73 (1997).

304. Simansky, K. J. & Vaidya, A. H. Behavioral mechanisms for the anorectic action of the serotonin (5-HT) uptake inhibitor sertraline in rats: comparison with directly acting 5-HT agonists. *Brain Res. Bull.* **25,** 953–60 (1990).

305. Suplicy, H. *et al.* A comparative study of five centrally acting drugs on the pharmacological treatment of obesity. *Int. J. Obes. (Lond).* **38,** 1097–103 (2014).

306. Wurtman, J. J. & Wurtman, R. J. Fenfluramine and fluoxetine spare protein consumption while suppressing caloric intake by rats. *Science* **198,** 1178–80 (1977).

307. Foltin, R. W. Effects of amphetamine, dexfenfluramine, diazepam, and other pharmacological and dietary manipulations on food ‘seeking’ and ‘taking’ behavior in non-human primates. *Psychopharmacology (Berl).* **158,** 28–38 (2001).

308. Breisch, S. T., Zemlan, F. P. & Hoebel, B. G. Hyperphagia and obesity following serotonin depletion by intraventricular p-chlorophenylalanine. *Science* **192,** 382–5 (1976).

309. Harvey, B. H. & Bouwer, C. D. Neuropharmacology of paradoxic weight gain with selective serotonin reuptake inhibitors. *Clin. Neuropharmacol.* **23,** 90–7

310. Bouwer, C. D. & Harvey, B. H. Phasic craving for carbohydrate observed with citalopram. *Int. Clin. Psychopharmacol.* **11,** 273–8 (1996).

311. Musil, R., Obermeier, M., Russ, P. & Hamerle, M. Weight gain and antipsychotics: a drug safety review. *Expert Opin. Drug Saf.* **14,** 73–96 (2015).

312. Shams, T. A. & Müller, D. J. Antipsychotic induced weight gain: genetics, epigenetics, and biomarkers reviewed. *Curr. Psychiatry Rep.* **16,** 473 (2014).

313. Alenina, N. *et al.* Growth retardation and altered autonomic control in mice lacking brain serotonin. *Proc. Natl. Acad. Sci. U. S. A.* **106,** 10332–7 (2009).

314. Savelieva, K. V *et al.* Genetic disruption of both tryptophan hydroxylase genes dramatically reduces serotonin and affects behavior in models sensitive to antidepressants. *PLoS One* **3,** e3301 (2008).

315. Dourish, C. T., Hutson, P. H. & Curzon, G. Low doses of the putative serotonin agonist 8-hydroxy-2-(di-n-propylamino) tetralin (8-OH-DPAT) elicit feeding in the rat. *Psychopharmacology (Berl).* **86,** 197–204 (1985).

316. Yadav, V. K. *et al.* A serotonin-dependent mechanism explains the leptin regulation of bone mass, appetite, and energy expenditure. *Cell* **138,** 976–89 (2009).

317. Avery, L. & Horvitz, H. R. Effects of starvation and neuroactive drugs on feeding in Caenorhabditis elegans. *J. Exp. Zool.* **253,** 263–70 (1990).

318. Srinivasan, S. *et al.* Serotonin regulates C. elegans fat and feeding through independent molecular mechanisms. *Cell Metab.* **7,** 533–44 (2008).

319. Lemieux, G. A. *et al.* Kynurenic Acid Is a Nutritional Cue that Enables Behavioral Plasticity. *Cell* **160,** 119–131 (2015).

320. Kellner, M., Porseryd, T., Porsch-Hällström, I., Hansen, S. H. & Olsén, K. H. Environmentally relevant concentrations of citalopram partially inhibit feeding in the three-spine stickleback (Gasterosteus aculeatus). *Aquat. Toxicol.* **158,** 165–70 (2015).

321. Hedgespeth, M. L., Nilsson, P. A. & Berglund, O. Ecological implications of altered fish foraging after exposure to an antidepressant pharmaceutical. *Aquat. Toxicol.* **151,** 84–7 (2014).

322. Weiger, W. A. Serotonergic modulation of behaviour: a phylogenetic overview. *Biol. Rev. Camb. Philos. Soc.* **72,** 61–95 (1997).

323. Gaspar, P. & Lillesaar, C. Probing the diversity of serotonin neurons. *Philos. Trans. R. Soc. Lond. B. Biol. Sci.* **367,** 2382–94 (2012).

324. Muto, A. & Kawakami, K. Imaging functional neural circuits in zebrafish with a new GCaMP and the Gal4FF-UAS system. *Commun. Integr. Biol.* **4,** 566–8 (2011).

325. Satou, C. *et al.* Transgenic tools to characterize neuronal properties of discrete populations of zebrafish neurons. *Development* **140,** 3927–31 (2013).

326. Liu, J. *et al.* Evolutionarily conserved regulation of hypocretin neuron specification by Lhx9. *Development* **142,** 1113–24 (2015).

327. Wen, L. *et al.* Visualization of monoaminergic neurons and neurotoxicity of MPTP in live transgenic zebrafish. *Dev. Biol.* **314,** 84–92 (2008).